STUDY OF NIFEDIPINE PHOTOCHEMISTRY INDUCED BY VISIBLE & UV-A LIGHT IN AQUEOUS LIPOSOME DISPERSIONS AND IN HYDROPHOBIC MEDIA

BY

WEIDONG JIA

A Thesis

Submitted to the Faculty of Graduate Studies

in Partial Fulfilment of the Requirements

for the Degree of

MASTER OF SCIENCE

Faculty of Pharmacy

University of Manitoba

Winnipeg, Manitoba, Canada

© January, 1996

National Library
of Canada

Acquisitions and
Bibliographic Services Branch

395 Wellington Street
Ottawa, Ontario
K1A 0N4

Bibliothèque nationale
du Canada

Direction des acquisitions et
des services bibliographiques

395, rue Wellington
Ottawa (Ontario)
K1A 0N4

Your file *Votre référence*

Our file *Notre référence*

The author has granted an irrevocable non-exclusive licence allowing the National Library of Canada to reproduce, loan, distribute or sell copies of his/her thesis by any means and in any form or format, making this thesis available to interested persons.

L'auteur a accordé une licence irrévocable et non exclusive permettant à la Bibliothèque nationale du Canada de reproduire, prêter, distribuer ou vendre des copies de sa thèse de quelque manière et sous quelque forme que ce soit pour mettre des exemplaires de cette thèse à la disposition des personnes intéressées.

The author retains ownership of the copyright in his/her thesis. Neither the thesis nor substantial extracts from it may be printed or otherwise reproduced without his/her permission.

L'auteur conserve la propriété du droit d'auteur qui protège sa thèse. Ni la thèse ni des extraits substantiels de celle-ci ne doivent être imprimés ou autrement reproduits sans son autorisation.

ISBN 0-612-13216-1

Canada

Name _____

Dissertation Abstracts International and *Masters Abstracts International* are arranged by broad, general subject categories. Please select the one subject which most nearly describes the content of your dissertation or thesis. Enter the corresponding four-digit code in the spaces provided.

PHARMACEUTICAL CHEMISTRY
SUBJECT TERM

0491
SUBJECT CODE

UMI

Subject Categories

THE HUMANITIES AND SOCIAL SCIENCES

COMMUNICATIONS AND THE ARTS
Architecture 0729
Art History 0377
Cinema 0900
Dance 0378
Fine Arts 0357
Information Science 0723
Journalism 0391
Library Science 0399
Mass Communications 0708
Music 0413
Speech Communication 0459
Theater 0465

EDUCATION
General 0515
Administration 0514
Adult and Continuing 0516
Agricultural 0517
Art 0273
Bilingual and Multicultural 0282
Business 0688
Community College 0275
Curriculum and Instruction 0727
Early Childhood 0518
Elementary 0524
Finance 0277
Guidance and Counseling 0519
Health 0680
Higher 0745
History of 0520
Home Economics 0278
Industrial 0521
Language and Literature 0279
Mathematics 0280
Music 0522
Philosophy of 0998
Physical 0523
Psychology 0525
Reading 0535
Religious 0527
Sciences 0714
Secondary 0533
Social Sciences 0534
Sociology of 0340
Special 0529
Teacher Training 0530
Technology 0710
Tests and Measurements 0288
Vocational 0747

LANGUAGE, LITERATURE AND LINGUISTICS
Language
- General 0679
- Ancient 0289
- Linguistics 0290
- Modern 0291

Literature
- General 0401
- Classical 0294
- Comparative 0295
- Medieval 0297
- Modern 0298
- African 0316
- American 0591
- Asian 0305
- Canadian (English) 0352
- Canadian (French) 0355
- English 0593
- Germanic 0311
- Latin American 0312
- Middle Eastern 0315
- Romance 0313
- Slavic and East European 0314

PHILOSOPHY, RELIGION AND THEOLOGY
Philosophy 0422
Religion
- General 0318
- Biblical Studies 0321
- Clergy 0319
- History of 0320
- Philosophy of 0322

Theology 0469

SOCIAL SCIENCES
American Studies 0323
Anthropology
- Archaeology 0324
- Cultural 0326
- Physical 0327

Business Administration
- General 0310
- Accounting 0272
- Banking 0770
- Management 0454
- Marketing 0338

Canadian Studies 0385
Economics
- General 0501
- Agricultural 0503
- Commerce-Business 0505
- Finance 0508
- History 0509
- Labor 0510
- Theory 0511

Folklore 0358
Geography 0366
Gerontology 0351
History
- General 0578
- Ancient 0579
- Medieval 0581
- Modern 0582
- Black 0328
- African 0331
- Asia, Australia and Oceania 0332
- Canadian 0334
- European 0335
- Latin American 0336
- Middle Eastern 0333
- United States 0337

History of Science 0585
Law 0398
Political Science
- General 0615
- International Law and Relations 0616
- Public Administration 0617

Recreation 0814
Social Work 0452
Sociology
- General 0626
- Criminology and Penology ... 0627
- Demography 0938
- Ethnic and Racial Studies 0631
- Individual and Family Studies 0628
- Industrial and Labor Relations 0629
- Public and Social Welfare 0630
- Social Structure and Development 0700
- Theory and Methods 0344

Transportation 0709
Urban and Regional Planning 0999
Women's Studies 0453

THE SCIENCES AND ENGINEERING

BIOLOGICAL SCIENCES
Agriculture
- General 0473
- Agronomy 0285
- Animal Culture and Nutrition 0475
- Animal Pathology 0476
- Food Science and Technology 0359
- Forestry and Wildlife 0478
- Plant Culture 0479
- Plant Pathology 0480
- Plant Physiology 0817
- Range Management 0777
- Wood Technology 0746

Biology
- General 0306
- Anatomy 0287
- Biostatistics 0308
- Botany 0309
- Cell 0379
- Ecology 0329
- Entomology 0353
- Genetics 0369
- Limnology 0793
- Microbiology 0410
- Molecular 0307
- Neuroscience 0317
- Oceanography 0416
- Physiology 0433
- Radiation 0821
- Veterinary Science 0778
- Zoology 0472

Biophysics
- General 0786
- Medical 0760

EARTH SCIENCES
Biogeochemistry 0425
Geochemistry 0996
Geodesy 0370
Geology 0372
Geophysics 0373
Hydrology 0388
Mineralogy 0411
Paleobotany 0345
Paleoecology 0426
Paleontology 0418
Paleozoology 0985
Palynology 0427
Physical Geography 0368
Physical Oceanography 0415

HEALTH AND ENVIRONMENTAL SCIENCES
Environmental Sciences 0768
Health Sciences
- General 0566
- Audiology 0300
- Chemotherapy 0992
- Dentistry 0567
- Education 0350
- Hospital Management 0769
- Human Development 0758
- Immunology 0982
- Medicine and Surgery 0564
- Mental Health 0347
- Nursing 0569
- Nutrition 0570
- Obstetrics and Gynecology .. 0380
- Occupational Health and Therapy 0354
- Ophthalmology 0381
- Pathology 0571
- Pharmacology 0419
- Pharmacy 0572
- Physical Therapy 0382
- Public Health 0573
- Radiology 0574
- Recreation 0575
- Speech Pathology 0460
- Toxicology 0383

Home Economics 0386

PHYSICAL SCIENCES
Pure Sciences
Chemistry
- General 0485
- Agricultural 0749
- Analytical 0486
- Biochemistry 0487
- Inorganic 0488
- Nuclear 0738
- Organic 0490
- Pharmaceutical 0491
- Physical 0494
- Polymer 0495
- Radiation 0754

Mathematics 0405
Physics
- General 0605
- Acoustics 0986
- Astronomy and Astrophysics 0606
- Atmospheric Science 0608
- Atomic 0748
- Electronics and Electricity 0607
- Elementary Particles and High Energy 0798
- Fluid and Plasma 0759
- Molecular 0609
- Nuclear 0610
- Optics 0752
- Radiation 0756
- Solid State 0611

Statistics 0463

Applied Sciences
Applied Mechanics 0346
Computer Science 0984
Engineering
- General 0537
- Aerospace 0538
- Agricultural 0539
- Automotive 0540
- Biomedical 0541
- Chemical 0542
- Civil 0543
- Electronics and Electrical 0544
- Heat and Thermodynamics ... 0348
- Hydraulic 0545
- Industrial 0546
- Marine 0547
- Materials Science 0794
- Mechanical 0548
- Metallurgy 0743
- Mining 0551
- Nuclear 0552
- Packaging 0549
- Petroleum 0765
- Sanitary and Municipal 0554
- System Science 0790

Geotechnology 0428
Operations Research 0796
Plastics Technology 0795
Textile Technology 0994

PSYCHOLOGY
General 0621
Behavioral 0384
Clinical 0622
Developmental 0620
Experimental 0623
Industrial 0624
Personality 0625
Physiological 0989
Psychobiology 0349
Psychometrics 0632
Social 0451

STUDY OF NIFEDIPINE PHOTOCEHMISTRY INDUCED BY VISIBLE & UV-A LIGHT IN AQUEOUS LIPOSOME DISPERSIONS AND IN HYDROPHOBIC MEDIA

BY

WEIDONG JIA

A Thesis submitted to the Faculty of Graduate Studies of the University of Manitoba in partial fulfillment of the requirements of the degree of

MASTER OF SCIENCE

© 1996

Permission has been granted to the LIBRARY OF THE UNIVERSITY OF MANITOBA to lend or sell copies of this thesis, to the NATIONAL LIBRARY OF CANADA to microfilm this thesis and to lend or sell copies of the film, and LIBRARY MICROFILMS to publish an abstract of this thesis.

The author reserves other publication rights, and neither the thesis nor extensive extracts from it may be printed or other-wise reproduced without the author's written permission.

ABSTRACT

The objective of the present work was to study the photodegradation mechanism of nifedipine in aqueous liposome dispersions, on hydrated albumin proteins and in hydrophobic organic solvents. For the liposome work, we studied both large unilamellar and multilamellar vesicles which were composed of saturated lipids, namely dimyristoyl-L-α-phosphatidylcholine (DMPC) and di-O-hexadecyl-DL-α-phosphatidylcholine (DHPC). We also chose to study hydrated bovine and human serum albumins because of their importance in binding nifedipine in blood plasma *in vivo*. Nifedipine was incorporated in the bilayer membranes of liposomes by a vortexing and extrusion technique and also adsorbed on the studied proteins by a simple vortexing method. The molar ratios of the lipids to the incorporated nifedipine were between 12:1 and 25:1 in the liposomes. The maximum observed molar ratio of the absorbed nifedipine/albumin was about 1 ± 0.1, which implied that nifedipine was possibly absorbed on specific protein binding sites. An electron paramagnetic resonance (EPR) study of the free radicals derived from the nifedipine photochemistry indicated that the free radicals were firmly bound to the albumins while they were relatively mobile in the bilayer membranes of liposomes.

As induced by visible and UV-A light, nifedipine underwent a faster photochemical conversion to the nitrosophenylpyridine (NTSP) product in bilayer lipid membranes than that observed in ethanol solutions. In agreement with some previous work, EPR spectral simulation of a partially resolved spectrum obtained from nifedipine in DMPC large unilamellar vesicles (LUVs) revealed the presence of two different nitroxide free radicals which were identified as the structures of Ar-NO$^{\bullet}$-C-Ar' (A) and Ar-NO$^{\bullet}$-H (B) at an approximate molar ratio 1:(0.65 ± 0.05). The total concentrations of these radicals in the liposome dispersions and in the protein aqueous solutions were between 10 μM and 20 μM relative to the initial nifedipine concentrations of (2 ± 0.5) mM. A possible intramolecular rearrangement mechanism involving a 1,4-dihydro-4-pyridinol derivative as an intermediate for the conversion of nifedipine to NTSP was proposed. Based on this mechanism, the formation of the observed radical adducts was explained in terms of the postulated intermediates.

UV-visible absorption measurements as a function of increasing nifedipine concentrations suggested the presence of at least nifedipine dimers in solution. We estimated the nifedipine dimer formation equilibrium constants (K) to be 8.0 ± 45%; 13.6 ± 26% and 49.0 ± 8% (M^{-1}) respectively in ethanol, 1-butanol and 1-octanol solutions. We suggest that the dimerization of nifedipine could be very important in the photochemistry where, for instance, radical A was produced from an intermolecular reaction involving NTSP and a photochemically produced reactive free radical.

ACKNOWLEDGEMENTS

I am sincerely grateful to Dr. Alan R. McIntosh for his supervision, encouragement, patience and financial aid during the period of study, research, and preparation of this thesis. I would like to extend my thanks to Dr. J. O'Neil (Department of Chemistry), Dr. J. F. Templeton and Dr. J. W. Steele (Faculty of Pharmacy) for their reviewing this thesis and for their valuable comments.

I gratefully acknowledge the generous financial support by Parke-Davis Company provided as the 'Parke-Davis Canada Centennial Pharmacy Research Award'. I would also like to acknowledge the financial assistance given by the Faculty of Pharmacy in the form of a teaching assistantship.

I am pleased to give my special thanks to my parents, my wife and my friends for their continued support, understanding and encouragement.

CONTENTS

LIST OF TABLES

LIST OF FIGURES

LIST OF ABBREVIATIONS

BSA	Bovine serum albumin
DHPC	Di-O-hexadecyl-DL-α-phosphatidylcholine
DHP(s)	1,4-Dihydropyridine derivative(s)
DMPC	Dimyristoyl-L-α-phosphatidylcholine
DMPO	5,5-Dimethyl-1-pyrroline-N-oxide
EPR	Electron paramagnetic resonance
HEPES	N-(2-Hydroxyethyl)piperazine-N'-2-ethanesulfonic acid, sodium salt
HSA	Human serum albumin
LDL	Low density lipoproteins
LUVs	Large unilamellar vesicles
MLVs	Multilamellar vesicles
MNP	2-Methyl-2-nitrosopropane
NFDP	Nifedipine
NTRP	2,6-Dimethyl-4-(o-nitrophenyl)-3,5-dimethylpyridinedicarboxylate
NTSP	2,6-Dimethyl-4-(o-nitrosophenyl)-3,5-dimethylpyridinedicarboxylate
PBN	N-t-Butyl-α-phenylnitrone
TEMPOL	4-Hydroxyl-2,2,6,6-tetramethylpiperidin-1-yloxy radical
TLC	Thin layer chromatography
UV-VIS	Ultraviolet and visible

PART I. INTRODUCTION

1.1 PHARMACOLOGY AND BIOAVAILABILITY

Nifedipine is a 1,4-dihydropyridine derivative, shown in Figure 1.1.1, and it has an important vasodilating effect on coronary arteries which is useful in cardiovascular therapy. As a primary cardiovascular drug, nifedipine has been extensively applied to the treatment of ischaemic disease and systemic hypertension (Nayler, 1988; Van Zwieten, 1989; Opie, 1990).

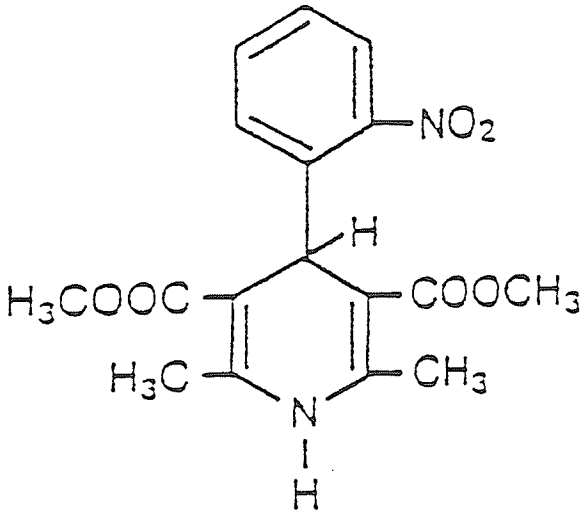

$C_{17}H_{18}N_2O_6$ MW=346.34

Dimethyl 1,4-dihydro-2,6-dimethyl-4-(o-nitrophenyl)-3,5-pyridinedicarboxylate.

Figure 1.1.1 Structure of nifedipine

Nifedipine selectively blocks the influx of calcium ions into cells at the slow calcium channels in the membranes of vascular smooth muscle and myocardial tissue (Nayler, 1990). The transmembrane flow of Ca^{2+} is known to regulate a wide variety of cellular processes including muscle contraction (Hagiwara and Byerly, 1981; Miller, 1987). The voltage-regulated calcium channel is a major regulator of calcium influx into these cells. Nifedipine shows a high affinity of binding at specific sites in the calcium channels which inhibits the opening of these ion channels. The binding sites of the channels have been extensively studied by radiolabeled nifedipine analogues (Hosey and Lazdunski, 1988).

Nifedipine is highly bound to serum albumin proteins in blood plasma which is thought to contribute to the long duration of action of the drug (Schlossman *et al*, 1975). Upon oral administration, up to 90% of a single dose of nifedipine is absorbed through the gastrointestinal tract (Hoster, 1975). Following enteric absorption, radiolabeled nifedipine is found to undergo hepatic oxidation to three pharmacologically inactive major metabolites (Kroneberg and Krebs, 1980) which are the nitrophenylpyridine metabolites I, II, and III as shown in Figure 1.1.2. Independent of the mode of administration, 70-80% of metabolites are eliminated via urine and up to 15% are excreted in faeces (Ramemsch and Sommer, 1983). Only about 0.1% of unchanged nifedipine is eliminated through renal clearance (Kleinbloesem *et al*, 1984).

1.2 ANTIOXIDANT PROPERTY

Lipid peroxidation by free radicals such as superoxide radical ($^{\cdot}O_2^-$) and hydroxyl radical ($^{\cdot}OH$) in biological systems has been implicated as a cause of membrane damage (Weglicki *et al*, 1990). The depression of lipid peroxidation in methyl oleate systems by nifedipine was first observed in 1984 (Tirzit *et al*, 1984). Recently the antioxidant effects

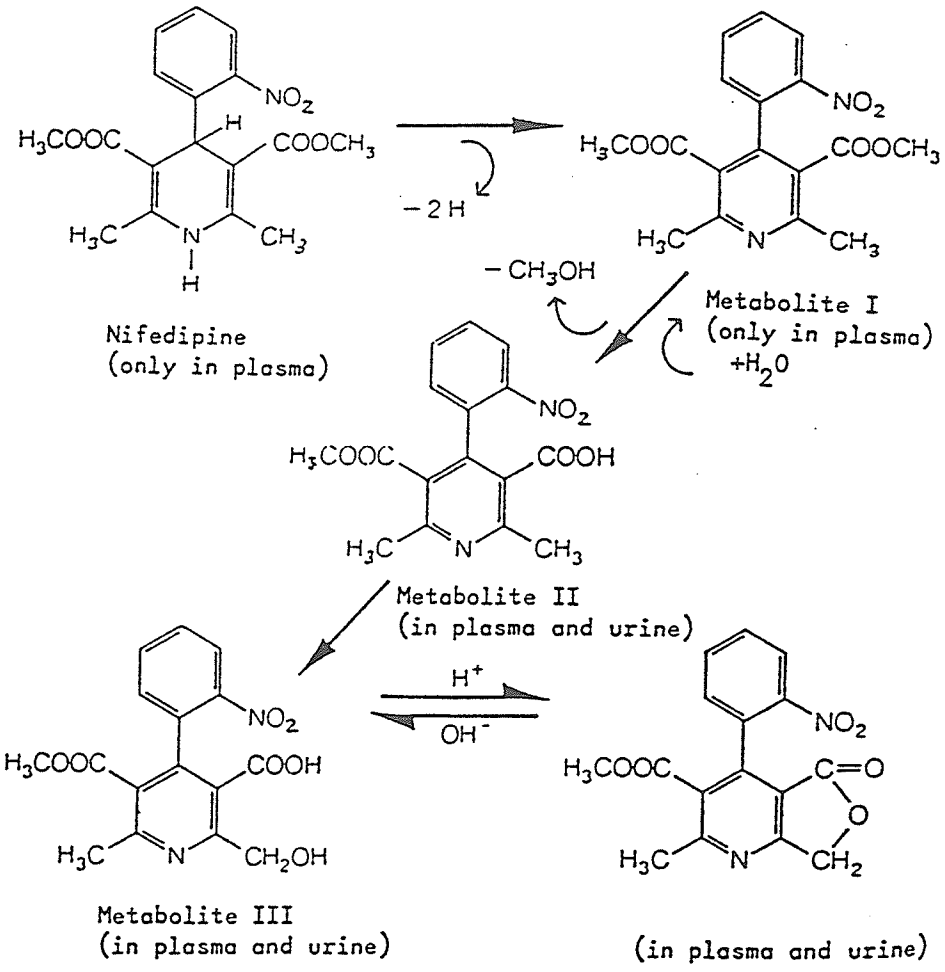

Figure 1.1.2 Metabolism of nifedipine (Kroneberg and Krebs, 1980)

of nifedipine and other calcium channel blockers against lipid peroxidation have been studied with increasing interest. Because of their lipophilic nature, calcium channel blockers bind to the phospholipid-rich membranes close to Ca^{2+} channels in addition to the serum albumin binding sites (Carvalho *et al*, 1989; Herbette *et al*, 1989). The antioxidant activity of nifedipine, verapamil and diltiazem were compared by using different *in vitro* models of low density lipoprotein (LDL) (Mak and Weglicki, 1990; Mak *et al*, 1992). The observed order of potency of these agents was nifedipine > verapamil > diltiazem. All three calcium blockers exhibited concentration-dependent (10-400 μM) inhibitory effects against lipid peroxidation, and nifedipine achieved a significant effect at 10 μM. The potency against free radical chain reactions in cardiac membranes was presumed to be related to the lipophilicity of the calcium channel blockers (Mak and Weglicki, 1990).

Ondrias *et al* and Misik *et al* reported their free radical results on the depression of lipid peroxidation of phosphatidylcholine liposomes by some calcium channel blockers including nifedipine (Ondrias *et al*, 1989, 1994; Misik *et al*, 1991, 1993). The study compared the antioxidant properties of nifedipine, illuminated nifedipine and nimodipine incorporated in diheptanoylphosphatidylcholine lipid dispersions. It was found that pure nifedipine incorporated in the lipids slightly inhibited lipid peroxidation but that both nonilluminated and illuminated nimodipine had no appreciable antioxidant potency. However, the illuminated nifedipine was several times more effective than the nonilluminated nifedipine. Misik *et al* (1993) proposed that 2,6-dimethyl-4-(o-nitrosophenyl)-3,5-dimethylpyridinedicarboxylate (NTSP), derived from the photodegradation of nifedipine (see Figure 1.3.1, page 7), played a role as an antioxidant in the lipid peroxidation. In a living organism, NTSP might be produced from nifedipine either enzymatically (Edwards, 1986) or by illumination through the skin (Thomas and Wood, 1986).

The antioxidative mechanism of nifedipine and its photochemical product, NTSP, probably involves a chain breaking reaction at the level of the membrane phospholipids because neither agent affected the primary hydroxyl radicals produced in the aqueous phase (Mak and Weglicki, 1990; Mak *et al*, 1992; Weglicki *et al*, 1990). The aromatic 'chain-breaking' antioxidants like nifedipine provide resonance stabilization for trapped radicals. As a nitroso compound, NTSP could also inhibit lipid peroxidation reactions in a pseudo Diels-Alder mechanism between nitroso compounds and the double bonds of unsaturated lipids (Sullivan, 1966).

1.3 PHOTOCHEMISTRY

1.3.1 Photodegradation

Nifedipine (NFDP) undergoes both a photochemical oxidation and reduction. Two main photodegradation products have been reported (Figure 1.3.1) (Syed, 1989). Ebel *et al* (1978) reported the formation of only the 4-(2-nitrosophenyl)pyridine (NTSP) product under both ultraviolet and visible light conditions, but Jacobsen *et al* (1979) and Testa *et al* (1979) found the NTSP product in visible light irradiations and the nitrophenylpyridine (NTRP) product when exposed to ultraviolet light. The wavelength of light significantly affected the molar fractions of nifedipine and the observed products in the photodegradation reactions. Nifedipine was easily decomposed by UV and visible light below 500 nm, and the degree of degradation reached a maximum around 380 nm (Matsuda *et al*, 1989). As the pyridine ring absorption bands are usually ≤ 330 nm and those for simple benzene derivatives are usually ≤ 280 nm, the absorption around 380 nm is correlated with the absorption bands of the dihydropyridine ring in nifedipine. Sadana and Ghogare (1991) indicated that the initial photodegradation of nifedipine yields the nitroso product (NTSP), and then slow air oxidation of NTSP produces nitrophenyl-pyridine

(NTRP). Similar results have also been reported elsewhere (Shim *et al*, 1988; Thoma and Kerker, 1992c).

Nifedipine usually undergoes a photochemical decomposition in solution by an apparent first-order reaction with a quantum efficiency of 0.42 (Thoma and Klimek, 1985). It is possible to observe zero-order kinetics at concentrations higher than 4×10^{-4} M and to observe pseudo-first order kinetics at lower concentrations (Majeed *et al*, 1987). The photooxidation of nifedipine is most rapid in ethanol, slower in diethyl ether and ethyl acetate, and slowest in toluene (Wang and Cheng, 1991). The solid state photodegradation of nifedipine follows apparent first-order kinetics (Matsuda *et al*, 1989). Polymer film coatings with UV absorbers and/or inorganic pigments (Bechard *et al*, 1992) does prevent or retard the photodegradation of nifedipine.

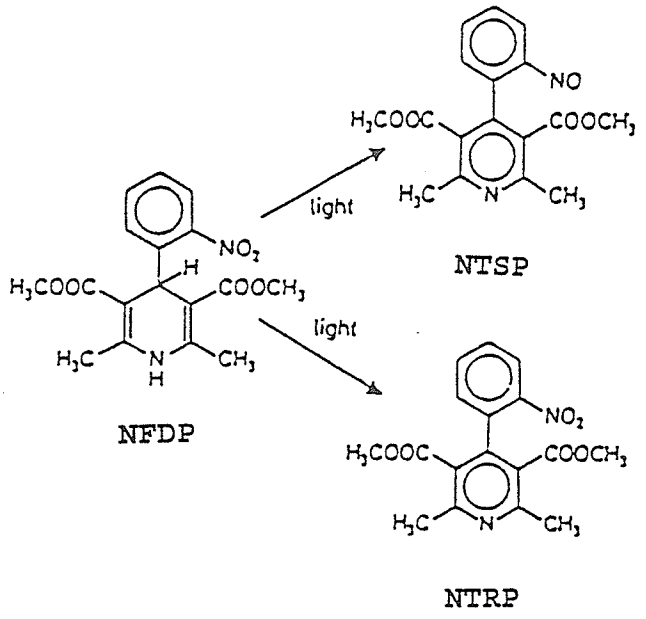

Figure 1.3.1 Nifedipine photodegradation *in vitro* (Syed, 1989)

1.3.2 State of the Photochemical Mechanism

As early as 1955, Berson and Brown reported the synthesis of 4-(2'-nitrophenyl)-1,4-dihydropyridine derivatives (Berson and Brown, 1955a) and the investigation of their photochemical behaviour (Berson and Brown, 1955b). In contrast to the 4-(4'-nitrophenyl)-1,4-dihydropyridine derivatives which are very stable even under intense irradiation by sun light or by a mercury arc (Philips, 1951), there is a facile photochemical conversion of 2'-nitrophenyl compounds to fully aromatic nitroso derivatives. Berson and Brown have suggested a mechanism which involves an intramolecular transfer of C_4 hydrogen to the nitro group.

More recently Stasko *et al* (1994) have studied the reactive radical intermediates formed from illuminated nifedipine in various organic solutions by EPR spectroscopy. An EPR spectrum observed from nifedipine incorporated in multilamellar lipid vesicles was also reported. Two relatively stable nitroxide radical products, A and B, (see Figure 1.3.2) were detected during the irradiation of nifedipine dissolved in benzene, acetonitrile and other solvents. In radical A, the X was an unknown EPR silent substituent. Upon irradiation, radical A formed immediately, whereas radical B increased upon prolonged irradiation. They suggested that radical B was formed by NTSP abstracting hydrogen from nifedipine, whereas four structures were assumed for radical A (Figure 1.3.2, NIF-2, NIF-3, NIF-4, NIF-5), among which structure NIF-5 was rather unusual but in agreement with the EPR parameters. As shown in Figure 1.3.3, a possible dimer complex was suggested as an important intermediate in the photochemical mechanism; but a complete mechanism was not proposed. Furthermore, each nifedipine stucture is nonplanar because of the intramolecular hydrogen bond to the nitro group.

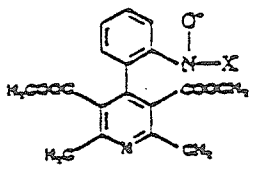

A

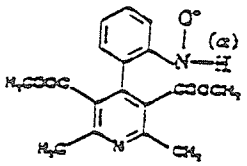

B

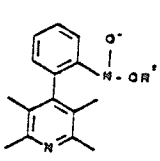

NIF-2

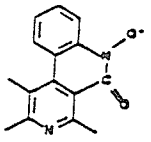

NIF-3

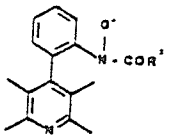

NIF-4

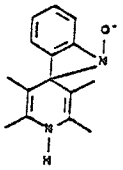

NIF-5

Figure 1.3.2 The two detected radicals A, B and

the possible structures of radical A in Stasko's work (Stasko *et al*, 1994)

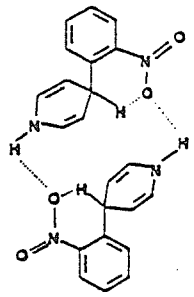

Figure 1.3.3 The assumed intermediate involved

in the photochemical conversion of nifedipine (Stasko *et al*, 1994)

(note: the above 1,4-dihydropyridine derivatives are nonplanar)

As detected by EPR spectroscopy, NTSP, not nifedipine, formed stable radical adducts when interacting with rat heart homogenates and dioleoylphosphotidylcholine lipids; and NTSP was effective in trapping free radicals formed by the thermal or photoinduced decomposition of 2,2'-azobisisobutyronitrile (Misik *et al*, 1991; Ondrias *et al*, 1994). In fact, Stasko *et al* employed NTSP as an endogenous spin trap (for the spin trapping technique, see page 26 for details) to study the photodegradation mechanism of nifedipine by the EPR method (Stasko *et al*, 1994).

The role of oxygen in the nifedipine photochemistry has been studied by the irradiation of nifedipine solutions in methanol under oxygen or nitrogen atmospheres with a 250W medium-pressure mercury lamp (Vargas *et al*, 1992). Irradiation in the presence of oxygen produced NTRP (III) with a yield of 73%, and the involvement of singlet oxygen was shown by trapping with 2,5-methylfuran to form hexene-2,5-dione. A control experiment under hypoxic conditions showed the same main photoproduct (III), but no formation of the dione product was observed.

1.4 OBJECTIVES OF THE PRESENT STUDY

As discussed in the previous section, nifedipine undergoes photodegradation when it is exposed to UV and visible light. For the purpose of quality assurance during its dosage preparation and its therapeutic application, many product analyses including kinetic studies have been carried out to find ways to minimize the photodegradation. Some studies related to the antioxidant properties of nifedipine also have been reported.

So far, relatively few studies have investigated the detailed mechanism of the nifedipine photochemistry. The intramolecular transfer of a C_4 hydrogen to the nitro group was first suggested in 1955 (Berson and Brown, 1955b), but the photochemical reaction

mechanism of nifedipine has not been completely elucidated at present. Stasko *et al* (1994) have proposed two specific free radical types (Figure 1.3.2, A & B) as stable photochemical products. However, we can pose several new questions with regard to this discovery. First, does a more reasonable structure exist for radical A?, Secondly, can we improve upon the suggested mechanism by which radical A and radical B are formed (Stasko *et al*, 1994)? Radicals A and B have been provisionally identified as the nitroxides shown in Figure 1.3.2, and they should be relatively stable because of their structures. In the same work, Stasko *et al* suggested one possible intermediate (Figure 1.3.3) to explain part of the observed nifedipine photodegradation. Furthermore, Vargas *et al* (1992) have studied the role of oxygen in the photoreaction, but the results indicated that NTRP was the main product under both oxic and hypoxic conditions. Obviously, more work is needed to clarify the photodegradation mechanism, the structures and formation pathway of the observed stable radical products and the role of oxygen in the photochemical reaction.

Interactions of nifedipine with lipids and proteins are very important *in vivo.* After administration, nifedipine is absorbed to and transferred from human serum albumin proteins in blood plasma (Schlossman *et al*, 1975). By using liposome model systems containing some unsaturated lipids, several reports have discussed some nifedipine interactions with low density lipoproteins where the antioxidant properties of nifedipine were revealed (Mak and Weglick, 1990; Mak *et al*, 1992; Weglicki *et al*, 1990). Presumably, the behaviour of nifedipine in saturated bilayer lipid membranes would be different. Another reason for choosing saturated lipids is to avoid the interference by the pseudo Diels-Alder reaction between unsaturated lipids and nifedipine or its degraded products (Sullivan, 1966). Finally, we chose to study nifedipine bound to bovine and

human serum albumin proteins separately from the lipid systems to determine if the photochemistry still proceeds in the hydrated protein environment.

In the present work, we will use EPR and UV-VIS spectroscopic methods to probe the nifedipine photochemical mechanism with respect to the formation pathway of the reported stable radicals (Stasko *et al*, 1994) and the role of oxygen in the reactions. We will also focus on the possible interactions of nifedipine with proteins (as described above) and separately with saturated bilayer lipid membranes. Our studied membranes consisted of large unilamellar vesicles (LUVs) and multilamellar vesicles (MLVs), composed of either DMPC (dimyristoyl-L-α-phosphatidylcholine) or DHPC (di-O-hexadecyl-DL-α-phosphatidylcholine), respectively ester and ether linked phospholipids.

Free radicals are clearly involved in the photochemical reactions of nifedipine (Stasko *et al*, 1994), and we will also rely upon EPR to study the stable free radicals which are formed. The trapping of the free radicals and the structural analysis of these adducts will assist us in a study of the detailed mechanism. Here, we emphasize once again the observed spin trapping properties of the nitroso compound NTSP (Misik *et al*, 1991), which may provide more information for our mechanistic objectives.

UV-VIS spectroscopy will be also applied in our study. Nifedipine and its photochemical products have characteristic UV-VIS absorption spectra. UV-VIS spectroscopy may provide qualitative and quantitative data to analyze the photodegradation reaction. Considering the intermolecular conversion model proposed in Stasko's work (Stasko *et al*, 1994), we assumed that nifedipine may have some tendency for self-association in solution due to some attraction between the nitrophenyl ring and the dihydropyridine ring in a nifedipine dimer complex through hydrogen bonding or electron donor-acceptor models. This complex could form more easily when the nifedipine

molecules are restricted to the bilayer lipid membranes of MLVs or LUVs. Therefore, the evaluation of the tendency for self-association of nifedipine by UV-VIS spectroscopy may provide useful data for a further evaluation of the nifedipine photochemical mechanism. For instance, the formation of the nitroxide photochemical products depends upon a bimolecular reaction between the nitroso molecule, NTSP, and a free radical molecule derived from nifedipine. This bimolecular reaction could be enhanced in a system where there was a strong tendency for molecular association of nifedipine and certain molecules which are nifedipine photoproducts.

PART II. METHODOLOGY

2.1 UV-VIS SPECTROSCOPY

Electronic transitions in molecules are excited by the absorption of UV/visible photons, and even the broad absorption bands which are commonly observed for polyatomic molecules are useful in the qualitative and quantitative analysis of chemical structures, equilibria and reactions (Jaffe and Orchin, 1962). Besides the fundamental Beer-Lambert Law, the development of techniques such as dual-wavelength, first derivative and luminescence-excitation spectroscopic methods have all facilitated the extension of the applications of UV-VIS spectroscopy (Perkampus, 1992). In this section, we will describe the Benesi-Hildebrand equation as a diagnostic test for complex formation between molecules, and we will also discuss the utility of first derivative absorption measurements.

2.1.1 Benesi-Hildebrand Equation

The evaluation of the equilibrium complex formation constant (K) is an application of UV-VIS spectroscopy in systems where light absorbing complexes exist. In general, the formation of a complex between donor (D) and acceptor (A) molecules in solution can be described by the following equilibrium where the equilibrium constant is given by Equation [1] for a 1:1 complex.

$$D + A \rightleftharpoons DA$$

$$K = \frac{C_{DA}}{(C_{0D} - C_{DA})(C_{0A} - C_{DA})} \qquad [1]$$

Here, K : equilibrium complex formation constant;

C_{0A} : initial concentration of acceptor;

C_{0D} : initial concentration of donor;

C_{DA} : concentration of complex DA at equilibrium.

Based on the Beer-Lambert Law and the measured absorbance values, several equations have been proposed for the determination of the equilibrium constant (K) (Perkampus, 1992). The well-known Benesi-Hildebrand Equation [2] (Benesi and Hildebrand, 1949) can be used for the evaluation of the equilibrium constant (K) by the graphical method of plotting $C_{0A}d/A_e$ against $1/C_{0D}$.

$$\frac{C_{0A} \cdot d}{A_e} = \frac{1}{K \cdot C_{0D} \cdot \varepsilon_{DA}} + \frac{1}{\varepsilon_{DA}} \qquad [2]$$

Here, ε_{DA} : molar extinction coefficient of the complex;

A_e : experimental absorptivity of the measured sample;

d : optical length of the cuvette.

During the development of the Benesi-Hildebrand Equation, the measured absorbance A_e at a selected wavelength was attributed to the equilibrium composition [3]:

$$A_e = \varepsilon_D \cdot (C_{0D} - C_{DA}) \cdot d + \varepsilon_A (C_{0A} - C_{DA}) \cdot d + \varepsilon_{DA} \cdot C_{DA} \cdot d \qquad [3]$$

Here, ε_D and ε_A are respectively the molar extinction coefficients of the donor and acceptor; the values of ε_D and ε_A were supposed to be zero at the measured wavelengths ($\varepsilon_A = \varepsilon_D = 0$); and several approximations such as $C_{0D} + C_{0A} > C_{DA}$ and $C_{0D} > C_{0A}$ were also used (Perkampus, 1992).

Several forms of the Benesi-Hildebrand Equation [2] have been applied

successfully to evaluate the equilibrium complex formation constant (K) for the case of distinct donor and acceptor molecules which form complexes. For a self-complexing case in which the donor and acceptor are the same compound, the Benesi-Hildebrand equation could not be applied. In general, for a self complexing reaction, the equilibrium would be:

$$nM \quad \rightleftharpoons \quad M_n$$

when n = 2, it is a dimerization:

$$2\,M \quad \rightleftharpoons \quad M_2 \text{ (or D)} \qquad (D = M_2)$$

$$\therefore \quad K = \frac{C_D}{C_M^{\,2}} \qquad [4]$$

Referring to the development of the Benesi-Hildebrand Equation [2], we proposed a modified Benesi-Hildebrand Equation [5] (see Appendix A) to evaluate the dimer-complex equilibrium formation constant in various organic solutions.

$$E = \frac{E_M}{(E_D - 2E_M)} = \frac{4CK+1 \pm \sqrt{(8CK+1)}}{8C_0K\left(\frac{A}{A_0} - \frac{C}{C_0}\right)} \qquad [5]$$

Here,

K : dimer-complex equilibrium formation constant;

C_D : concentration of the dimer at equilibrium;

C_M : concentration of the monomer at equilibrium.

E_M : molar extinction coefficient of monomer;

E_D : molar extinction coefficient of dimer;

C_0 : starting low concentration of monomer;

C : higher concentration of monomer.

A_0 : absorbance corresponding to C_0;

A : absorbance corresponding to C;

In Equation [5], there are two problems for the determination of the K value: first, both K and E_D are unknown; and secondly, the equation is nonlinear which means it cannot be solved directly by graphical methods. However, K should be independent both of wavelength and concentration, and E_D should be dependent on wavelength but independent of concentration. With these further conditions, a simple iteration method could give a solution to yield at least the equilibrium constant, K. To the best of our knowledge, this specific method may not have been used explicitly in the case of identical donor and acceptor molecules. We will attempt to use Equation [5] for the evaluation of nifedipine's tendency for self-association in homogeneous solution.

2.1.2 First Derivative Spectroscopy

The first and second derivatives as well as higher derivatives of an absorption spectrum may be calculated as a function of the wavelength (λ). In general, by differentiation of the Beer-Lambert Law, Equation [6] is obtained:

$$\frac{d^n A}{d\lambda^n} = \frac{c \cdot d \cdot d^n \varepsilon}{d\lambda^n} \qquad [6]$$

In Equation [6], it is clear that the value $d^nA/d\lambda^n$ is directly proportional to the concentration. Derivative spectroscopy was introduced in the 1950s, and some UV-VIS spectrometers are equipped with the capability to display directly $d^nA/d\lambda^n$ (usually, n=1, 2, 3 or 4).

Derivative spectroscopy has several applications, both in qualitative and

quantitative analysis. For instance, the determination of concentration can be facilitated in some multicomponent systems where light-scattering occurs. O'Haver and Green have detailed the errors involved in applying the method to the quantitative analysis of mixtures (O'Haven and Green, 1976). In light scattering systems such as in turbid solutions and in some biological systems, there can be significant baseline sloping in simple absorption spectra due to light scattering. It was found that first and second derivative spectra derived from simple differentiation [7] could eliminate the effect of light scattering because the baseline slope is often constant over limited wavelength domains for most particle scattering systems (O'Haven and Green, 1976; Talsky, 1979).

$$A(\lambda) = A_N(\lambda) + A_S(\lambda) = A_N(\lambda) + \text{linear function}$$

$$dA(\lambda)/d\lambda = dA_N(\lambda)/d\lambda + \text{constant} \qquad [7]$$

Here, A_N is the normal absorbance from the solution and A_S is the constant sloping baseline caused by scattering. In the above equation, the constant can be subtracted to give the desired result. Usually, the UV-VIS derivative spectral method will not improve the sensitivity of the absorption measurement, but it can give an improvement when a sloping baseline occurs in a UV-VIS spectrum.

UV-VIS spectroscopy has been applied in the quality control of nifedipine (Kracma *et al*, 1988). A simple and rapid method was reported for the determination of NTSP in nifedipine preparations by second derivative UV-VIS spectrophotometry (Carlucci *et al*, 1990). In the present work, the liposome dispersions act as a light-scattering system and cause spectral baseline sloping. First or second derivative spectrometry may be one of the choices to determine the concentration of nifedipine in our samples.

2.2 EPR SPECTROSCOPY

2.2.1 Fundamentals

Electron paramagnetic resonance (EPR), which was developed in 1945, is still the best spectroscopic method to detect or characterize free radicals or molecules possessing one or more unpaired electrons. An EPR spectrometer basically consists of a radiation source (microwave klystron source including a microwave bridge), a sample absorption cell (microwave cavity with magnet) and a diode detector (Figure 2.2.1). Usually, a 100 kHz modulation of the magnetic field with phase sensitive detection at the same frequency is employed in an EPR spectrometer, and a first derivative spectrum is displayed (Knowles *et al*, 1976).

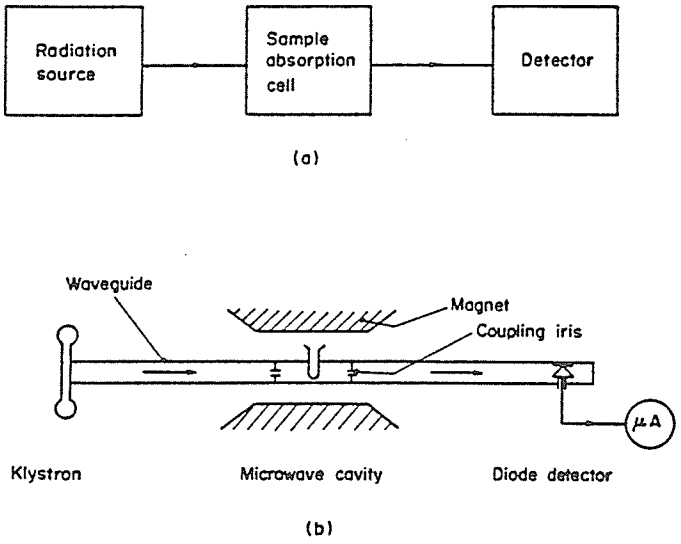

Figure 2.2.1 Schematic layout of an absorption spectrophotometer (a) and simple form of an EPR absorption spectrometer (b) (Knowles *et al*, 1976, page 209).

An unpaired electron with a net magnetic moment has a spin of either +1/2 or -1/2, and it can align itself either parallel or antiparallel to the external magnetic field. Magnetic resonance absorption can be observed when the unpaired electron absorbs a microwave photon which has an energy equivalent to the difference between the two quantized electron spin energy levels, thus provoking a change in the orientation of the electron spin. Usually, the assignment and EPR spectral interpretation for a given free radical can be characterized by *g* factors and hyperfine splitting constants *(A)* for either isotropic or anisotropic spectra.

1) *g* Factor

The absolute magnetic field position of the lines of an EPR spectrum is characterized by the *g* factor, $g=h\nu/\beta H_r$, where H_r is the external magnetic field (gauss) at resonance, ν is the microwave frequency (Hz), h is the Planck's constant and β is the Bohr magneton. The theoretical *g* value is 2.0023 (g_e=2.0023) for a completely free electron in a vacuum. Deviations from the free electron *g* factor can give some information about the chemical structure of the free radical. The isotropic *g* factors observed for nitroxide free radicals (g = 2.0050 - 2.0060), for instance, tend to be significantly higher than that of the free electron *g* factor.

As a quantity characteristic of the molecule in which the unpaired electrons are located, the g factor can be used to identify the origin of an unknown signal. By comparison with well known free radicals, the g factor of an unknown free radical can be determined, based on Equation [8] (Wertz and Bolton, 1972, page 465; Swartz *et al*, 1972, page 100).

$$g_x = \frac{g_s \cdot H_s}{H_x} = g_s \cdot \left(1 + \frac{\Delta H}{H_s} \right) \qquad [8]$$

Here, g_x is the unknown g factor; g_s is the g factor of the standard used; H_s and H_x are the resonant magnetic fields for standard and unknown, respectively; $\Delta H = H_s - H_x$. As long as ΔH is small (less than 1 percent), compared with the magnetic field H_s at the centre of the standard EPR spectrum, Equation [8] can be used for the determination of the g factor of the unknown. Mn^{2+} ion in a solid inorganic matrix ($g_s = 2.0012 \pm 0.0002$) is often used as a standard for the measurement of unknown g factors. SrO powder usually contains sufficient Mn^{2+} to give a strong EPR signal with very narrow lines (~1.5 G).

2) Hyperfine splittings

The lines in an EPR spectrum can be split by interaction of the paramagnetic electron with the magnetic moments of neighbouring nuclei. The interaction of an unpaired electron with a nuclear magnetic moment is defined as the nuclear hyperfine interaction which greatly enhances the application of the EPR technique to the identification of free radicals.

The hyperfine splitting of the energy levels can be given by *a* (in gauss), and the resonant field for each line can be derived from Equation [9] for the interacting electron-nuclear spin system. For example, the nitroxide free radical can have one electron spin interacting with one nitrogen nuclear spin.

$$H_r = H' - aM_I \qquad [9]$$

For the nitrogen nucleus, $M_I = \pm 1, 0$ are the nuclear spin quantum numbers, *a* is known as the hyperfine splitting constant, and H' is the resonant field when $a = 0$. The hyperfine splitting constant can be obtained by measuring the separation between lines in simple spectra or by spectral analysis and simulation for more complicated spectra. The number of hyperfine lines from a particular nucleus depends on the nuclear spin (I), and this

number is given by $(2I + 1)$. Therefore, a proton with $I = 1/2$ gives two lines while a ^{14}N nucleus with $I = 1$ gives rise to three hyperfine lines. Usually, ^{13}C hyperfine structure will be unobservable in most biological systems because of the low ^{13}C natural abundance; and the common ^{12}C isotope has a zero nuclear moment.

Figure 2.2.2 shows the hyperfine splittings for a nuclear spin with $I = 1$ (e.g., ^{14}N) as a function of the magnetic field. The hyperfine splittings in the EPR spectrum clearly mirror the energy level splittings, and the number of lines is characteristic of the value of the nuclear spin (I) (Knowles *et al*, 1976, page 175). Here, A is defined as the hyperfine splitting constant with units of energy (e.g., ergs).

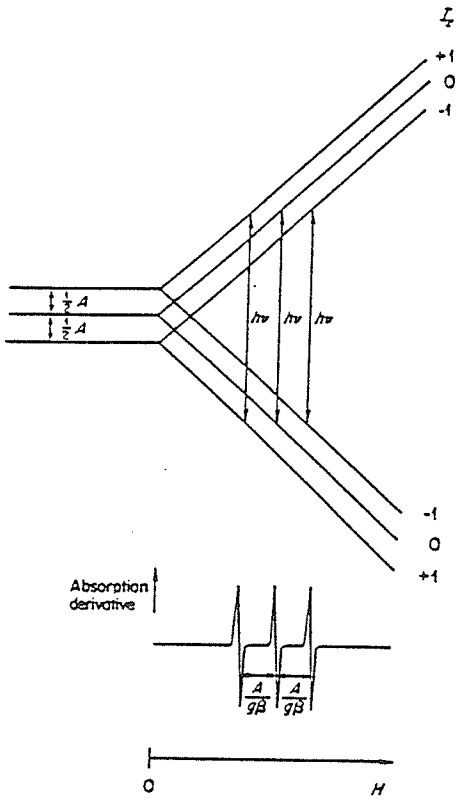

Figure 2.2.2 Hyperfine splitting energy levels as a function of magnetic field for an electron spin interacting with ^{14}N with nuclear spin $I = 1$. (Knowles et al, 1976, page 175)

3) Isotropic and anisotropic spectra

Anisotropic g factors and anisotropic hyperfine interactions are observed when a free radical is immobilized relative to the strong magnetic field. The EPR lines are now dependent on the orientation of the molecular axes relative to the magnetic field. This is one important feature of immobilized EPR spectra. For instance, when the radical is restricted to a single crystal host, the spectral anisotropy is observed for fixed orientations of the principal molecular axes (x,y z) of a free radical relative to the magnetic field; and three principal g factors (g_{xx}, g_{yy}, g_{zz}) and hyperfine constants (A_{xx}, A_{yy}, A_{zz}) can now be measured. In some cases, the molecular system is axially symmetric and then has the principal values: $g_{\parallel} = g_{zz}$, $g_{\perp} = g_{xx} = g_{yy}$ and $A_{\parallel} = A_{zz}$, $A_{\perp} = A_{xx} = A_{yy}$.

For the specific case of free radicals in solutions of low viscosity, no anisotropy can be seen because of the rapid molecular tumbling. In this case, we observe an isotropic spectrum with narrow lines and well-resolved hyperfine splittings; and the isotropic or average g factor is observed:

$$g_{av} = (g_{xx} + g_{yy} + g_{zz})/3 \qquad [10]$$

Nitroxide radicals are of some interest in the present study, and we will briefly describe their potentially anisotropic EPR spectra. The nitroxide unpaired electron is partly localized in the *p* orbital on nitrogen (e.g., Figure 2.2.3a) in the pictured symmetric molecule. Figure 2.2.3*b,c* shows two possible anisotropic spectra for this nitroxide when it is immobilized in different media while Figure 2.2.3d shows the isotropic spectrum for a freely rotating molecule.

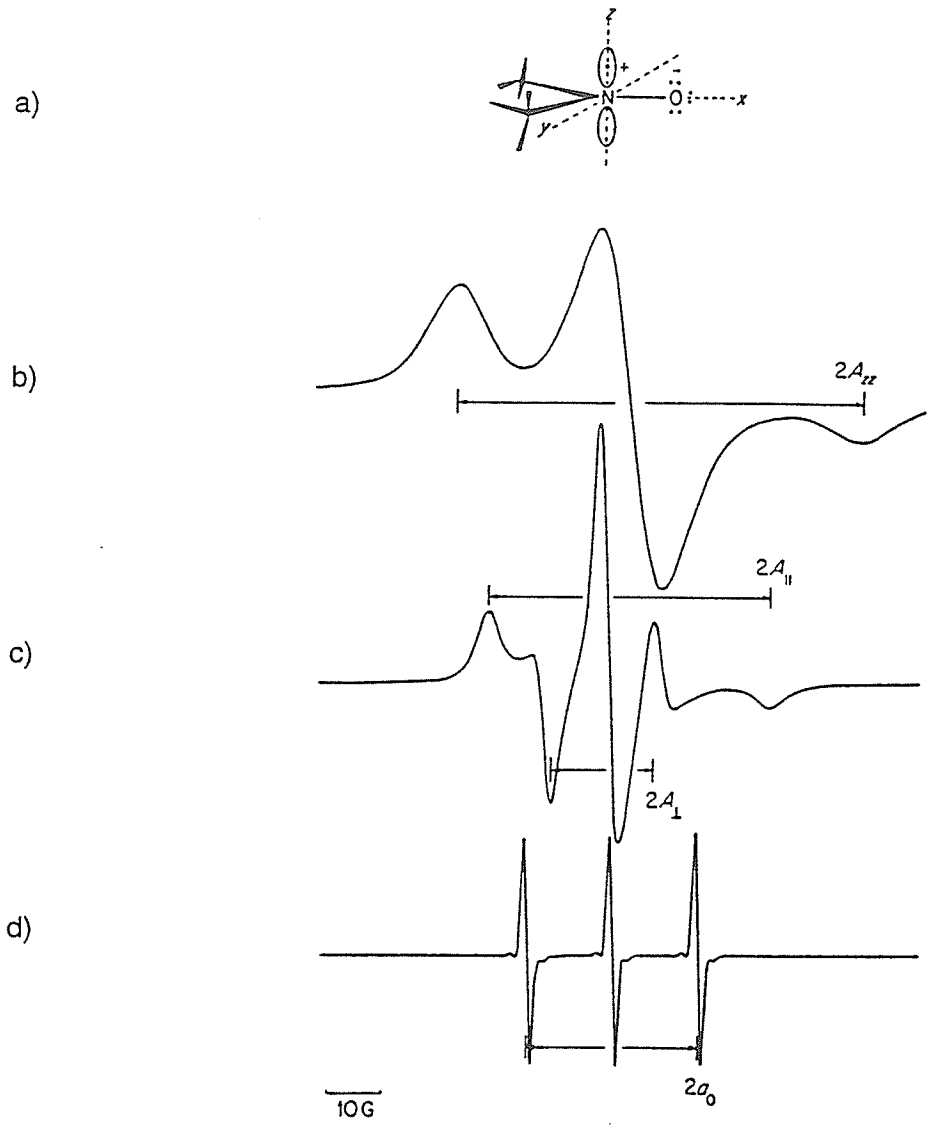

Figure 2.2.3 Electronic structure of a nitroxide radical and its anisotropic EPR spectra under various conditions of motion (Knowles *et al*, 1976, page 185).

(a) Electronic structure of nitroxide radical; (b) Powder spectrum from a nitroxide randomly and rigidly oriented in frozen solution; (c) Lipid dispersion spectrum from a nitroxide spin label in a randomly oriented lipid dispersion; (d) Isotropic spectrum from a non-viscous solution.

2.2.2 Spin Trapping Technique

Because of their extremely short lifetimes, many free radicals cannot be directly detected by EPR. The spin trapping technique has been extensively applied in detecting such free radicals both *in vivo* and *in vitro* (Evans, 1979; Janzen and Haire, 1990). This technique involves the addition of the reactive free radical to a diamagnetic 'spin trap' to form a more stable free radical which can be detected with EPR.

Usually spin traps can be divided into two categories: nitroso compounds and nitrone compounds. Nitroso spin traps give more distinctive hyperfine splitting constants and more information about their trapped radicals because the reactive free radical adds directly to the nitrogen atom of the spin trap and has a strong interaction with the ^{14}N nucleus with $I = 1$. However, the adducts of free radicals with nitroso spin traps are often chemically unstable, particularly if the free radicals are oxygen-centred (Evans, 1979). The adducts of nitrone spin traps are formed from reactive free radicals adding to the nitrone carbon atom of the spin traps, and this provides less direct spectral information about the trapped radical. However, the better chemical stability of the resulting spin adducts is the main advantage for using the nitrone spin traps.

The spin trapping methodology has proven to be a useful tool for studies in biological systems (Swartz *et al*, 1972). Figure 2.2.4 shows the chemical structures of four important spin traps and some radical adducts. As mentioned before, NTSP was found to be effective as a spin trap, particularly as an endogenous spin trap in the nifedipine photochemistry (Stasko *et al*, 1994). We simply note that NTSP is similar to 2-methyl-2-nitrosopropane (MNP) of Figure 2.2.4 because both are nitroso-type spin traps.

		Spin-trap	Adduct
I.	a) NTSP:	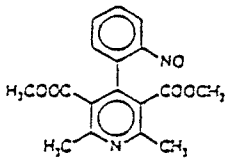	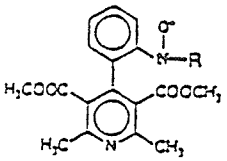
	b) MNP	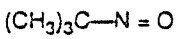	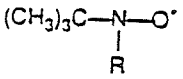
II.	c) PBN	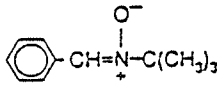	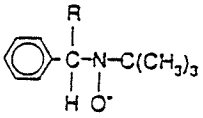
	d) DMPO	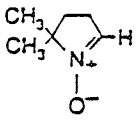	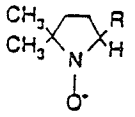

Figure 2.2.4 Chemical structures of some important spin traps and their adducts with reactive free radicals (R·).

(I: nitroso spin traps; II: nitrone spin traps; a. NTSP: Dimethyl 1,4-dihydro-2,6-dimethyl-4-(o-nitrosophenyl)-3,5-pyridinedicarboxylate; b. MNP: 2-methyl-2-nitrosopropane; c. PBN: phenyl-N-tert-butylnitrone; d. DMPO: 5,5-dimethyl-1-pyrroline N-oxide.)

PART III. EXPERIMENTAL

3.1 MATERIALS AND INSTRUMENTS

3.1.1 Materials

01. Nifedipine (NFDP)

    M.W. 346.3; 10 g pkg, Sigma Chemical Co., USA; stored in the freezer at -10°C.

02. L-α-Phosphatidylcholine, Dimyristoyl (C14:0) (DMPC)

    M.W. 677.9; 1 g pkg, 99+%, Sigma Chemical Co., USA; stored in the freezer at -10°C.

03. DL-α-Phosphatidylcholine, Di-O-hexadecyl (DHPC)

    M.W. 706.1; 100 mg pkg, 99%, Sigma Chemical Co., USA; stored in the freezer at -10°C.

04. 5,5-Dimethyl-1-pyrroline N-oxide (DMPO)

    M.W. 113.16; 1 g pkg, Sigma Chemical Co., USA; stored in the freezer at -10°C.

05. N-*t*-Butyl-α-phenylnitrone (PBN)

    M.W. 177.2; 5 g pkg, Sigma Chemical Co., USA; stored at room temperature.

06. 4-Hydroxyl-2,2,6,6-tetramethylpiperidin-1-yloxy radical (Tempol)

    M.W. 172.25; Sigma Chemical Co., USA; stored at room temperature.

07. Albumin, bovine (BSA)

    M.W. 66,000; initial fraction by cold alcohol precipitation, Fraction V, 96-99% albumin; 10 g pkg, Sigma Chemical Co., USA; stored in a desiccator and kept at 2-5°C.

08. Albumin, human (HSA)

    Fraction V, 96-99% albumin; 1 g pkg, Sigma Chemical Co., USA; stored in the freezer at -10°C.

09. N-(2-Hydroxyethyl)piperazine-N'-2-ethanesulfonic acid sodium salt (HEPES)

M.W. 260.3; 100g pkg, Sigma Chemical Co., USA; stored at room temperature.

10. Silica gel plates for TLC

Coating silica gel, 250 μM layer, fluorescence-UV_{254}; backing polyester 20 x 20 cm; Whatman Ltd., England.

11. Chloroform

spectrophotometric grade; 500 ml pkg, Mallinckrodt, USA; stored at room temperature.

12. Benzene, Methanol and 1-Octanol

analytical reagent; 4 l pkg, Mallinckrodt, USA; stored at room temperature.

14. Ethanol (anhydrous)

25 l pkg, Commercial Alcohol Inc., Canada; stored at room temperature.

15. 1-Butanol

Chromatographic reagent; 500 ml pkg, the British Drug Houses Ltd., England; stored at room temperature.

16. Deionized and quartz-distilled water.

3.1.2 Instruments

01. Varian Associates Model E-12 Electron Paramagnetic Resonance Spectrometer with:
    a) Model 4111 Temperature Controller, Bruker, Germany;
    b) Model 1180 Computer, Nicolet Instrument Co., USA.;
    c) Model 2090 Transient Recorder, Nicolet Instrument Co., USA.;
    d) Tungsten-halogen lamp with a fibre optic light-pipe: Model 180; 200 W; Dolan-Jenner Industries, Inc., USA; always filtered with a Schott BG-38 cut-off light filter.

02. Shimadzu UV-260 UV-Visible Recording Spectrophotometer, Shimadzu Corporation, Japan, with the light sources of Deuterium (D_2) lamp and Halogen (WI) lamp (50W) (Lamp change-over wavelength range: 322–392 nm).

03. Nuclear Magnetic Resonance Spectrometer, ^1H 300 MHZ, Bruker, Germany

04. Type 37600 Mixer, Barnstead/Thermolyne, USA.

05. Extruder, Lipex Biomembranes, Inc.(Canada), with
25 mm (0.1 μm pores) Polycarbonate Membranes, Nuclepore Co., USA.

06. Mettler AE 160 Balance, Mettler Instrument Co., USA.

07. Fisher Accumet Model 620 pH Meter, Fisher Scientific Company, USA.

08. Refrigerated Centrifuge Model B-20, International Equipment Co., USA.

3.2 PREPARATIONS AND INCORPORATIONS

1) 20 mM HEPES/150 mM NaCl buffer:

The amount of 5.206 g (0.020 mol) HEPES (M.W. 260.3) and 7.768 g (0.15 mol) sodium chloride (M.W. 58.45) were weighed and dissolved with 900 ml of doubly distilled water by stirring in a 1000 ml beaker. The pH value was adjusted with 2N HCl to 7.40 ± 0.01 using a Fisher Accumet pH meter (Model 620). The solution was transferred to a 1 litre volumetric flask and made up to 1,000 ml. Finally, the pH of the solution was readjusted to the required range and stored in container for use.

2) 20 mM HEPES buffer:

The solution was prepared in a similar way to the above without the addition of sodium chloride.

3) **3 M 5,5-Dimethyl-1-pyrroline-N-oxide (DMPO)/HEPES buffer stock solution:**

The amount of 0.345 ml (0.350 mg, 3.0945 mmol) of DMPO (M.W. 113.16, *d* 1.015) was diluted to 1.032 ml by adding 0.687 ml of HEPES buffer (without sodium chloride). The concentration was determined by ultraviolet spectrometry (ε_{225nm}=7.22 x 10^3 M^{-1} cm^{-1}) (Floyd *et al*, 1984) and the solution was stored in the freezer at -10°C for use.

4) **1 M N-tert-Butyl-α-phenylnitrone (PBN)/EtOH stock solution:**

The amount of 177.2 mg (1 mmol) PBN (M.W. 177.2) was dissolved in a 1-ml volumetric flask in a small amount of ethanol (95%, v/v). The solution was made up to 1 ml and stored in the freezer at -10°C for use.

5) **4-Hydroxyl-2,2,6,6-tetramethylpiperidin-1-yloxy radical (Tempol) standard solution:**

i) The amount of 8.6 mg (5.0 x 10^{-5} mol) Tempol (M.W. 172.25) was dissolved in HEPES-NaCl buffer (pH 7.4), diluted to 25 ml in a volumetric flask and a 2.0 mM solution was obtained. The 100 μM Tempol/HEPES-NaCl buffer solution was prepared by transferring and diluting 0.5 ml of the 2.0 mM solution to 10 ml in a 10-ml volumetric flask. The prepared final solution was used within four hours of preparation.

ii) The amount of 0.185 mg Tempol was dissolved in anhydrous ethanol in a 10 ml volumetric flask and a 0.11 mM ethanol solution of Tempol was obtained.

iii) The amount of 0.290 mg Tempol was dissolved in benzene in a 10 ml volumetric flask and a 0.17 mM benzene solution of Tempol was obtained.

6) 100 mg/ml Lipid/chloroform stock solutions:

Solutions of lipids DMPC, DHPC in chloroform were prepared. For example, 1.0 g (1.475 mmol) DMPC (M.W. 677.9) was dissolved in a 10-ml volumetric flask in a small amount of chloroform. The solution was made up to 10 ml and stored in the freezer at -10°C for use.

7) 10 mM Nifedipine/chloroform stock solution:

The amount of 34.6 mg (0.10 mmol) nifedipine (M.W. 346.3) was dissolved in a 10 ml volumetric flask in a small amount of chloroform and made up to 10 ml. The solution of 10 mM nifedipine in chloroform was stored in the freezer at -10°C before use.

8) Albumin/HEPES-NaCl buffer solution:

Stock solutions of 3.5%, 14% albumin (bovine, BSA) and 14% albumin (human, HSA) were prepared. For example, the solution of 14% BSA in the buffer was obtained by dissolving 140 mg BSA and diluting it to 1 ml in a 1-ml volumetric flask with 20 mM HEPES/150 mM NaCl buffer. The solutions were used immediately.

9) Preparation of 2,6-dimethyl-4-(o-nitrosophenyl)-3,5-dimethylpyridinedicarboxylate (NTSP)

A 20 ml volume of the 50 mM Nifedipine/CH_2Cl_2 solution was exposed to the filtered tungsten lamp at the distance of 15 cm at a fixed intensity of 70% of the maximum during 24 hrs. The reaction was monitored by TLC silica gel plates (fluorescent-UV_{254}) with the developer of petroleum ether/methylene chloride/methanol (1:1:0.1) until only one spot showed on the TLC plate. After evaporation of the solvent, a yellow-greenish crystalline

compound was obtained and dried under vacuum for up to 8 hours. NMR ^1H and UV-VIS spectra characterized the compound as NTSP·H_2O (NMR ^1H: δ1.60-1.65 2H, broad singlet; δ2.67 6H, singlet; δ3.38 6H, singlet; δ6.54-6.57 1H, doublet; δ7.41-7.44 1H, singlet; δ7.50-7.52 1H, singlet; δ7.69-7.74 1H. UV-VIS: 680-860 nm broad absorption).

10) Incorporation in multilamellar vesicles (MLVs):

Multilamellar vesicles containing nifedipine or NTSP were prepared by vortexing the solution of lipid in HEPES/NaCl buffer. For example, 350 μl 100 mg DMPC/chloroform solution was mixed with 50 μl 10 mM nifedipine/chloroform solution. The mixture was evaporated in a test tube under argon purge to form dry lipid films to which 1 ml HEPES/NaCl buffer (pH 7.4) was added. The lipid film-buffer solution was vortexed (1 min X 10) and alternately warmed (1.5 min X 10 at 37°C) in the water bath. Multilamellar vesicles were obtained from this procedure. A blank sample containing only lipids was also prepared as a reference.

11) Incorporation in large unilamellar vesicles (LUVs):

Large unilamellar vesicles containing nifedipine or NTSP were prepared from multilamellar vesicles with the extrusion technique by using Nuclepore polycarbonate filters (25 mm in diameter with pore sizes of 0.1 μm) and an Extruder of a 10 ml capacity equipped with a thermobarrel accessory to control the temperature during extrusion. For example, the prepared multilamellar vesicles were extruded by using a suitable argon pressure (10 times at 37°C) and kept warm (1.5 min X 10 at 37°C water bath) during the extrusion. The concentrations of nifedipine incorporated in the LUVs were determined by UV-visible spectra. The LUVs were kept at ambient temperature with protection from light

and used as soon as possible. Blank samples containing only lipids were also prepared as reference material.

12) Nifedipine incorporation in albumin aqueous solutions:

Nifedipine was incorporated in hydrated bovine and human serum albumins also by a vortexing method. For instance, a 200 μl volume of the 15 mM nifedipine/chloroform solution was evaporated in a 5-ml test tube under argon purge to form a dry film to which 0.5 ml of the 14% (w/v) albumin aqueous solution was added. The mixture was vortexed up to 15 minutes and centrifuged up to 3 minutes at 2,000 rpm. The upper solution was transferred to another tube and the concentration was determined by the UV-visible spectrophotometer. The solutions were used as soon as possible, and blank samples were also prepared as references.

3.3 QUANTITATIVE ANALYSIS

3.3.1 UV-VIS Spectroscopy

Nifedipine and its photodegradation products have strong UV-VIS absorption bands because of the presence of the phenyl, 1,4-dihydropyridine and pyridine chromophores in these molecules. A Shimadzu UV-260 UV-VIS recording spectrophotometer was used with 1 mm pathlength quartz cells for the measurement of concentration in all samples and for the kinetic study of the nifedipine photochemistry. The baseline was adjusted relative to air. All the UV-VIS spectra were recorded employing reference samples containing no nifedipine. For instance, the spectra of nifedipine incorporated in vesicles were recorded by using blank vesicle samples without nifedipine as a reference to minimize the sloping baseline in the absorption spectra caused by the strong light

scattering of these lipid dispersions.

1) Measurement of concentration

In order to determine the concentrations of nifedipine or NTSP in all samples, we first measured the molecular extinction coefficients (ε) of nifedipine and NTSP and calibrated the concentration dependence of the first derivative spectral absorptivity (A') in ethanol solutions.

The molecular extinction coefficients (ε) of nifedipine and NTSP were determined by their standard solutions of 1.00 mM in ethanol and chloroform respectively. The standard solutions were prepared as in the following: 17.3 mg (0.05 mmol) of nifedipine or NTSP·H_2O were dissolved in a 50 ml volumetric flask in either ethanol or chloroform. The standard solutions were used directly to measure the absorptivities of these samples at precise wavelengths. The molecular extinction coefficients (ε) were calculated based on the Beer-Lambert Law.

The concentration dependence of the first derivative spectral absorptivity (A') of nifedipine was calibrated by a series of standard solutions in ethanol at different concentrations. The standard solutions were prepared by diluting the 10 mM nifedipine/EtOH stock solution (0.10 mmol in 10 ml volumetric flask) to the concentrations of 5, 2.5, 1, 0.5 mM. The first derivative spectral absorptivities of the standard solutions at 400 nm were recorded.

It is important to know how quickly nifedipine is converted under the typical experimental conditions used in the EPR work. Therefore, we used the calibrated concentration dependence of the first derivative UV-VIS spectral absorptivity in the kinetic analysis of the nifedipine photochemistry. Specifically, we irradiated the solution of 2.5

mM nifedipine/EtOH and the dispersions of nifedipine/LUVs with the same filtered light source at the same light intensity (70% of the maximum light output) at a distance of 15 cm. The UV-VIS spectra of the irradiated samples at different time intervals were recorded for further analysis.

2) Measurement of self-association

The self-association of nifedipine was studied by UV-VIS spectroscopy where ethanol, 1-butanol and 1-octanol were used as solvents. The concentrations of nifedipine in the solvents varied in the range of 1 mM to 40 mM. In the case of the 1 mM nifedipine concentration, a 1 mm pathlength quartz cuvette was used for absorbance measurements, while at higher nifedipine concentrations, a stainless steel cuvette with a very short pathlength was used.

The pathlength of the steel cuvette was calibrated by measuring the absorbance of the 1 mM nifedipine solution in anhydrous ethanol at 235 nm. We then applied the result of the measured molar extinction coefficient (ε) (from Table 4.1.1), $\varepsilon_{235\ nm}$ = 19150 $(M \times cm)^{-1}$, in the Beer-Lambert equation:

$$A = \varepsilon dc,$$

Here, $A_{235\ nm} = 0.094$

Therefore, $d = A/\varepsilon c$

$= 0.094 / 19150\ (M \times cm)^{-1} \times 1.0 \times 10^{-3}\ (M)$

$= (4.91 \pm 0.05) \times 10^{-3}\ (cm)$

3.3.2 EPR Spectroscopy

Electron Paramagnetic Resonance (EPR) spectra of the free radicals or spin adducts produced by the photolysis of nifedipine were recorded with a Varian Associates Model E-12 EPR spectrometer which was interfaced with a Nicolet Instruments Model 1180 computer. A Bruker Model 4111 Temperature Controller was employed to control the sample temperatures in the cavity of the EPR spectrometer.

Usually a sample of 60 µl was held in a 0.8 mm inner diameter capillary tube which was put into a 4 mm outer diameter one-end sealed tube. In some cases, two 60 µl samples were held in side-by-side teflon tubes which were put into a 4 mm outer diameter unsealed tube. Besides the capillary holder, a 2.4 mm inner diameter one-end sealed suprasil tube was used for the measurement of nifedipine/organic solvent systems with an active sample volume of about 135 µl. The samples in thin walled teflon tubes were exposed to a steady stream of either air or argon, and complete gas exchange through these teflon walls occurred in less than 30 seconds. Furthermore, it was verified that there were no bubbles in the measured samples in the EPR cavity. The spectral output profile of the light source which provided mostly visible and some UV-A (330 - 400 nm) light as filtered by a Schott BG-38 filter is shown in Figure 3.3.1 (Dr. McIntosh, private communication).

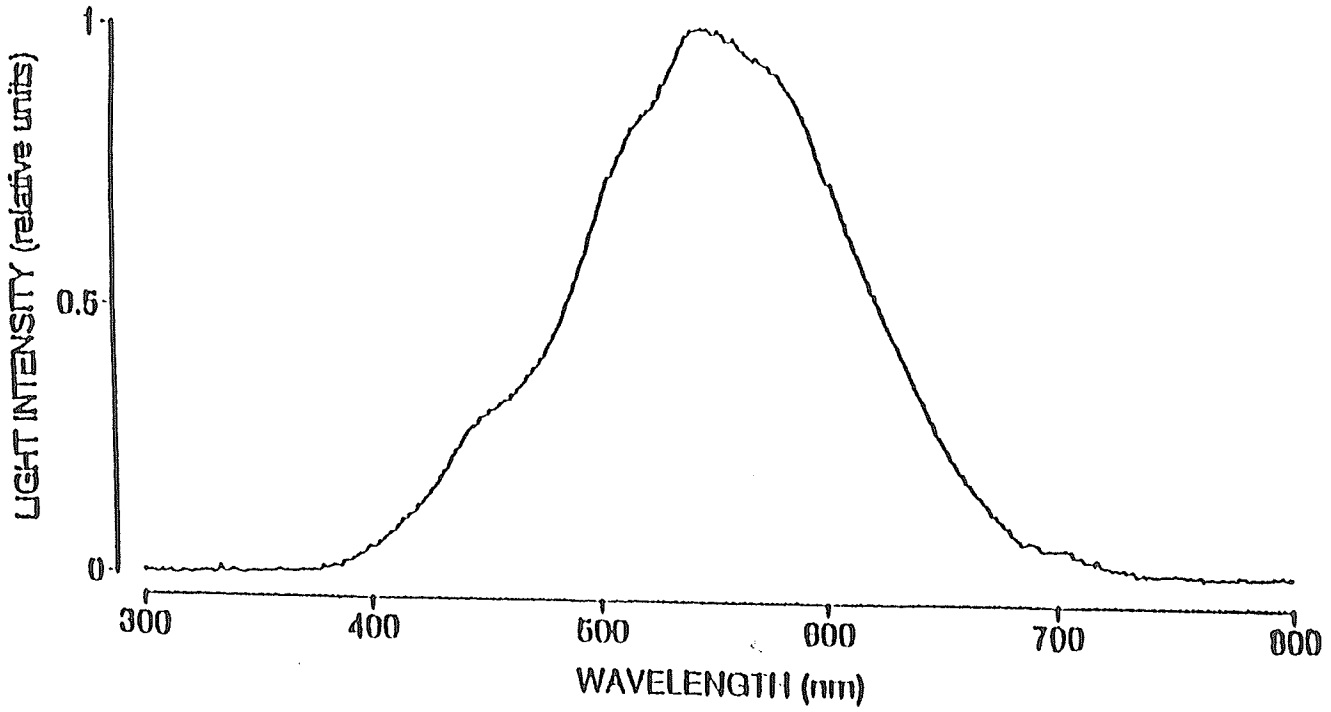

Figure 3.3.1 Spectral output profile of the tungsten-halogen-lamp filtered by a Scholt BG-38 filter (Dr. McIntosh, private communication).

1) Instrumental parameters:

The EPR spectra were recorded with several similar instrumental conditions, but a typical condition for EPR spectra measured in LUV dispersions was:

modulation amplitude	:	0.5 Gauss;
microwave power	:	10 mW;
receiver gain	:	2×10^3;
time constant	:	0.10 second;
scan range	:	100 Gauss;
field set	:	3215 Gauss;
cavity temperature	:	37°C;
light source	:	visible and UV-A light at a distance of 15 cm;
light filter	:	Schott BG38, AM-7181;
atmosphere	:	air/argon

2) Spin trapping assay:

As described in the Introduction, the nitroso group in the nitrosophenylpyridine (NTSP) molecule is capable of spin trapping; and this molecule is derived from the photochemistry of nifedipine (Misik *et al*, 1991). In this work, the EPR spectra derived from illuminated nifedipine samples were measured without the addition of exogenous spin traps. As a confirmation of relative spin trapping efficacy, the spin trap PBN was added to some samples in our study. The concentration of PBN was usually 50 mM in the measured samples. The spin traps were added to the samples immediately before the EPR spectral measurements. For example, the sample of nifedipine/LUVs and 50 mM

PBN was made by mixing 5 μl 1 M PBN-Ethanol solution and 95 μl nifedipine LUVs in a test tube. About 60 μl of this sample was introduced into a capillary tube for immediate spectral analysis during photolysis in the EPR cavity.

3) Spectrum acquisition:

EPR spectra of all the samples in the present study were recorded by the standard operating procedure of field sweep time averaging. The spectrometer was placed under computer control which slowly swept the 100 G domain of the magnetic field in about fifty seconds. The EPR spectra were acquired as the sum of repetitive multiple sweeps of the magnetic field for each sample.

Isotropic spectral simulations were also performed for several free radicals by using the NTCESR computer program written by Nicolet Technology Corporation (Madison, WI). The spectral simulation routine can simulate EPR spectra of free radicals with couplings to many magnetic nuclei. This method is helpful to clarify the possible structures for a given measured EPR spectrum. To determine the structures of the observed radicals in this work, the splitting constants were obtained by analyzing the recorded spectra. According to these measured splitting constants, some models for the analyzed radicals were then proposed and were further confirmed by spectral simulation.

4) Determination of radical concentration:

The double integrals of the EPR spectra were also calculated in order to determine concentrations of the detected free radicals, and these integrations were also performed on the measured spectra with the NTCESR program. Normally, the double integral value (A) of an EPR spectrum is proportional to radical concentration (C), receiver gain (G) and

scan number (N). If all other conditions are unchanged, the ratio of A/(C x G x N) should be the same for the same type of radical. If s and m are used respectively as subscripts to represent a standard of known concentration and a measured sample of unknown concentration, then we obtain

$$\frac{A_s}{C_s G_s N_s} = \frac{A_m}{C_m G_m N_m} \qquad [11]$$

$$C_m = \frac{A_m G_s N_s}{A_s G_m N_m} C_s \qquad [12]$$

Here, the double integral value, A_s for the standard can be defined conveniently to be a reference value, and all subsequent calculations of the double integral A_m will be relative to this definition. In order to make this comparison valid, it is extremely important that the sample and instrumental conditions such as modulation amplitude, microwave power, temperature, and solvent or medium are virtually identical for the two compared samples.

In our work, 4-hydroxyl-2,2,6,6-tetramethylpiperidin-1-yloxy (Tempol) was chosen as the standard nitroxide radical in solutions of known concentrations. The solution of 100 μM Tempol in pH 7.4 HEPES/NaCl buffer was chosen as the standard sample of nitroxide free radicals for the calibration of radicals produced in liposomes and in proteins (both primarily aqueous samples). The A_s value of the standard solution for instrumental conditions of modulation amplitude 0.8 Gauss, microwave power 10 mW, receiver gain 2 x 10^3, temperature 27°C and purging with air was defined as 888. All double integrals of photochemically produced radicals were carefully compared with this standard value taking into account any difference in receiver gain. The results of these double integral calculations are listed in Appendix C. Finally, by comparing the double integrals of new

samples with the double integral data of the standard solution under identical instrumental conditions, the concentrations of nifedipine nitroxide free radicals in liposomes and in proteins were determined. Under routine conditions, the double integral method usually gives a measured radical concentration with a precision of ± 15 %; and under ideal conditions, the precision can be about ± 10%.

The calibration of radical concentrations was also performed in 0.168 mM Tempol/benzene solution and in 0.107 mM Tempol/ethanol solution under the conditions: modulation amplitude 0.5 G, microwave power 10 mW, cavity temperature 25°C, sample of 135 μl volume in a suprasil tube, time constant 0.1 second, but receiver gain $2x10^2$ for a benzene solution and $2x10^3$ for an ethanol solution. The A_s values for these samples were defined as 100 for each standard solution. The measured samples in the same solvents were analyzed immediately after the definition of the corresponding standard solution.

PART IV. RESULTS

4.1 CONCENTRATION DETERMINATION

4.1.1 Calibration of Concentrations

To develop a method to measure the concentrations of nifedipine and NTSP (present in illuminated samples), we measured the UV-VIS zero-order and first-order derivative spectra (Figure 4.1.1) and their respective molecular extinction coefficients (ε) (Table 4.1.1) for both nifedipine and NTSP solutions. In ethanol solution, nifedipine has a sharp maximum in its absorption spectrum close to 235 nm and a broad maximum around 360 nm. NTSP has absorption maxima at 220 nm, 280 nm and 310 nm in ethanol solution. The gradual decrease in absorbance at 360 nm during the photolysis of a nifedipine solution was attributed to the aromatization of the 1,4-dihydropyridine ring and the formation of NTSP. We found that NTSP has almost no optical absorption at wavelengths greater than 380 nm, and furthermore, nifedipine shows a characteristic minimum in the first derivative absorption spectrum near 400 nm which we used to determine the concentrations of nifedipine present in our samples.

It is clear that the partitioning of nifedipine either to binding sites on albumin proteins or into the bilayer membranes of lipid dispersions can cause changes in measured extinction coefficients which are essential for precise concentration measurements. It is also important to point out that the solubility of nifedipine in water is extremely slight (see next Section 4.1.2, page 52), and the measured octanol/water partition coefficient is about 10^4:1 (Syed, 1989). Therefore, for the protein and lipid vesicle samples of this work, it is reasonable to conclude that nifedipine was respectively extensively bound to albumin proteins or essentially all located in the lipid bilayer membranes in the vesicle samples. It is extremely difficult to measure precise extinction coefficients in these two types of samples, and we chose to calibrate the nifedipine concentrations with reference to the measured extinction coefficients in ethanol solution as a mimic of the hydrophobic binding sites of nifedipine in the hydrated albumin proteins

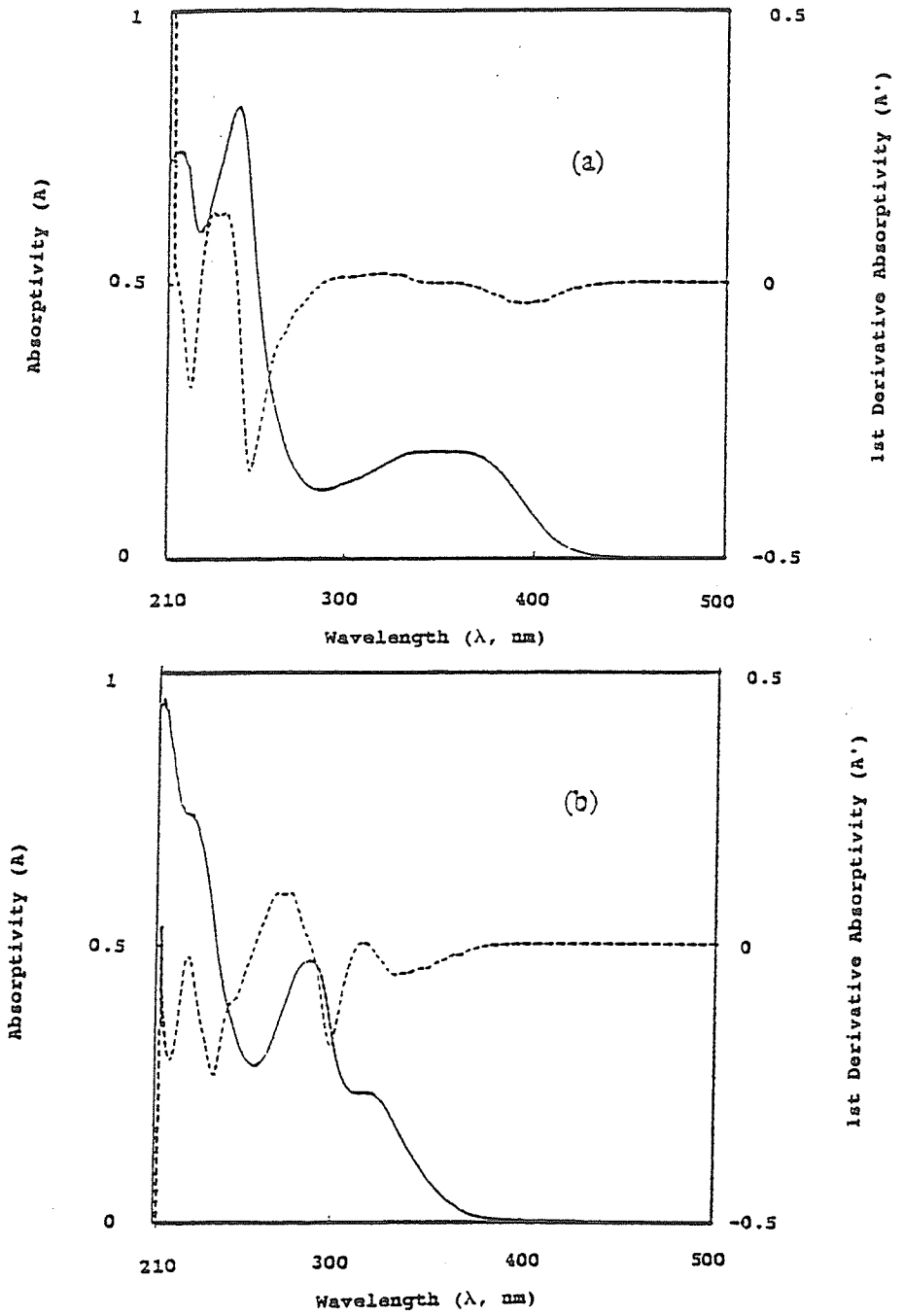

Figure 4.1.1 UV-VIS absorption spectra (shown in solid line) and first derivative absorption spectra (shown in dotted line) of nifedipine (a) and NTSP (b) in ethanol solutions

Table 4.1.1. Spectral molar extinction coefficients (ε)

for nifedipine and NTSP solutions

λ (nm)	Extinction Coefficient, ε $(M \cdot cm)^{-1}$			
	$CHCl_3$ Solution		EtOH Solution	
	NFDP	NTSP	NFDP	NTSP
400	710	-	1440	-
390	1410	-	2450	-
380	2440	-	3530	-
360	4150	590	4650	450
330	4760	3590	4610	3470
310	4760	6400	3900	5660
280	3110	9510	2740	11510
250	10340	6660	9060	6860
235	17670	12150	19150	10140
230	15810	12880	17640	12830

Note: all data were measured with 1 mM of corresponding sample solutions and a 0.1 cm pathlength cuvette was used.

and in the bilayer lipid membranes. The first derivative absorbance of nifedipine at 400 nm in ethanol was chosen for the preparation of solutions of known concentrations. Figure 4.1.2 shows the measured first order derivative absorptivity plotted against the concentration of nifedipine in ethanol from 0.5 mM to 10 mM at 400 nm (measured in a 0.1 cm pathlength cuvette). It is evident that the relation is nonlinear at high concentrations because of the lack of homogeneous light absorption in the most concentrated samples. For estimates of concentration which are in error by only a few percent, the linear relationship between the first derivative absorptivity (A') and the concentration of nifedipine (C) can still be applied up to about C = 5 mM. Therefore, an acceptable linear relation is A' = kC, where the k value (k_{400nm} = 0.050 mM^{-1}) was determined from the slope of the plot in Figure 4.1.2.

We deliberately used concentrations as high as 10 mM to know the range of concentration for which the linear absorptivity-concentration relationship would work in ethanol solutions. It is highly probable that the real local nifedipine concentrations in liposomes could be even > 10 mM, particularly when the molecules are restricted to the very small volumes of bilayer lipid membranes. In fact, the *measured* concentrations of nifedipine dispersed in liposomes or absorbed on proteins in our experiments were mostly about 2 ± 0.5 mM. The first derivative absorptivities of the samples with the concentrations of 2 ± 0.5 mM were close to 0.100 ± 0.025 with the 0.1 cm optical path length. Therefore, the calibrated linear absorptivity relationship of Figure 4.1.2 could be applied in the liposome and protein samples in which the concentrations of incorporated nifedipine were about 2 mM. We estimate that there are errors of the order of a few percent in the measured concentrations which are due to any differences in the nifedipine extinction coefficient in the protein and bilayer membrane environments relative to the calibrated extinction coefficient in ethanol.

Table 4.1.2 First derivative spectral absorptivity (A')

as a function of nifedipine concentration

measured at 400 nm in ethanol solution

[NFDP] (mM)	0.50	1.00	2.50	5.00	10.0
$A'_{400\ nm}$	0.025	0.049	0.127	0.248	0.489
k & S_R	k = 0.050 $(mM)^{-1}$; S_R = 1.73 (%)				

Notes:

$A'_{400\ nm}$: first derivative absorptivity of nifedipine at the wavelength of 400 nm; k: linear coefficient between A' and C; S_R : relative standard deviation in the determined value for k.

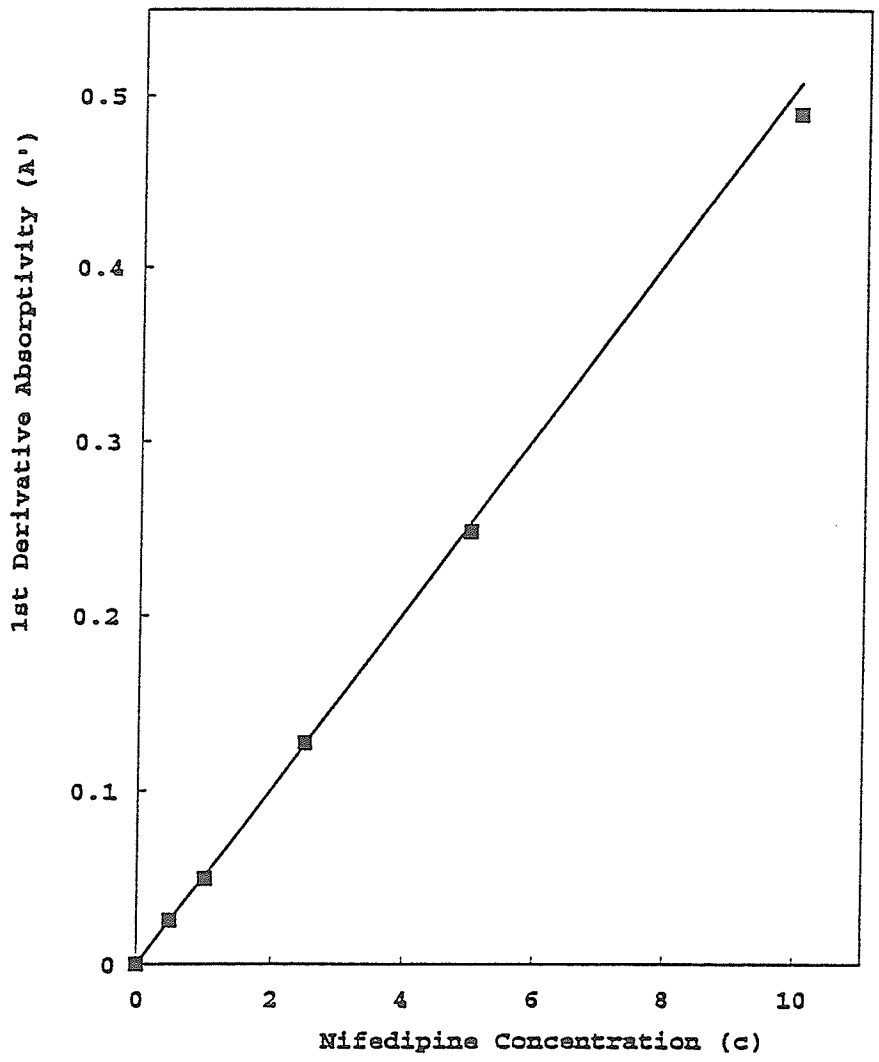

Figure 4.1.2 Concentration dependence of first derivative spectral absorptivity (A') of nifedipine in ethanol solution at 400 nm.

4.1.2 Incorporated Nifedipine Concentrations

Large unilamellar vesicles (LUVs) serve as good models for biological membranes and drug delivery systems (Brock *et al*, 1994; Elorza *et al*, 1993). The methods for the production of LUVs by sonication (Saunders *et al*, 1962), organic solvent dilution (Deamer and Bangham, 1976) and detergent dialysis (Bruner *et al*, 1976) have been reported. The extrusion technique using moderate pressures is also available for the production of LUVs from multilamellar precursors composed of synthetic and biological phospholipids (Nayar *et al*, 1989). The extrusion method has the particular advantage of generating LUVs with nearly the same vesicle diameters as verified by several sizing determinations (Nayar *et al*, 1989). In order to work with a homogeneous population of vesicles we chose the extrusion method in this work for the preparation of LUVs, and the procedures have been described in detail (see page 34).

Based on the absorptivity calibrations, the concentrations of nifedipine in the bilayer membranes of the MLVs and LUVs were determined. From Table 4.1.3, we found that DMPC LUVs effectively trapped nifedipine with a recovery around 70% of the maximum value, and this gave a molar ratio of DMPC/NFDP in the range of 11 to 25. From Table 4.1.4, we observed a recovery of about 40-50% of nifedipine in DHPC LUVs in our experiments. This difference in recovery profiles may be related to morphological and dynamic changes in the structure of the bilayer membranes due to differences in the molecular structure of the constituent phospholipids: either ether or ester lipids.

As a comparison, nifedipine was also incorporated in hydrated proteins: human serum albumin (HSA) and bovine serum albumin (BSA). As previously discussed, nifedipine should be incorporated in the hydrophobic sites of the proteins because of nifedipine's high hydrophobicity. The proteins can be dissolved in water to form the usual

homogeneous yellowish solution which does not appear to be a dispersion on the basis of there being no light scattering in these samples. Interestingly, no matter what concentration of nifedipine was used between 0.5 mM and 2 mM, the molar ratio of nifedipine and BSA protein roughly remained 1:1 (Table 4.1.5). Based on this observation, it is possible that nifedipine could be absorbed on a specific site on the BSA protein, but we have no more detailed information. By assuming the HSA average molecular weight to be 66,000, a molar ratio for nifedipine binding to HSA protein was found to be 0.72 : 1.0 (also Table 4.1.5).

To confirm that nifedipine was really bound to the proteins and located in bilayer lipid membranes of vesicles rather than in the aqueous phases in each case, we measured the solubility of nifedipine in HEPES-NaCl buffer. We found that A_{360nm}=0.009 (0.1 cm cell), and as shown below the saturated nifedipine solution is only 16.3 μM in nifedipine in the HEPES-NaCl buffer. It is clear that nifedipine must be bound to proteins and to bilayer membranes for concentrations as high as 2.5 mM in nifedipine in the protein and vesicle samples.

$$C = A_{360nm} / (\varepsilon_{360nm} \times d) = 0.009 / (5500 \times 0.1)$$

$$= 1.63 \times 10^{-5} \text{ (M)}$$

$$= 16.3 \times 10^{-3} \text{ (mM)}$$

here, ε_{360nm}(in H_2O) = 5500 (Syed, 1989).

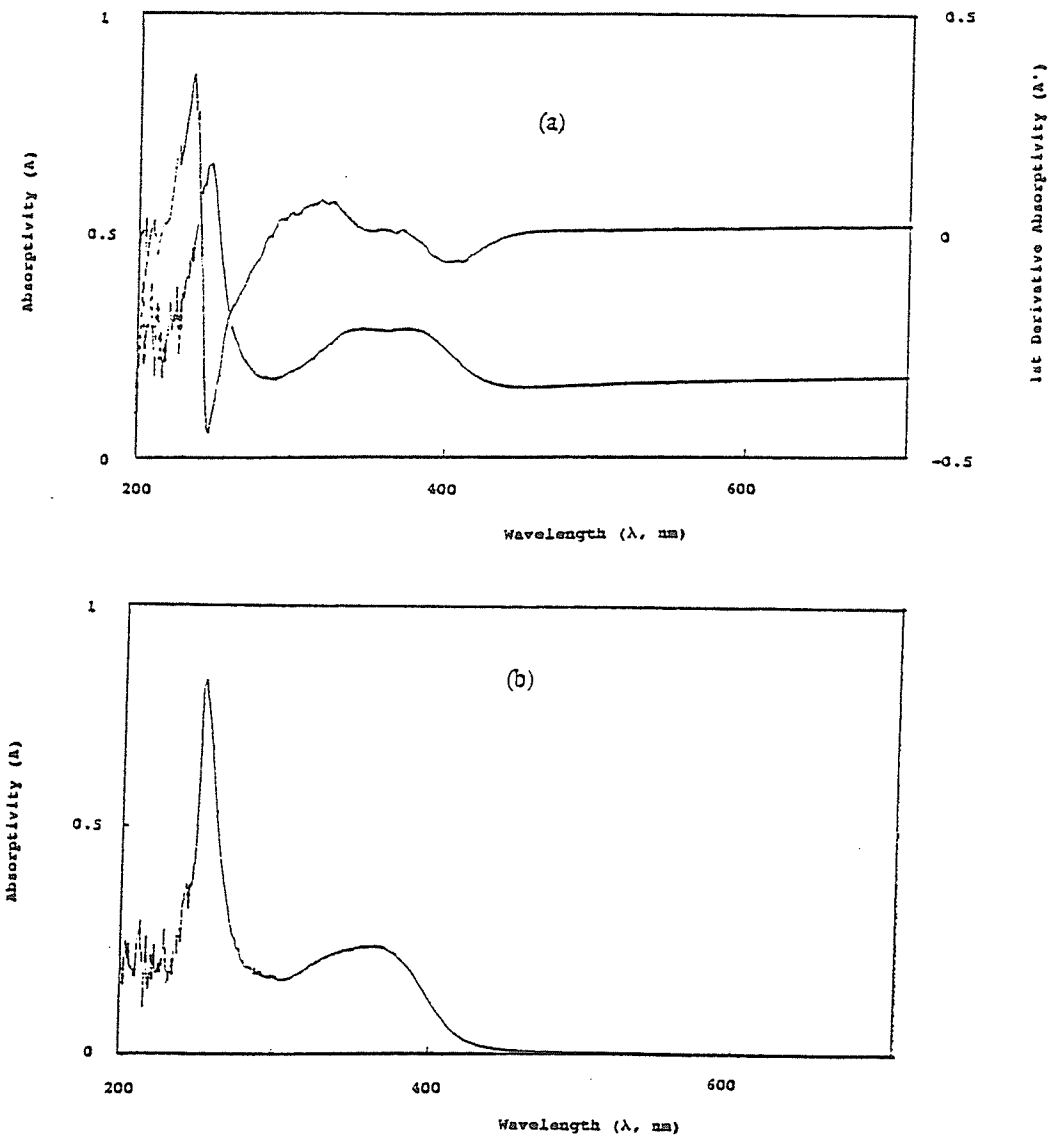

Figure 4.1.3 (a) UV-VIS spectrum (lower trace) and first derivative spectrum (upper trace) of nifedipine dispersed in DMPC/LUVs; (b) UV-VIS spectrum of nifedipine absorbed on bovine serum albumins

Table 4.1.3 Data for the incorporation of nifedipine in DMPC LUVs

Experiment Number	[NFDP] (mM)	[DMPC]/[NFDP] (molar ratio)	NFDP(%) (incorporated)
1	2.20	24.10	73
2	2.16	24.51	72
3	4.32	12.27	72
4	4.69	11.30	75

Notes:

Incorporation temperature: 37±1°C; UV-VIS spectral reference: DMPC LUVs without nifedipine.

Table 4.1.4. Data for the incorporation of nifedipine in DHPC LUVs

Experiment Number	[NFDP] (mM)	[NFDP]/[DHPC] (molar ratio)	NFDP(%) (incorporated)
1	3.09	16.50	52
2	2.92	17.45	49
3	2.45	20.83	41

Notes:

Incorporation temperature: 54±1°C; UV-VIS spectral reference: DHPC LUVs without nifedipine.

Table 4.1.5. Data for the complexing of nifedipine with bovine serum albumin (BSA) and human serum albumin (HSA)

Protein	Protein% (w/w in H_2O)	[NFDP] (mM)	[NFDP]/[PROTEIN] (molar ratio)	Yield (%)
BSA	3.5	0.57	1.08	10
BSA	14	2.15	1.01	36
HSA	14	1.55	0.72	26

Notes:

Sample temperature: 20°C; UV-VIS spectral reference: corresponding BSA or HSA aqueous solutions without nifedipine; The MW of BSA is 66,000 and the MW of HSA was supposed to be the same as the MW of BSA.

4.2. DIMER-COMPLEX ASSAYS

We decided to search for evidence of dimer-complex formation for nifedipine in solution by looking for changes in its absorption spectrum as a function of increasing concentration. Some changes in the absorption spectra were apparent in several solvents, and we attempted to determine the corresponding equilibrium dimer-complex formation constants (K). We measured the absorbance values for 1-10 mM nifedipine in 1-octanol solutions, 1-20 mM nifedipine in ethanol solutions and 1-20 mM nifedipine in 1-butanol solutions. We could not prepare a solution of nifedipine in 1-octanol at a concentration as high as 20 mM. The three previous alcoholic solvents show a range of hydrophobicity with the longer chains being more hydrophobic, and we looked systematically for evidence of nifedipine dimer-complex formation. Finally, it was extremely unlikely that impurities were responsible for the observed changes in the nifedipine spectra at high concentrations.

We attempted to determine the equilibrium dimer-complex formation constants (K) and the extinction coefficients (E_D) by employing an iteration method based on the modified Benesi-Hildebrand Equation [5] we proposed (see page 17). This method was not successful probably due to significant overlapping between the monomer and presumed dimer spectra which were quite similar. Typical comparative spectra are presented in Figure 4.2.1 as the observed absorbance ratios at each wavelength in each solvent for a ten fold increase in nifedipine concentration in 1-octanol and for twenty fold increases in ethanol and 1-butanol, each relative to 1 mM nifedipine reference concentrations. Given the absence of any new distinct absorption bands at higher nifedipine concentrations, it was then proposed that the monomer E_M value was similar to the (presumed) dimer E_D value at all of the measured wavelengths. In order to make

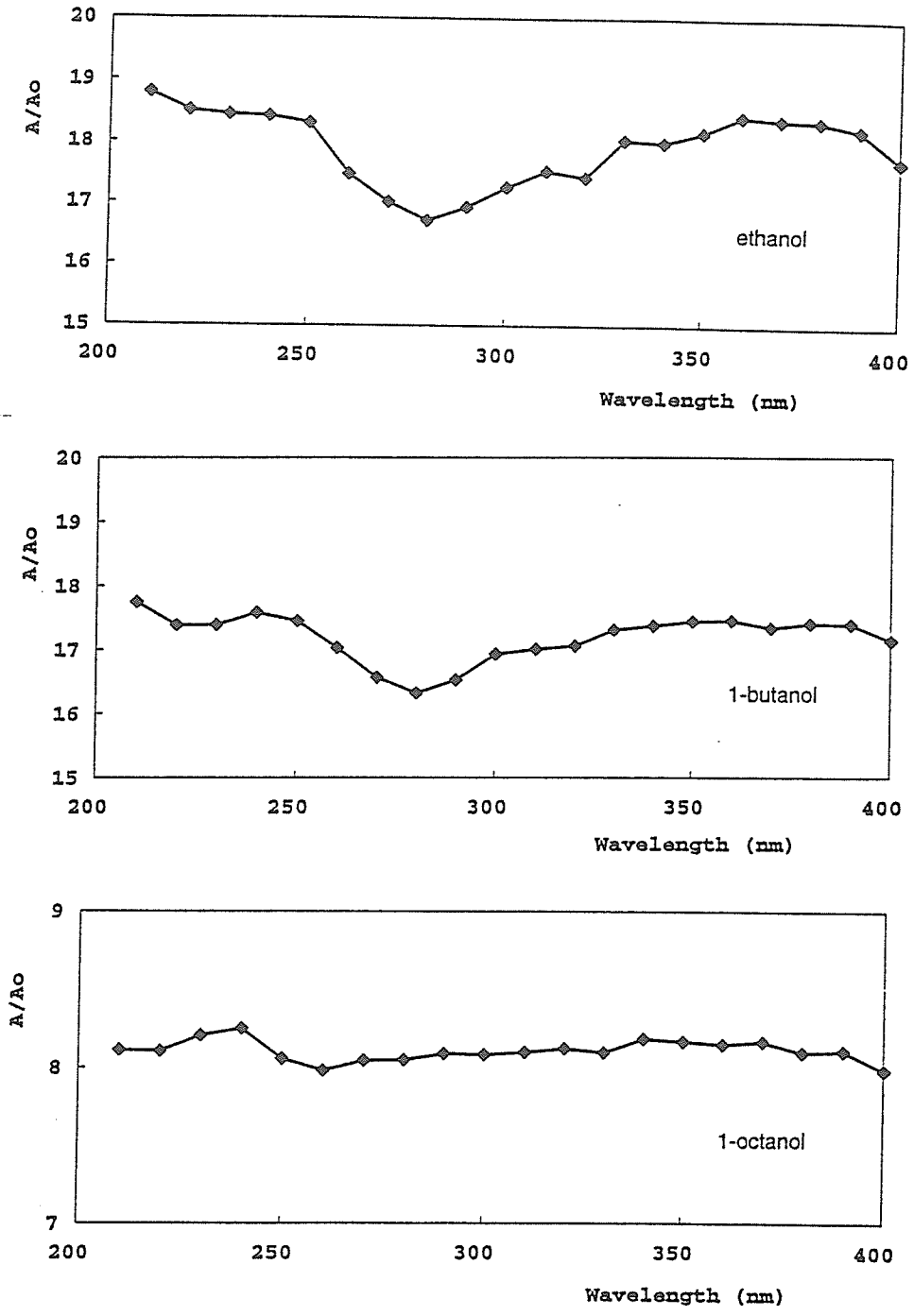

Figure 4.2.1 Plots for nifedipine solutions of the ratio A/A_0 against wavelength (λ).

(A is the absorbance of 10 mM nifedipine/1-octanol solution, 20 mM nifedipine/ethanol or nifedipine/1-butanol solutions; A_0 is the absorbance of 1 mM nifedipine in the corresponding solvents.)

an estimate of the equilibrium association constant, we assumed that the latter proposition was true; and we further simplified the problem by taking the E_D and E_M values to be identical. In this case, the analysis is reduced to a simple calculation based on Equations [13], [14] and [15] below.

For a dimer association reaction, we now derive the simple equilibrium association constant (K) of Equation [13]:

$$2M \rightleftharpoons D$$

for no association:	C_0	0
for some association:	$C_0 - 2C_D$	C_D

The K value:

$$K = \frac{C_D}{(C_0 - 2C_D)^2} \qquad [13]$$

Here, C_D is the concentration of dimer complex at equilibrium, and C_0 is the concentration of monomer before association occurs. With some dimerization, the measured absorbance A_e at a selected wavelength is due to presence of both monomer and dimer species:

$$A_e = A_M + A_D = E_M \cdot (C_0 - 2 \cdot C_D) \cdot d + E_D \cdot C_D \cdot d$$
$$= E_M \cdot C_0 \cdot d - (2 \cdot E_M - E_D) \cdot d \cdot C_D$$

Here, A_M and A_D are the absorbances of the monomer and dimer species; E_M and E_D are their respective molar extinction coefficients; and d is the optical pathlength. For $A_0 = E_M \cdot C_0 \cdot d$ we obtain:

$$A_e = A_0 - (2 \cdot E_M - E_D) \cdot d \cdot C_D$$

and $$\Delta A = A_0 - A_e = (2 \cdot E_M - E_D) \cdot d \cdot C_D$$

$$C_D = \frac{\Delta A}{(2 \cdot E_M - E_D) \cdot d} \qquad [14]$$

For the case of negative deviation to Beer-Lambert Law, $A_0 > A_e$,

then, $\Delta A = (A_0 - A_e) > 0$

and therefore, $(2 \cdot E_M - E_D) > 0$, $E_D < 2E_M$

Obviously, the value of E_D will be: $0 < E_D < 2E_M$.

With the simplifying assumption, $E_D = E_M$; then

$$C_D = \frac{\Delta A}{E_M \cdot d} \qquad [15]$$

Therefore, Equation [14] has been simplified to Equation [15], and we can now make an estimate of the concentration of the dimer complex. Furthermore, with the same simplifying assumption, $E_D = E_M$, we can now estimate the values of the dimer association constant (K) with Equation [13]. The estimated K values and the corresponding dimer concentration values are listed in Table 4.2.1. The detailed absorbance ratio data is also listed in Appendix B.

Table 4.2.1 Estimates of the equilibrium dimer association constants (K) for nifedipine in alcoholic solutions

Solutions	C_D (mM)[a]	K (M^{-1})[b]
20 mM NFDP/Ethanol	2.03 (27.3%)[c]	7.98 (45.6%)[c]
20 mM NFDP/1-Butanol	2.81 (13.3%)[c]	13.59 (26.0%)[c]
10 mM NFDP/1-Octanol	1.89 (3.59%)[c]	49.03 (8.00%)[c]

Notes:

(a) C_D: the equilibrium concentration of dimer complex (units of mM); (b) K: the dimer association constant (units of M^{-1}); (c) Data in the parentheses are standard deviations (S_R).

4.3 PHOTODEGRADATION ASSAYS

4.3.1 Product and Kinetic Analyses

Although the nitrosophenylpyridine derivative (NTSP) (Figure 1.3.1) was reported to be a major product from the irradiation of nifedipine with fluorescent lights (Thoma and Kerker, 1992b), mercury arc (Matsuda *et al*, 1989) and sunlight (Sadana and Ghogare, 1991), the nitrophenylpyridine derivative (NTRP) was also reported as a major product (73%) with mercury arc irradiation (Vargas *et al*, 1992). Given the contradictory nature of the literature, it was decided to confirm the identity of the photochemical products formed with visible light. We also desired to isolate the main photoproduct to compare its photochemistry with that of nifedipine.

The product analysis was attempted following photolysis of 1 mM nifedipine in anhydrous ethanol solution and 50 mM nifedipine in methylene dichloride, using the tungsten-halogen light source. The entire reaction was monitored by UV-VIS spectroscopy and thin layer chromatography (TLC). Separation of nifedipine from its photoproducts by TLC is fast, convenient, and well documented (Ebel, 1978; Thoma and Klimek, 1985). The TLC results in the present work are listed in Table 4.3.1. The TLC results indicate that before the irradiation, there was only nifedipine; during the irradiation, one new spot appeared in addition to nifedipine; and finally nifedipine disappeared and only one product was present according to TLC. Furthermore, the mixtures of nifedipine and its photoproduct(s) were also checked in different developer systems, and still only one photoproduct was evident. Considering the accuracy of the separation method (TLC), we can only conclude that the purity of the single photoproduct was about 95% under the conditions of our irradiations; and we are unable to confirm the identity of products which may constitute only 5% of the total product(s).

Table 4.3.1 Results of the TLC analysis

of the photodegradation products of nifedipine

Sample[a]	Developer I[b]			Developer II[b]		
	Rf_{NFDP}	Rf_{NTSP}	ΔRf^{c}	Rf_{NFDP}	Rf_{NFDP}	ΔRf^{c}
A	0.34	0.55	0.21	0.57*	0.68*	0.11*
B	0.45	0.74	0.29	0.40	0.62	0.22
C	0.42	0.63	0.21	-	-	-
D	-	0.59	-	-	-	-

Notes:

a) Sample A: NFDP (10 mM, EtOH) and NTSP (12.5 mM, $CHCl_3$) were spotted separately on the same plate;

Sample B: 1:1 molar ratio mixture of NFDP (10 mM, EtOH) and NTSP (12.5 mM, $CHCl_3$);

Sample C: a mixture of NFDP and NTSP taken from 50 mM NFDP/CH_2Cl_2 solution after an irradiation of 4.5 hrs;

Sample D: 1:1 molar ratio mixture of NTSP (from 12.5 mM NFDP/$CHCl_3$ solution exposed to sunlight) and NTSP (from 50 mM NFDP/EtOH solution exposed to the filtered tungsten-halogen lamp).

b) Developer I: petroleum ether/methylene chloride/methanol: 1:1:0.1;

Developer II: petroleum ether/ethyl acetate: 1:0.8; *: using developer of petroleum ether/ethyl acetate: 1:1.

c) ΔRf: the difference between the retention factors for NFDP (Rf_{NFDP}) and NTSP (Rf_{NTSP}) on the same plate.

The structure of the separated photoproduct was analyzed by ^{1}H NMR and UV-VIS spectroscopies. The ^{1}H NMR spectrum and its interpretation are shown in Figure 4.3.1. We found literature ^{1}H-NMR spectra for nifedipine (Syed, 1989) and for the nitrophenyl pyridine derivative (NTRP) (Antonin *et al*, 1984), but not for the nitrosophenylpyridine derivative (NTSP). Compared with the ^{1}H NMR spectrum of nifedipine (Syed, 1989), the protons at δ2.67 and at δ3.38 were Ar-CH_3 and -COOCH_3, respectively. The disappearance of N_1-H and C_4-H proved the aromatization of the dihydropyridine ring. The results of decoupling designated the chemical shifts of the protons in the benzene ring (H_6, δ7.71; H_3, δ6.55; H_5, δ7.44; H_4, δ7.52). Deuterium exchange indicated that the two protons (from integrated amplitudes) δ1.65 may come from an intramolecular H_2O hydrogen bonding between the nitroso group -N=O and the neighbouring carbonyl group. Further confirmation for the nitroso group assignment came from the UV-VIS spectrum where a characteristic broad band at about 775 nm was observed. In contrast, the nitro group does not absorb at this wavelength (Orger, 1972). Therefore, the NMR and UV-VIS analytical results both confirmed that the main photodegradation product in these experiments was the nitrosophenylpyridine compound (NTSP).

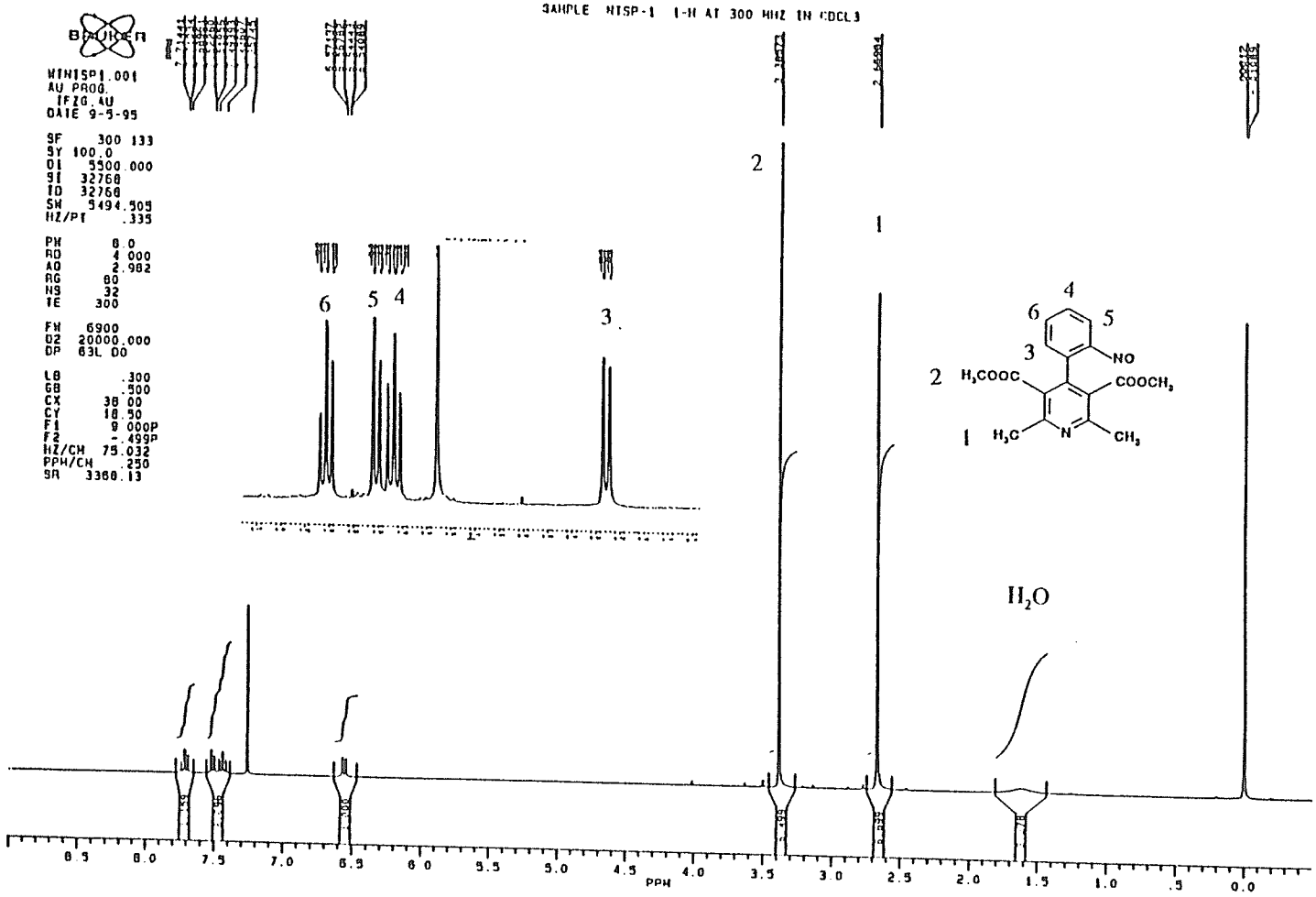

Figure 4.3.1 ^{1}H NMR spectrum of the nitrosophenylpyridine (NTSP) compound which was found to be the main photochemical product.

To the best of our knowledge, the photokinetic behaviour of nifedipine in liposomes has not been reported. These measurements were undertaken in order to determine how quickly nifedipine was converted to the NTSP product in the parallel EPR study with the same tungsten-halogen light source. Therefore, the photochemical kinetics of the nifedipine irradiation were studied with 2.5 mM nifedipine in DMPC LUVs as well as with 2.5 mM nifedipine in ethanol solution for a direct comparison. The comparable kinetic results are shown in Table 4.3.2 and in Figure 4.3.2. The first derivative UV-VIS spectral absorptivity at 400 nm was used for the purpose of measuring the photoconversion kinetics. These studies indicated that the conversion of nifedipine to NTSP was close to 90% complete in only five minutes. Furthermore, the photochemistry followed an apparent first order reaction in nifedipine, both in DMPC LUVs and in ethanol solutions. It was significant that the photochemistry was faster in the DMPC LUV samples than in ethanol solutions. The faster photoconversion of nifedipine in DMPC aqueous dispersions may be related to the probably higher concentration of the nifedipine molecules in the bilayer membranes of the vesicles. We will return to a discussion of the role of dimer complexes in the photochemical mechanism later. Finally, no obvious difference was observed in the comparison of photoconversion kinetics either with or without the BG-38 filter which was used primarily to remove the large infrared output from the tungsten-halogen lamp. It is clear that this infrared component was not important in promoting the observed photochemistry.

Table 4.3.2 Kinetic results of nifedipine photodegradation in DMPC LUVs and in ethanol solution

t^a (min)	$A'_{400}{}^b$		$C_{NFDP}{}^c$ (mM)	
	LUV	EtOH	LUV	EtOH
0	0.126	0.125	2.52	2.50
1.0	0.089	0.103	1.78	2.06
2.0	0.061	0.084	1.22	1.68
3.0	0.039	0.069	0.78	1.38
4.0	-	0.056	-	1.12
Kinetics in LUV	$C = C_0 * e^{-kt}$; $k = 0.367\ min^{-1}$; $t_{1/2} = 1.9$ min.			
Kinetics in EtOH	$C = C_0 * e^{-kt}$; $k = 0.198\ min^{-1}$; $t_{1/2} = 3.5$ min.			

Notes:

a) t: irradiation time by using a filtered tungsten-halogen lamp with the irradiation intensity of 70% at the distance of 15 cm between the sample and the lamp; b) A'_{400}: 1st derivative UV-VIS spectral absorptivity at 400 nm; c) C_{NFDP}: concentration of nifedipine in the samples.

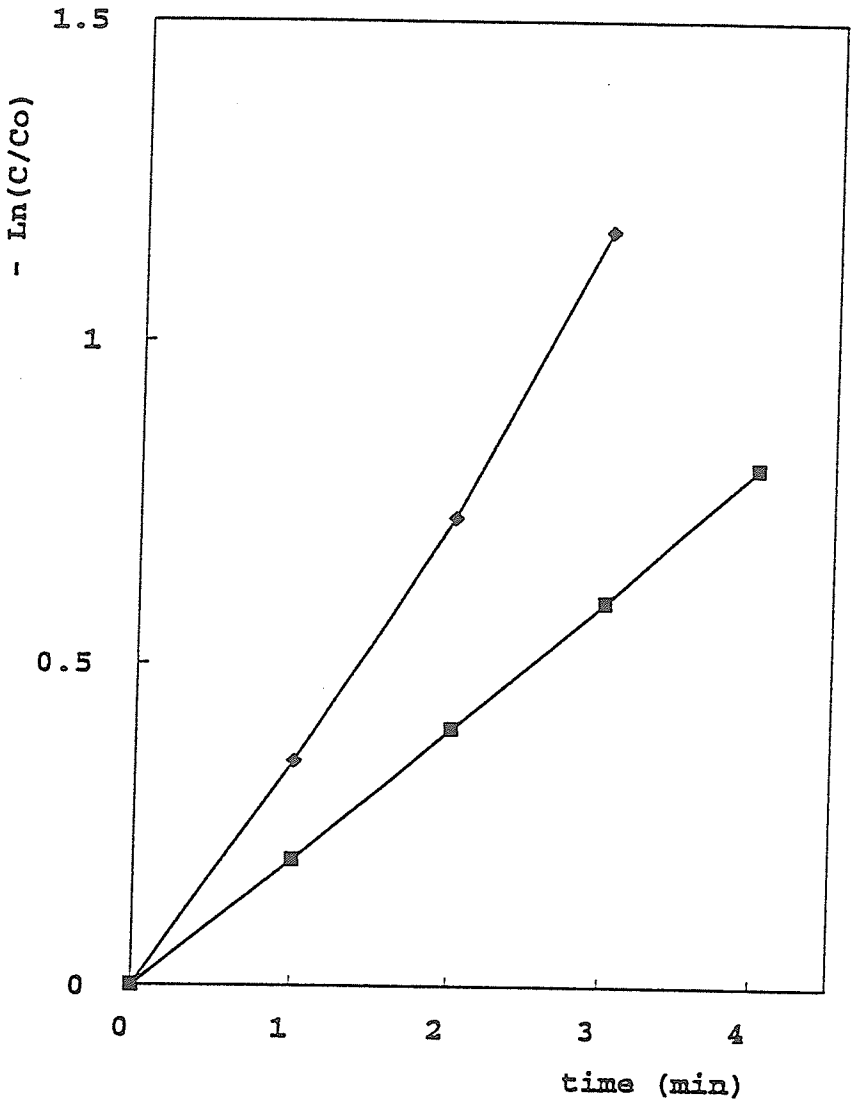

Figure 4.3.2 First order kinetic plots of [$-ln(C/C_0)$] versus *time* for the nifedipine photodegradation in DMPC LUVs (♦) and in ethanol solution (■).

(*t*: irradiation time, units of minutes; *C*, C_0: nifedipine concentrations at time *t* and at the start; [$-ln(C/C_0)$]: negative natural logarithm of the ratio C/C_0.)

4.3.2 Radical Detection

By using TLC separation methods along with UV-VIS and ^{1}H NMR spectroscopies, we have confirmed that NTSP (Figure 1.3.1, III) is a major photochemical product. Furthermore, it only took about five minutes of irradiation with the filtered tungsten-halogen lamp in this study to achieve about 90% conversion of nifedipine to NTSP. We also separated the product NTSP with a purity of about 95% (see Section 4.3.1). In order to clarify the nature of the free radicals produced in biological environments, the nifedipine photochemistry was studied in liposome dispersions, in albumin protein aqueous solutions and in organic solutions by using electron paramagnetic resonance (EPR) spectroscopy. As previously discussed, EPR is a powerful method to investigate a mechanism which involves free radicals. In our experiments, samples which did not contain nifedipine were utilized as appropriate controls, but these control results were not listed in the tables or figures unless a measurable result was observed. The concentrations of free radicals listed in the tables were determined by the double integration of the experimental first derivative EPR spectra, and they were calibrated against standard samples of the nitroxide free radical, Tempol, which was similar to the radicals detected in our experiments.

1) Detection in liposome aqueous dispersions

Either dimyristoyl-L-α-phosphatidylcholine (DMPC) or di-O-hexadecyl-DL-α-phosphatidylcholine (DHPC) were chosen as the lipids for making liposomes. Nifedipine was incorporated first in the membranes of multilamellar vesicles (MLVs), and then these were transformed into large unilamellar vesicles (LUVs) by the extrusion process. Both the MLVs and LUVs were studied as incorporation models.

The EPR data for the irradiation of nifedipine incorporated in DMPC LUVs are given in Tables 4.3.3 and 4.3.4 under specific conditions, and the related spectra are shown in Figures 4.3.3 and 4.3.4. Tables 4.3.6 to 4.3.8 give the EPR data for the irradiation of nifedipine incorporated in DHPC liposomes (both LUVs and MLVs), and the corresponding spectra are shown in Figures 4.3.6 to 4.3.8.

The isolated photodegradation product 2,6-dimethyl-3,5-dimethoxycarbonyl-4-[2'-nitrosophenyl]-pyridine (NTSP) was also studied by EPR in DMPC LUVs; the corresponding data are listed in Table 4.3.5 and typical spectra are given in Figure 4.3.5. As previously discussed, NTSP has good spin trapping properties as an endogenous agent (Stasko *et al*, 1994). For comparison, the effects of adding an exogenous spin trap, PBN, were also studied. The data are presented in Tables 4.3.4 and 4.3.5 and in Figures 4.3.4 and 4.3.5.

The effects of ambient air (oxibiotic) and hypoxic conditions were studied in DMPC LUVs (Table 4.3.3 and Figure 4.3.3). The term 'oxibiotic' means a normal concentration of oxygen in our aqueous samples, e.g., about 200 micromolar oxygen at 37°C, and the term 'hypoxic' means a much lower oxygen concentration. The oxibiotic and hypoxic conditions in the samples were achieved by purging the samples in very thin teflon tubing respectively with air or argon as described in the EPR experimental section (page 38).

Also in the case of nifedipine/DHPC LUV samples, the effect of temperature on the photoinduced reaction was found to be important and was studied. These results are shown in Table 4.3.8 and in Figure 4.3.8 on the following pages.

2) Detection in aqueous solutions of albumin proteins

To compare the difference between the interactions of nifedipine with lipids and with proteins, bovine albumin and human albumin were chosen as proteins and these systems were irradiated. The EPR data for the irradiation of nifedipine incorporated in bovine and human albumins is given in Tables 4.3.9 and 4.3.10, and the corresponding spectra are shown in Figures 4.3.9 and 4.3.10.

The average g-factor of the very strongly immobilized radical(s) was measured with a standard sample of Mn^{2+} ions as an impurity in SrO powder at 37° C according to Equation [8] (see page 21):

$$g_x = \frac{g_s \cdot H_s}{H_x} = g_s \cdot \left(1 + \frac{\Delta H}{H_s} \right) \qquad [8]$$

Here, $g_s = 2.0012 \pm 0.0002$ (Swartz *et al*, 1972, page 100) is the g-factor of the standard sample. From the spectrum in Figure 4.3.9b, we estimated $\Delta H = 5.8 \pm 0.1$ (G). The magnetic field we used was $H_0 = 3218$ (G). Substituting these values in the above equation, we obtained $g_x = 2.0048 \pm 0.0002$.

3) Detection in organic solutions

The photochemical behaviour of nifedipine was studied in several organic solvents including benzene and ethanol. Table 4.3.12 and Figure 4.3.12 show the respective EPR data and spectra for these irradiations of nifedipine in benzene and ethanol solutions.

Table 4.3.3 EPR data for the irradiation of 4.69 mM nifedipine/DMPC LUVs under ambient oxibiotic or hypoxic conditions

Experiment[a] No.	Atmosphere (litre/hr)	Irradiation Time (min)	[R•][b] (μM)	Yield (%)
NFDMB.02	1.25 (argon)	5	9.1	0.19
NFDMB.03	1.25 (argon)	20	17.5	0.37
NFDMB.04	1.25 (argon)	40	17.2	0.37
NFDMC.05	2.50 (air)	5	9.9	0.21
NFDMC.06	2.50 (air)	20	20.1	0.43
NFDMC.07	2.50 (air)	40	19.1	0.41

Notes:

a) Experimental conditions: 0.5 G modulation amplitude; 10 mW microwave power; 100 G scan range; 2 x 10^3 receiver gain; sample temperature at 37°C; 70 x 2 μl sample volume in teflon tubes.

b) [R•]: radical concentration measured by double integration of the EPR spectrum with a precision of ±15%.

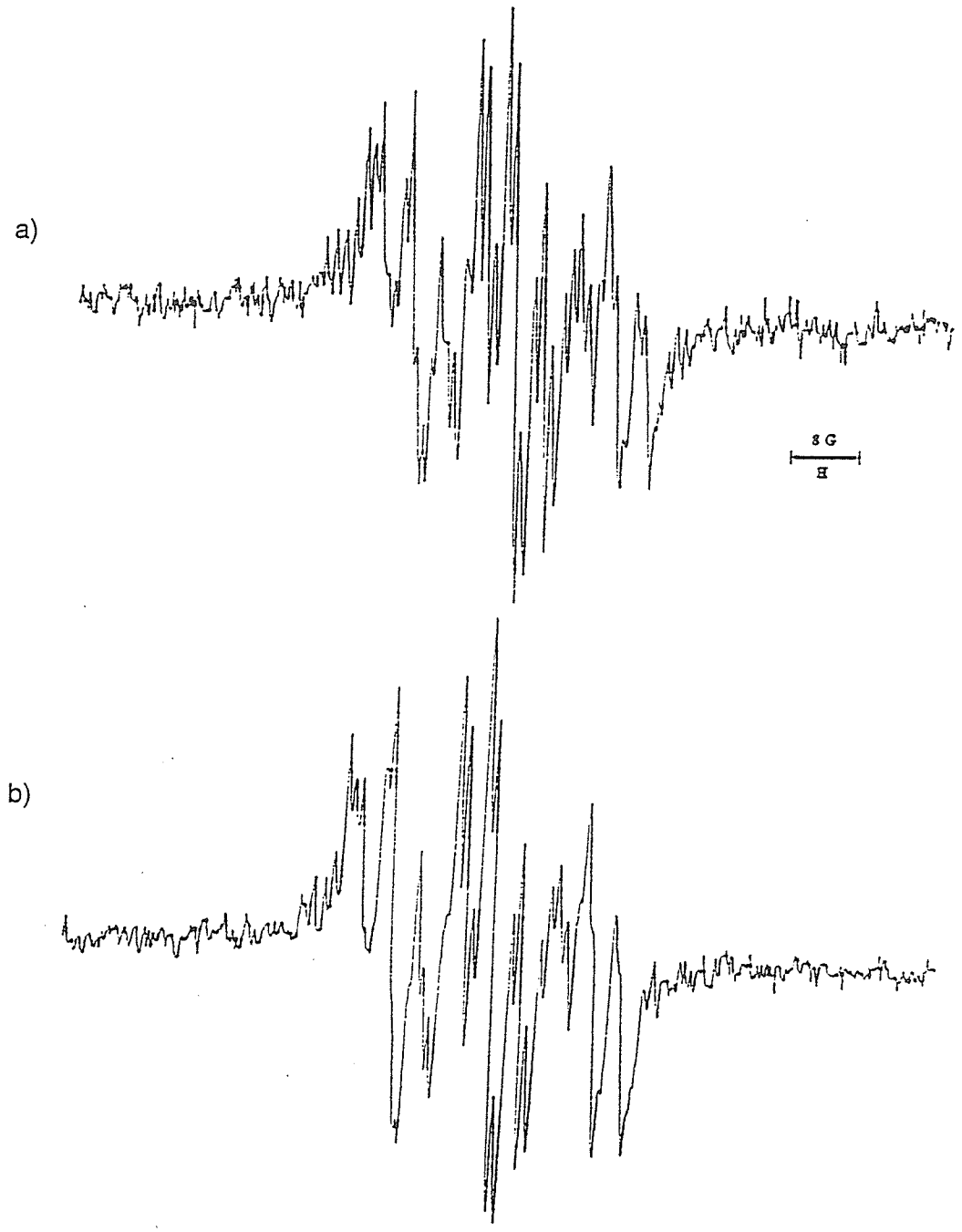

Figure 4.3.3 EPR spectra observed from the irradiation of NFDP/DMPC LUVs under ambient oxibiotic (a) and hypoxic (b) conditions.

a) NFDMB.04: 4.69 mM NFDP/DMPC-LUVs;

b) NFDMC.07: 4.69 mM NFDP/DMPC-LUVs.

Table 4.3.4 EPR data for the irradiation of

2.20 mM nifedipine/DMPC LUVs with/without PBN spin-trap

Experiment[a] No.	Spin Trap	Irradiation Time (min)	[R·][b] (μM)	Yield (%)
NF3L.02	-	5	7.9	0.36
NF3L.03	-	10	11.4	0.51
NF3L.04	-	15	11.6	0.53
NF3L.05	-	20	12.6	0.57
NF3L.07	PBN, 50 mM	5	7.9	0.36
NF3L.08	PBN, 50 mM	10	11.5	0.52
NF3L.09	PBN, 50 mM	15	12.9	0.59
NF3L.10	PBN, 50 mM	20	13.7	0.62

Notes:

a) Experimental conditions: the same as described in Table 4.3.3 (page 72) except for 0.8 G modulation amplitude and 60 μl sample volume in glass capillary.

b) [R·]: the same as defined in Table 4.3.3 (page 72).

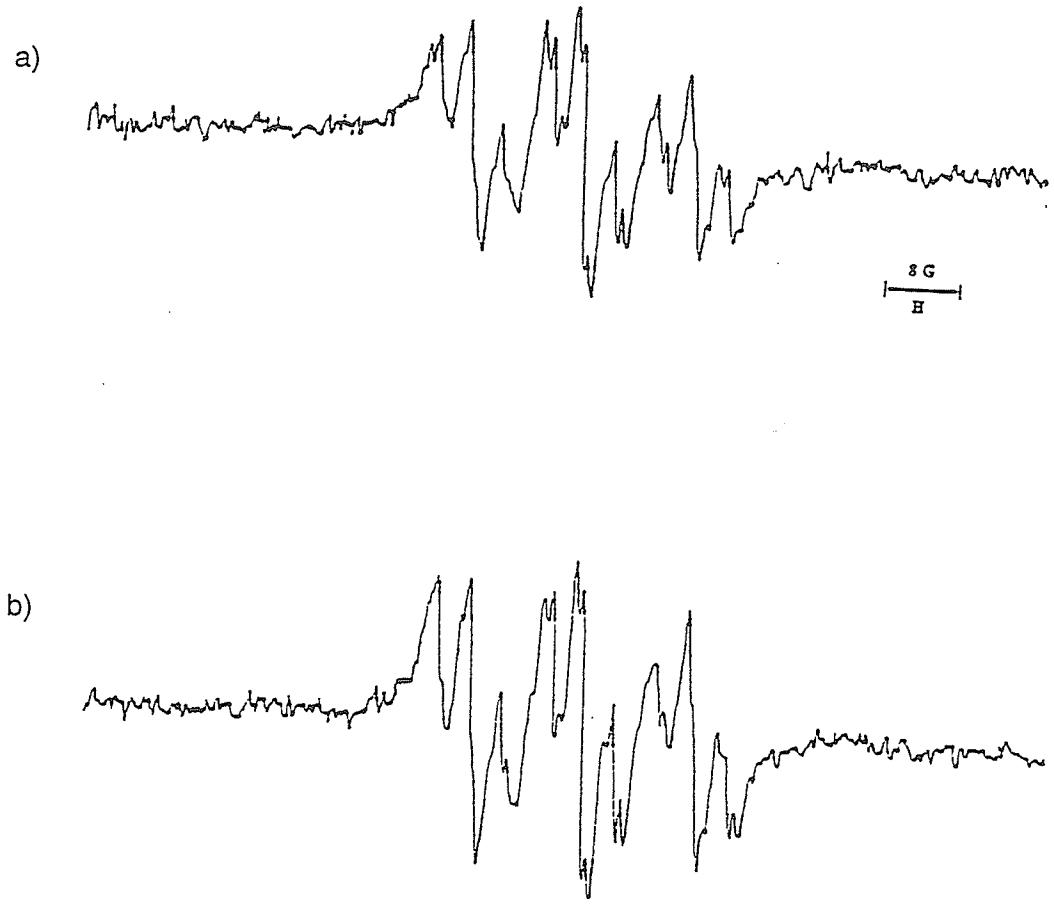

Figure 4.3.4 Comparison of EPR spectra

for the irradiation of NFDP/DMPC LUVs with/without PBN spin trap

a) NF3L.05: 2.2 mM NFDP/DMPC-LUVs, PBN 0 mM;

b) NF3L.10: 2.2 mM NFDP/DMPC-LUVs, PBN 50 mM.

Table 4.3.5 EPR data for the irradiation of 2.5 mM NTSP/DMPC LUVs with/without PBN spin-trap

Experiment[a] No.	Spin Trap	Irradiation Time (min)	[R•][b] (μM)	Yield (%)
NF3L.12	-	5	-	-
NF3L.13	-	10	4.3	0.17
NF3L.14	-	15	5.3	0.21
NF3L.15	-	20	4.8	0.19
NF3L.17	PBN, 50 mM	5	7.8	0.31
NF3L.18	PBN, 50 mM	10	8.7	0.35
NF3L.19	PBN, 50 mM	15	9.9	0.40
NF3L.20	PBN, 50 mM	20	9.7	0.39

Notes:

a) Experimental conditions: the same as described in Table 4.3.3 (page 72) except for 0.8 G modulation amplitude and 60 μl sample volume in glass capillary.

b) [R•]: the same as defined in Table 4.3.3 (page 72).

Figure 4.3.5 Comparison of EPR spectra

for the irradiation of NTSP/DMPC LUVs with/without PBN spin trap.

a) NF3L.15: 3 mM NTSP/DMPC-LUVs, PBN 0 mM;

b) NF3L.20: 3 mM NTSP/DMPC-LUVs, PBN 50 mM;

Table. 4.3.6 EPR data for the irradiation of

nifedipine/DHPC LUVs or MLVs

Experiment[a] No.	Irradiation Time (min)	[R•][d] (μM)	Yield (%)
NFDHA.02 (LUV)[b]	15	13.5	0.44
NFDHA.03 (LUV)[b]	30	14.1	0.46
NFDHA.04 (LUV)[b]	45	11.8	0.38
DHNF.03 (MLV)[c]	10	8.3	0.28
DHNF.04 (MLV)[c]	20	13.8	0.46
DHNF.05 (MLV)[c]	40	15.9	0.53

Notes:

a) Experimental conditions: the same as described in Table 4.3.3 (page 72) except for 70 μl x 2 sample volume in teflon tubes under hypoxic conditions.

b) Concentration of nifedipine incorporated in DHPC LUV: 3.09 mM.

c) Concentration incorporated in DHPC MLV: 3 mM.

d) [R•]: the same as defined in Table 4.3.3 (page 72).

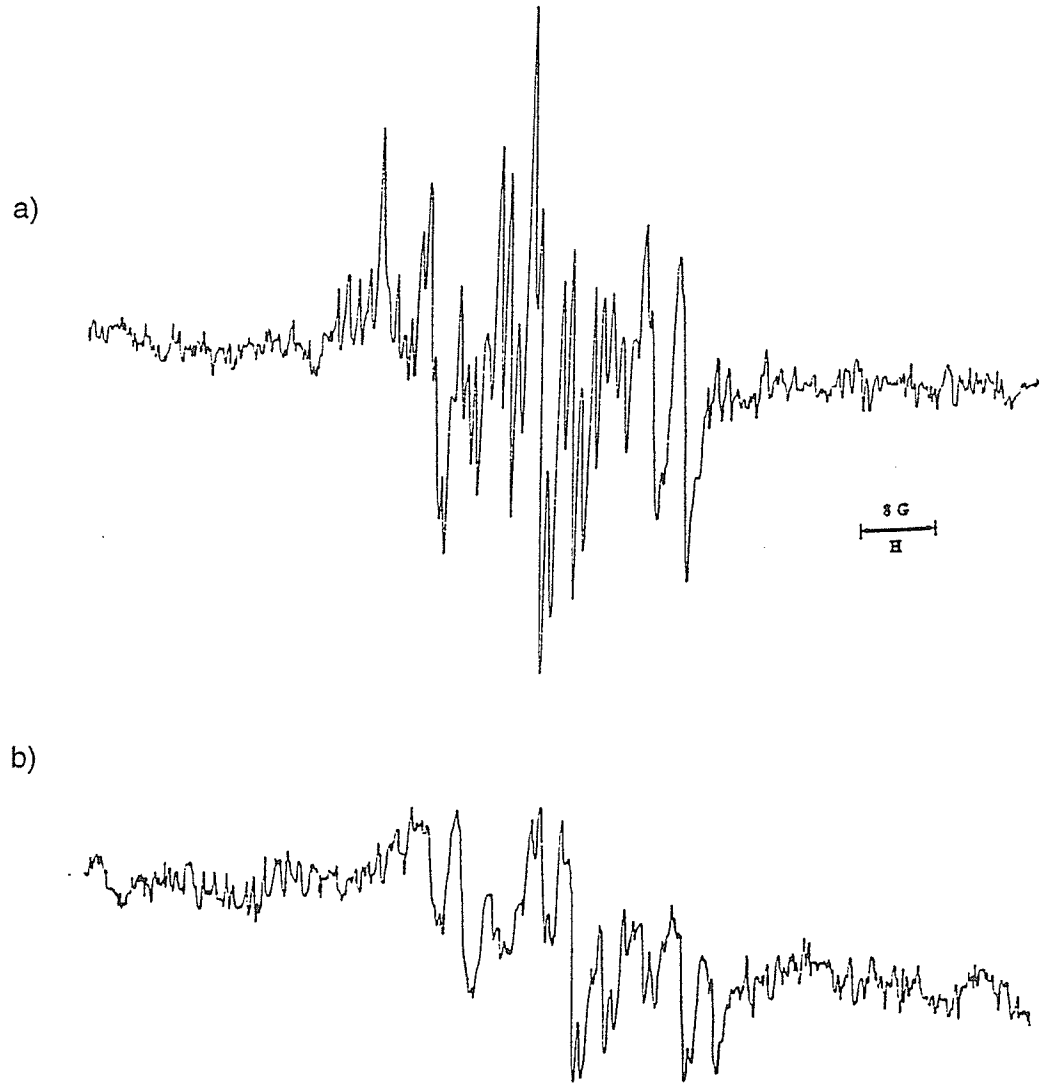

Figure 4.3.6 Comparison of EPR spectra

for the irradiation of NFDP/DHPC in LUVs and MLVs

a) NFDHA.04: 3.09 mM NFDP/DHPC-LUVs;

b) DHNF.05: 3 mM NFDP/DHPC-MLVs.

Table 4.3.7 EPR data for nifedipine/DHPC LUVs in the dark

for the same length of time as for the irradiation

Experiment[a] No.	[NFDP] (mM)	T (°C)	Scan Time (min)	[R•][b] (μM)	Yield (%)
NFDHE.01	2.45	16	40	3.0	0.12
NFDHA.05	3.09	37	40	5.4	0.17
NFDHA.06	3.09	37	80	5.2	0.17
NFDHD.01	2.92	47	40	4.2	0.14

Notes:

a) Experimental conditions: the same as described in Table 4.3.3 (page 72) except for 70 μl x 2 sample volume in teflon tubes under hypoxic conditions.

b) [R•]: the same as defined in Table 4.3.3 (page 72).

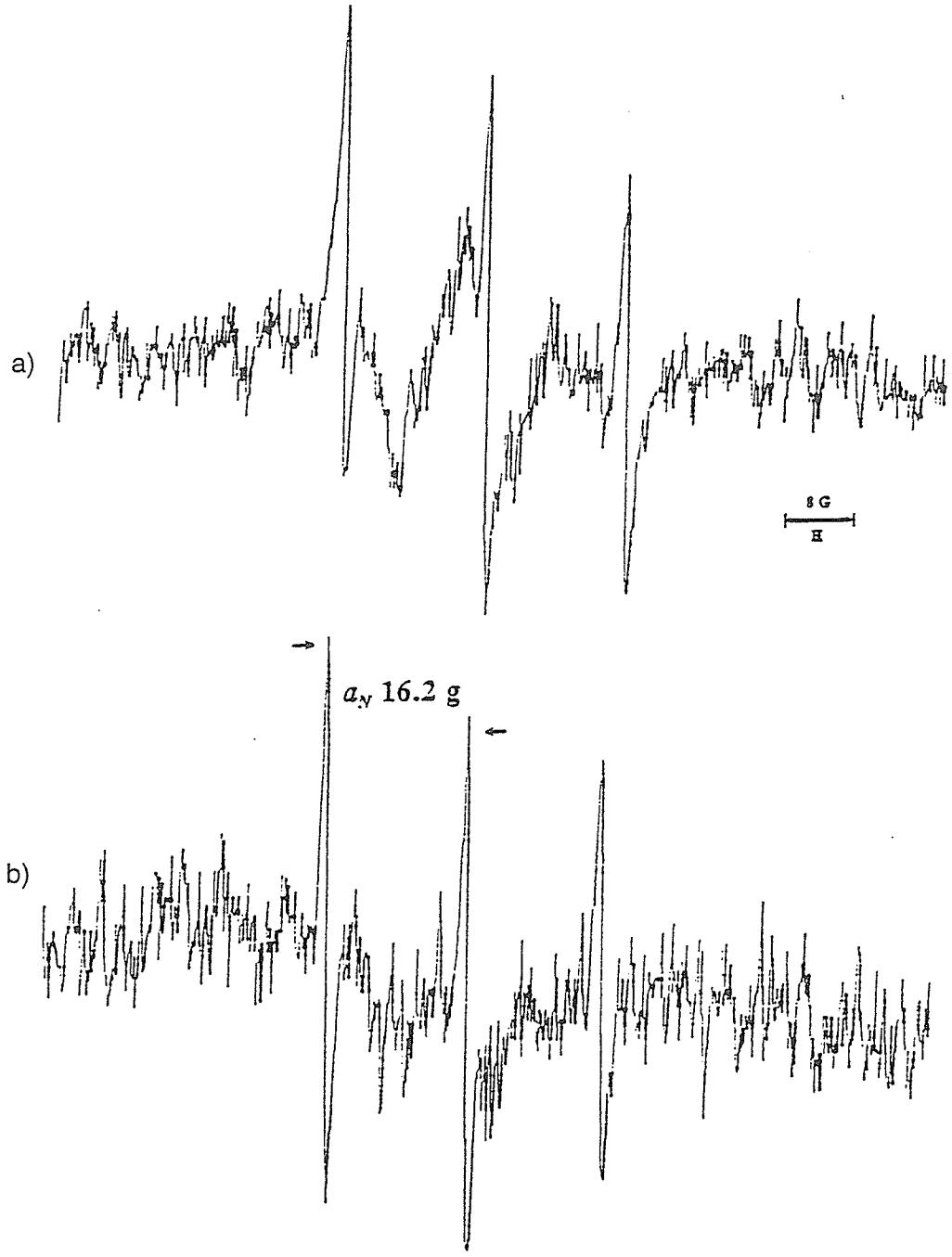

Figure 4.3.7 EPR spectra for NFDP/DHPC LUVs in the dark

for the same length of time as for the irradiation in Figure 4.3.8

a) NFDHD.01: 2.92 mM NFDP/DHPC-LUV, 47°C;

b) NFDHA.04: 3.09 mM NFDP/DHPC-LUV, 37°C.

Table 4.3.8 EPR data for the irradiation of nifedipine/DHPC LUVs at different temperatures

Experiment[a] No.	[NFDP] (mM)	Temperature (°C)	[R•][b] (μM)	Yield (%)
NFDHE.04	2.45	16	10.6	0.44
NFDHC.04	2.92	27	13.5	0.46
NFDHA.09	3.09	37	12.8	0.41
NFDHD.04	2.92	47	13.2	0.45

Notes:

a) Experimental conditions: the same as described in Table 4.3.3 (page 72) except for 40 minute irradiation time and 70 μl x 2 sample volume in teflon tubes under hypoxic conditions.

b) [R•]: the same as defined in Table 4.3.3 (page 72).

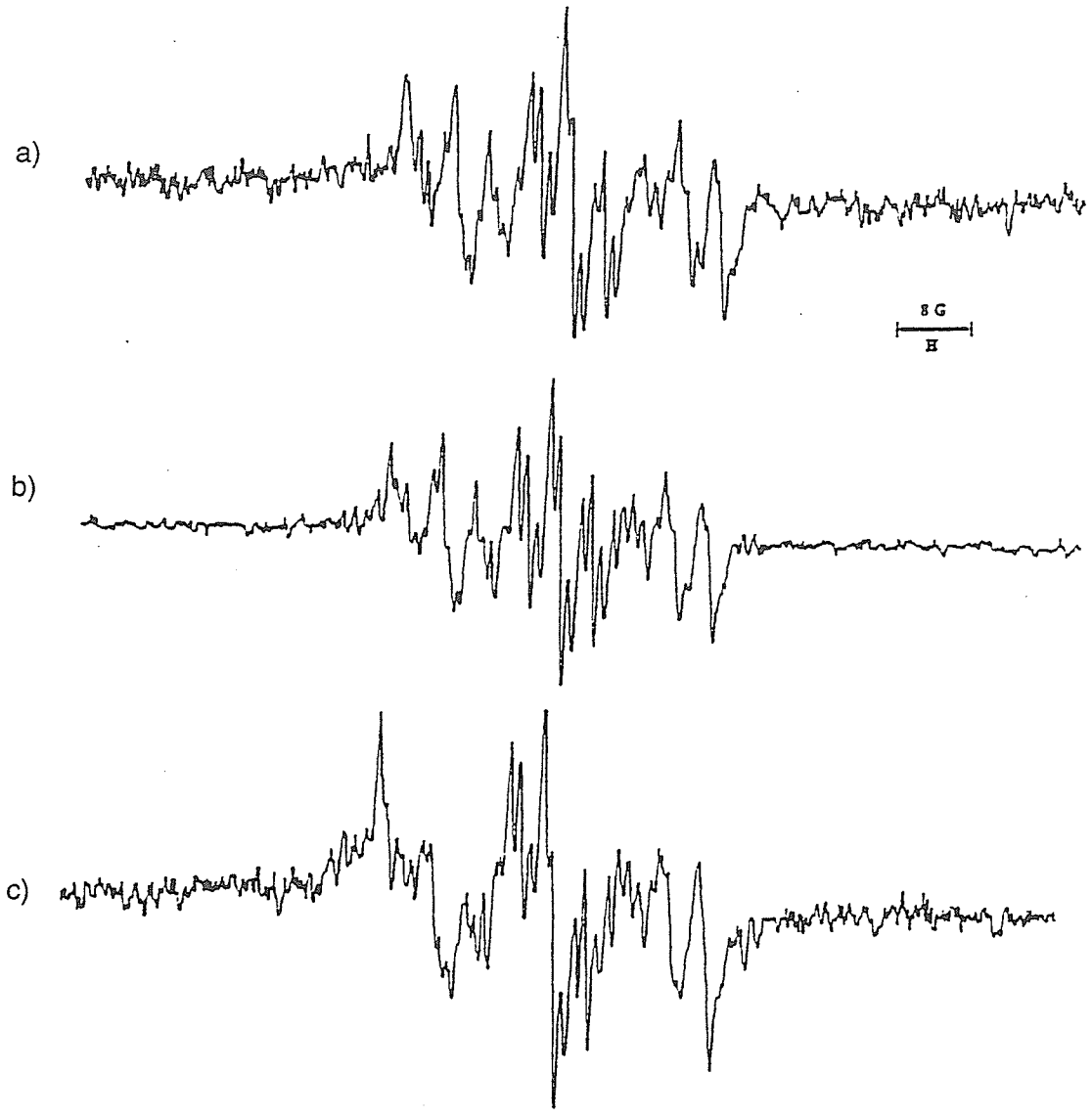

Figure 4.3.8 The effect of temperature on EPR spectra

for the irradiation of NFDP/DHPC LUVs

a) NFDHE.04: 2.45 mM NFDP/DHPC-LUV, at 16°C;

b) NFDHA.09: 3.09 mM NFDP/DHPC-LUV, at 37°C;

c) NFDHD.04: 2.92 mM NFDP/DHPC-LUV, at 47°C.

Table 4.3.9 EPR data for the irradiation of nifedipine complexed with bovine serum albumin in aqueous solutions

Experiment[a] No.	[NFDP] (mM)	Irradiation Time (min)	Modulation Amplitude(G)	[R•][b] (μM)	Yield (%)
ABNFA.01	0.6	40	0.5	3.9	0.65
ABNFB.02	2.1	40	0.5	14.0	0.65
ABNFB.07	2.1	40	2.5	14.1	0.66
ABNFB.08	2.1	80	2.5	23.7	1.10

Notes:

a) Experimental conditions: the same as described in Table 4.3.3 (page 72) except for 60 μl sample volume in glass capillary under oxibiotic conditions.

b) [R•]: the same as defined in Table 4.3.3 (page 72).

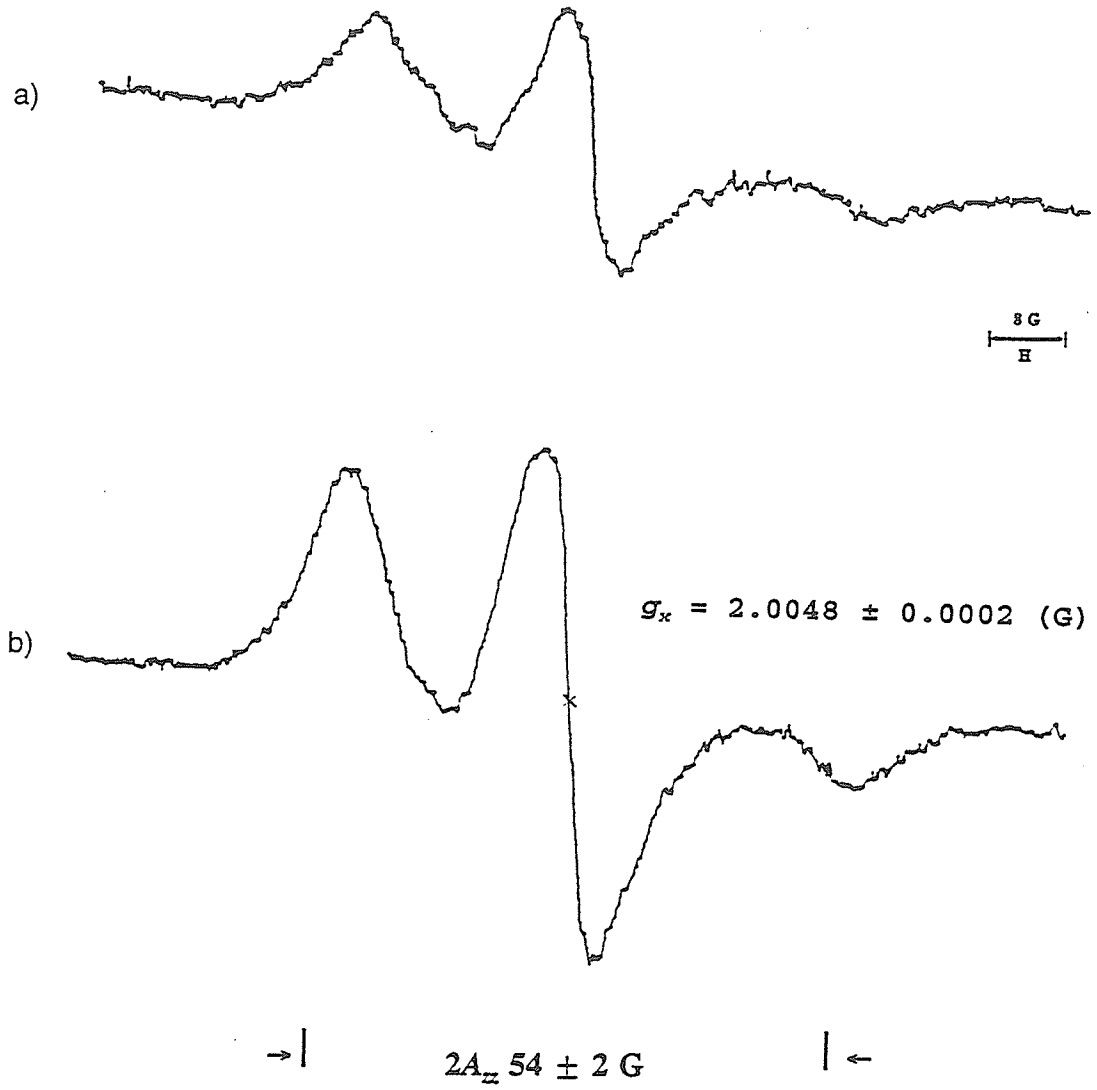

Figure 4.3.9 EPR spectra for the irradiation of nifedipine complexed with bovine serum albumin in aqueous solutions a) ABNFB.07: 2.15 mM NFDP/BSA; b) ABNFB.08: 2.15 mM NFDP/BSA.

Table 4.3.10 EPR data for the irradiation of 1.55 mM nifedipine complexed with human serum albumin in aqueous solutions

Experiment[a] No.	Modulation Amplitude(G)	Irradiation Time (min)	[R•][b] (μM)	Yield (%)
NFABH.02	2.5	20	5.9	0.38
NFABH.03	2.5	40	9.2	0.59
NFABH.04	2.5	80	20.1	1.30
NFABH.05	2.5	120	23.1	1.49
NFABH.09	1.25	40	9.2	0.59

Notes:

a) Experimental conditions: the same as described in Table 4.3.3 (page 72) except for 60 μl sample volume in glass capillary under oxibiotic conditions.

b) [R•]: the same as defined in Table 4.3.3 (page 72).

a)

b)

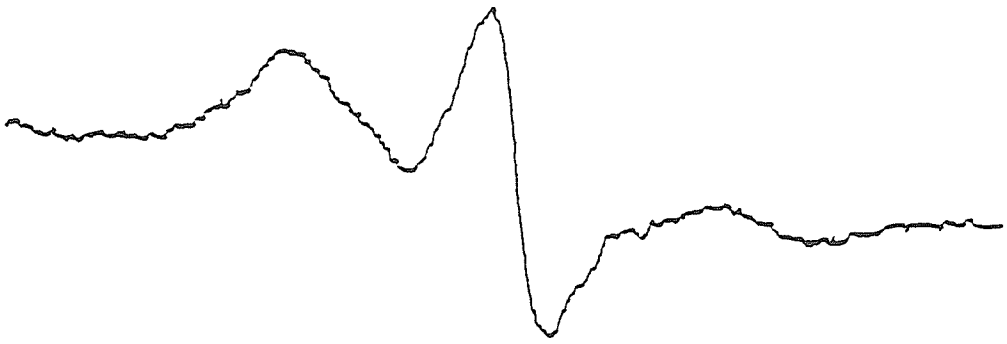

Figure 4.3.10 EPR spectra for the irradiation of nifedipine complexed with human serum albumin in aqueous solutions for different irradiation times. a) NFABH.03: 40 minutes; b) NFABH.05: 120 minutes.

Table 4.3.11 EPR data for the irradiation of

1 mM nifedipine in benzene and ethanol solutions

Experiment[a] No.	Solvent	[R•][b] (μM)	Yield (%)
NFBENZ.04	Benzene	4.0	0.4
NFETOH.04	Ethanol	1.5	0.1

Notes:

a) Experimental conditions: the same as described in Table 4.3.3 (page 72) except for 40 minute irradiation time, sample temperature at 25°C and 400 μl sample volume in glass tube under oxibiotic conditions.

b) [R•]: the same as defined in Table 4.3.3 (page 72).

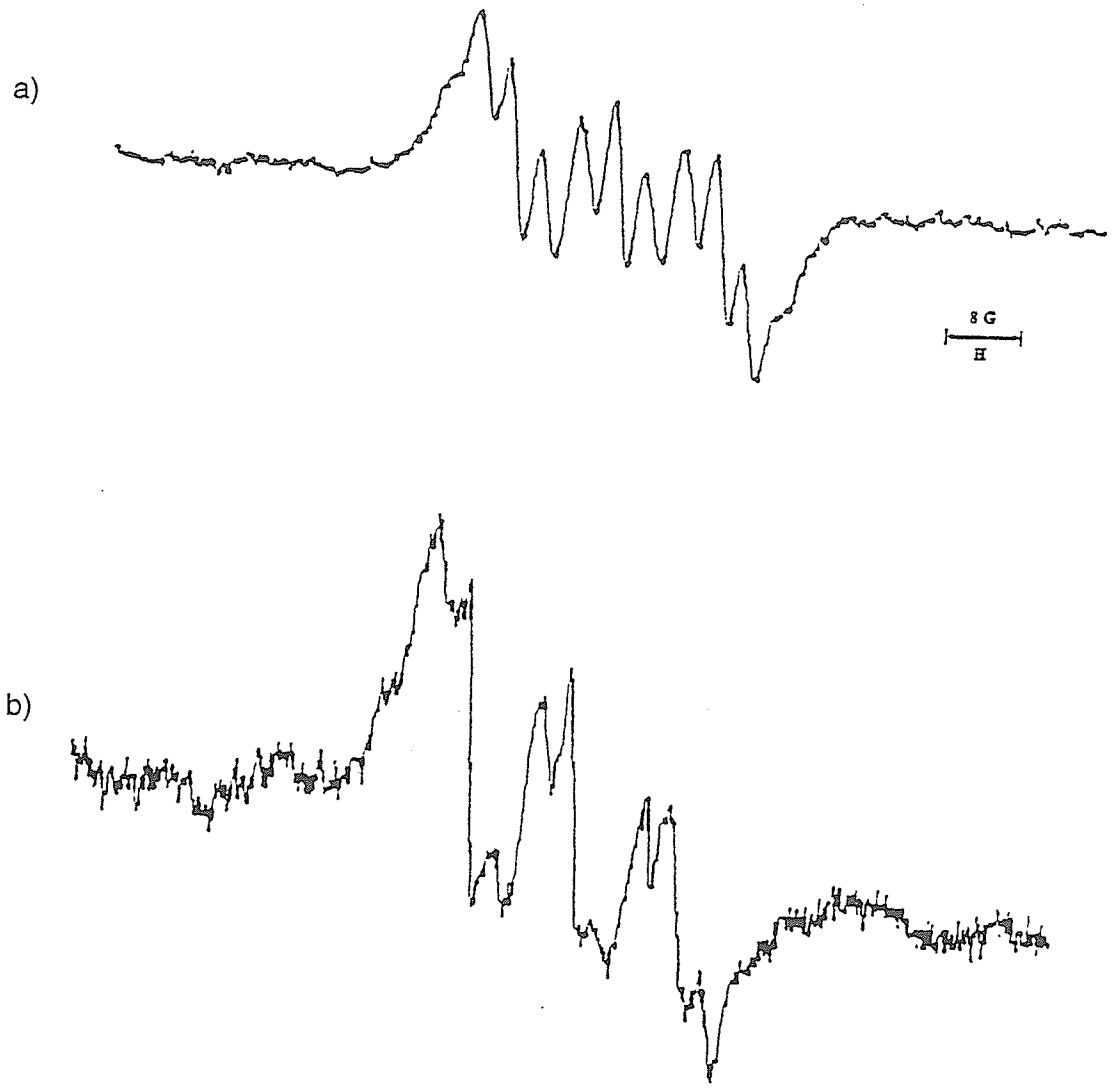

Figure 4.3.11 EPR spectra for the irradiation of nifedipine in benzene (a) and ethanol (b) solutions

PART V. DISCUSSION

5.1 DIMER-COMPLEX FORMATION

Changes in absorption spectra often occur when molecular association takes place during complex formation resulting in dimers or even oligomers. When these complexes are formed, their absorption spectra are different from those of the individual monomer species and the presence of these complexes must be taken into account to explain the observed spectra and to show that the Beer-Lambert Law is still obeyed by all of the light-absorbing species which are present in solution. UV-VIS spectroscopy provides a method to study complex-forming equilibria which may involve specific H-bonded complexes or charge-transfer (donor-acceptor) complexes in which at least one component absorbs in the spectral region (Perkampus, 1992).

On the basis of the lack of obvious new absorption bands associated with the presumed dimer association of this work, we conclude that there must be only weak association occurring between the nifedipine monomers. This weak association probably takes the form of hydrogen bonding interactions between the monomer units. Nonetheless, there were pronounced spectral changes as a function of concentration, and we have further assumed that the extinction coefficients of the dimer (E_D) and the monomer (E_M) were identical. The only justification we can offer for this latter assumption is that the monomer and dimer structures are so similar that their spectra are also similar. Clearly, more work is required to prove this rather drastic assumption.

Using this simplification, we could estimate the dimer concentrations and the dimer association equilibrium constants (K) in several solvents. From Table 4.2.1, the values of nifedipine dimer association equilibrium constants (K) in 1-octanol, 1-butanol and ethanol solutions were found respectively to be 49.3, 13.6, 7.98 (M^{-1}) which would indicate the relative occurrence of the dimer association of nifedipine. The increasing trend of the K

values in the order of increasing solvent hydrophobicity was an interesting observation. It suggests that polar interactions are still important in the presumed monomer association process. These interactions could be either hydrogen bonding or of a charge transfer type, but our absorption spectral evidence suggests that the hydrogen bonded interaction is more probable.

It is worthwhile to speculate about the size of the K value in lipid bilayer membranes even though we cannot measure it directly. Compared with the slightly hydrophobic 1-octanol solution, the K value for nifedipine dimer-complex formation in DMPC LUV or DHPC LUV systems probably should be greater because of the higher hydrophobicity of bilayer membranes. If we assume that the K value of nifedipine self-association in DMPC liposomes was > 50 M^{-1} (or > 0.05 mM^{-1}), and the concentration of nifedipine was 2.5 mM; it was found that about 10% of nifedipine in a 2.5 mM nifedipine/DMPC LUVs was in the dimeric form according to Equation [13] and the following calculation, Here, C_D is the concentration of the dimer-complex at equilibrium; C_0 is the initial concentration of nifedipine; and K is the equilibrium constant.

$$K = \frac{C_D}{(C_0 - 2C_D)^2} \qquad [13]$$

$$50 = C_D/(0.025 - 2C_D)^2$$

$(C_D)_1 = 7.25$ (mM) (unreasonable);

$(C_D)_2 = 0.25$ (mM) (reasonable).

dimerized nifedipine % = $100 \cdot (C_D/C_0) = 100 \times 0.25/2.5 = 10$ (%).

5.2 PHOTODEGRADATION MECHANISM

As confirmed in this work, nifedipine underwent a fast photodegradation to form NTSP as a major product. The elucidation of the mechanism involved in the conversion of nifedipine to NTSP is important for us to understand the photochemical reaction and to explain the formation route of the stable radicals observed by EPR spectroscopy. We noticed the reported differences in photostability between 4-(2'-nitrophenyl)-1,4-dihydropyridine derivatives and 4-(4'-nitrophenyl)-1,4-dihydropyridine derivatives (Berson and Brown, 1955a; Philips, 1951). The 4'-nitrophenyl compounds are photochemically stable even under intense irradiation by sunlight or mercury arc lamps. We believe that the suggested involvement of an *intramolecular* transfer of C_4 hydrogen to the 2'-nitro group plays a very important role in the photochemical reaction of nifedipine (Berson and Brown, 1955a).

In fact, hydrogen abstraction by the photoexcited nitro group and formation of the *aci*-nitro structure (Figure 5.2.1, reaction a) was deemed to be probable due to the existence of low-lying n,π^* excited states (de Mayo, 1960). A number of photochemical molecular rearrangements of *ortho*-nitrobenzylic hydrogen to the nitro group have been reported, in which the nitro group is reduced to a nitroso group while an oxygen atom is apparently inserted into a C-H bond located in an *ortho* position (Figure 5.2.1, reaction b). The requirement of *ortho* orientation was recognized, probably for the first time, by Sachs and Hilpert, who proposed that 'all aromatics which have a hydrogen ortho to a nitro group will be light sensitive' (Sachs and Hilpert, 1904). Typical examples of their mechanisms are discussed in the photoreactions of *o*-nitrobenzaldehyde (Leighton and Lucy, 1934) and *o*-nitrophenyldiphenyl methane (Tanasescu, 1926). As shown in Figure 5.2.1 (reaction c), nitrosobenzene also abstracts a hydrogen atom which is less reactive and forms a free radical which tends to dimerize (Mauser and Hertzer, 1965).

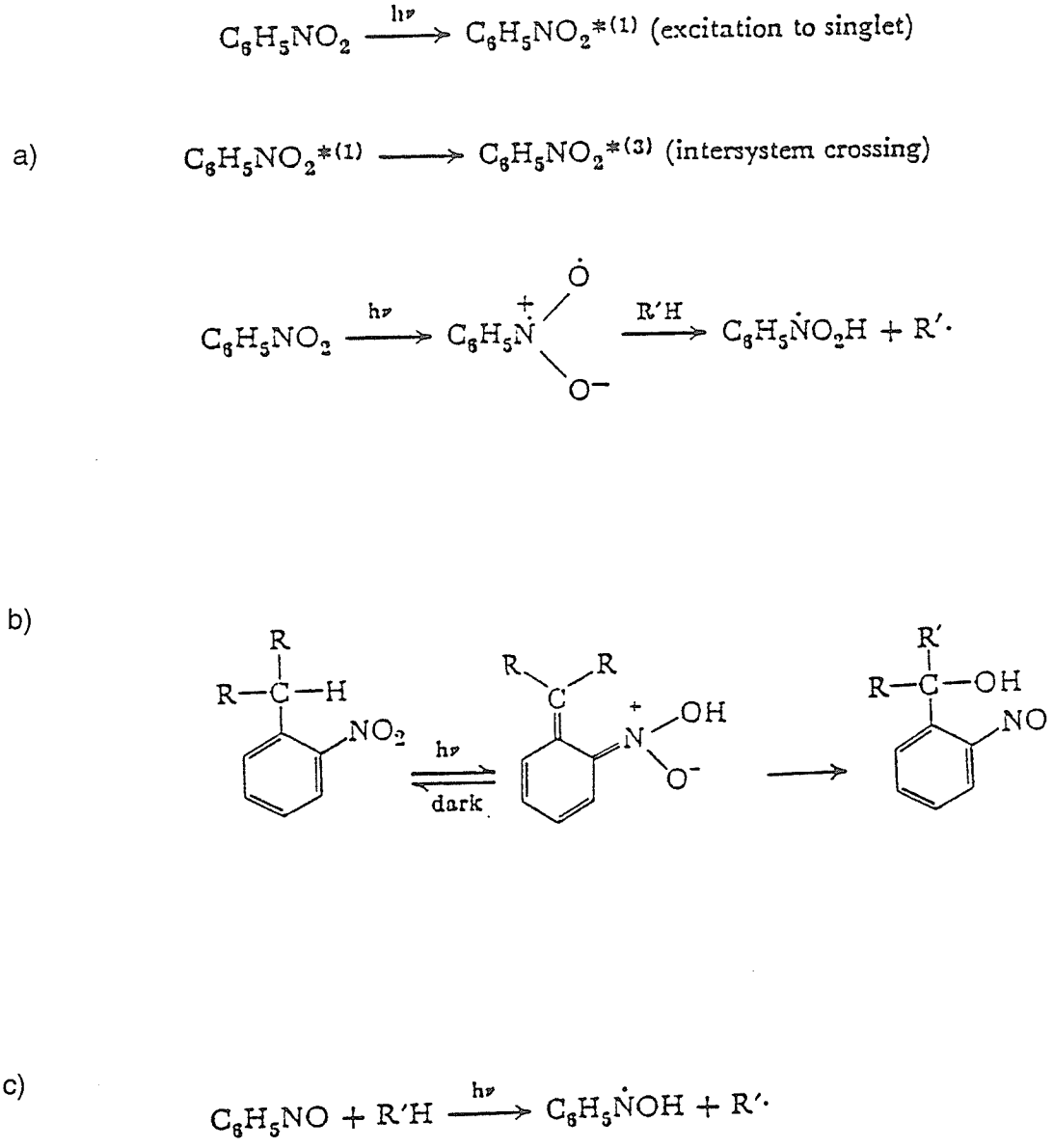

Figure 5.2.1 Related hydrogen abstraction and oxygen insertion reactions.

Similar to other *ortho*-nitrobenzylic compounds, we propose that nifedipine undergoes a photochemical reaction mechanism according to the one shown in Figure 5.2.2. The nitrobenzene moiety of nifedipine (Figure 5.2.2, structure I) will be excited to form a n,π^* triplet state (Figure 5.2.2, structure II) which is probably responsible for the hydrogen abstraction. The excited nitro group of nifedipine abstracts the C_4-hydrogen to form an *aci*-nitro compound with a carbon-centred free radical (Figure 5.2.2, structure III). However, neither the biradical molecule itself nor its spin trap adducts were observed in our experiments. This may suggest chemical instability resulting from a very fast intramolecular rearrangement to form an EPR silent intermediate (Figure 5.2.2, structure IV). Through an intramolecular reaction, the intermediate changes into the 2'-nitrosophenyl-1,4-dihydropyridinol derivative (Figure 5.2.2, structure V) which is aromatized by intramolecular dehydration to form 2'-nitrosophenylpyridine (NTSP) (Figure 5.2.2, structure VI).

To the best of our knowledge, none of the known nifedipine photochemical studies to date have suggested the existence of the 1,4-dihydro-4-pyridinol derivatives. In our monitoring of the products observed with the irradiation of the filtered tungsten-halogen lamp, room light and sunlight, we only found the presence of NTSP as a major product. We also could not find any reports on the preparation or properties of 1,4-dihydro-4-pyridinol or 1,2-dihydro-2-pyridinol derivatives. This dearth of information most probably points to the instability of 1,4-dihydro-4-pyridinol which easily forms the aromatized pyridine ring by dehydration. The suggested 1,4-dihydro-4-pyridinol intermediate may play an important role in the photodegradation mechanism of nifedipine, particularly in conjunction with the o-nitrophenyl group.

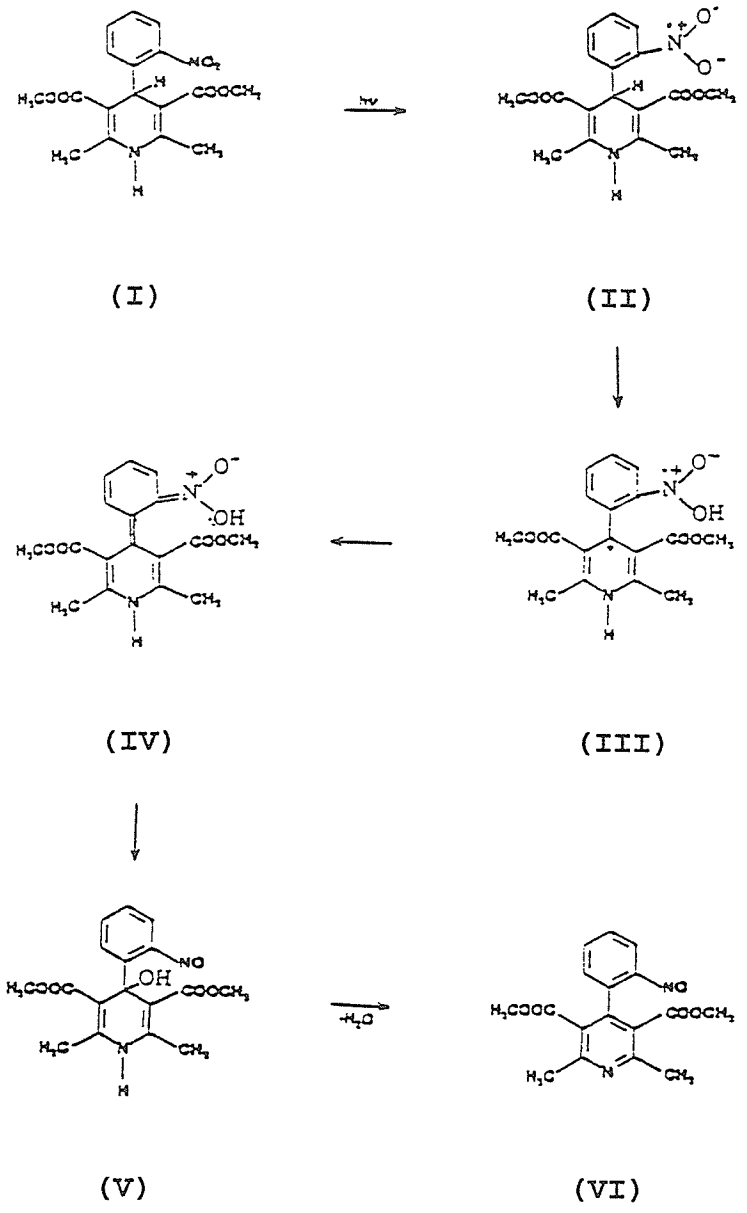

Figure 5.2.2 Proposed mechanism for the nifedipine photodegradation.

5.3 RADICAL ANALYSIS

5.3.1 Radical Formation

1) Formation in liposome aqueous dispersions

We chose DMPC and DHPC lipids in the form of large unilamellar vesicles (LUVs) and multilamellar vesicles (MLVs) as model systems to study the interaction of nifedipine with the lipids. DMPC is a saturated diester phospholipid with a gel-to-liquid crystal transition temperature (T_c) of 37°C, whereas DHPC is a saturated diether phospholipid with a gel-to-liquid crystal transition temperature (T_c) of 50°C (Marsh, 1990).

For both the DMPC and DHPC lipids, it was observed that nifedipine incorporated in LUV bilayer membranes always gave higher resolution spectra for the radicals than those observed in MLVs of the same lipids (Figure 4.3.6). However, there was not a large difference between the measured concentrations of the radicals produced in the LUVs and MLVs (Table 4.3.6). The lower spectral resolution seen for the radicals detected in the MLV samples may be related to the diversity of lipid structures present in these samples which were prepared by a simple vortexing technique. Since there was no extrusion of these MLV lipid dispersions, the possible structures formed would include some micelles and brick-like structures besides the majority of multilamellar structures. This kind of heterogeneity is expected to occur in the phase diagrams for all lipids (Marsh, 1990) when the dispersions are studied at temperatures close to and above their respective T_c values.

At the temperatures of 16°C, 27°C, 37°C and 47°C, the concentrations of the free radicals detected in NFDP/DHPC LUVs were almost the same (Table 4.3.8), but the spectrum obtained at 37°C showed the best resolution (Figure 4.3.8b). An optimum temperature around 37°C may result from the dual benefits of low viscosity in the bilayer membranes of the liposomes and sufficient thermal stability of the detected radicals at this

temperature.

We found that the DHPC lipids with nifedipine always showed a triplet signal even in the dark (Figure 4.3.7). The splitting constant of the triplet is $a_N \approx 16.2$ gauss which is typical for many nitrogen centred radicals. One of the explanations might be the existence of a trace of peroxide as an impurity in the ether lipid. Nifedipine could be reduced by the peroxide compound to a nitroso compound which may function as a spin trap (Figure 5.3.1).

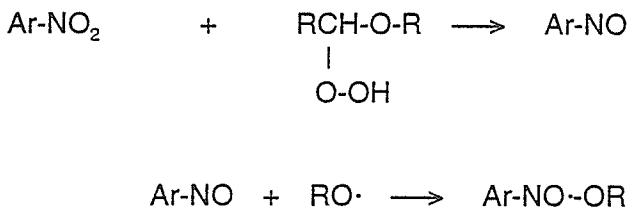

Figure 5.3.1 Formation of nitroso compound in the presence of peroxide

2) Formation of radicals bound to albumins in aqueous solutions

Compared with the high resolution spectra obtained from NFDP/LUVs, the EPR spectra of NFDP incorporated in albumins always gave a strongly immobilized free radical spectrum with approximate EPR spectral parameters of $2A_{zz} = 54 \pm 2$ gauss (assuming cylindrical symmetry for a nitroxide radical) and $g_{av} = 2.0048 \pm 0.0002$ (Figures 4.3.9 and 4.3.10). The growth in the observed free radical signals approached a plateau steady state value after about 100 minutes of irradiation (Tables 4.3.9 and 4.3.10). The consistent observation of strongly anisotropic spectra indicated clearly that the radicals had extremely limited motions on the EPR timescale (nanoseconds to microseconds) and that they were immobilized on the proteins. In this case, the radical adducts would have random

orientations with respect to the strong magnetic field. For a nitroxide free radical with cylindrical symmetry, A_{zz} is much greater than A_{xx} and A_{yy} and it can be measured directly from the spectrum with a reasonable accuracy (McConnell and McFarland, 1970). Similar spectra have been reported in the system of nifedipine incorporated in low-density lipoproteins, but it was not certain if nifedipine was immobilized primarily in lipids or in the protein component (Ondrias *et al*, 1994). The present experiments clearly indicate that there are very different behaviours for nifedipine associated with either pure lipids or proteins. Nifedipine shows a relatively free motion in bilayer lipid membranes, whereas it is strongly immobilized on the albumin proteins. This result is consistent with the observation that nifedipine can penetrate various biological membranes but be absorbed strongly on the hydrophobic portion of albumin plasma proteins.

3) Formation under ambient oxibiotic or hypoxic conditions

The formation of the radicals under ambient oxibiotic and hypoxic conditions was studied (Figure 4.3.3 and Table 4.3.3). There was no obvious evidence to show that oxygen was important or even involved in the photochemical mechanism in this work, either as a participant or as a quencher. This result is not in agreement with the work reported by Vargas *et al* (1992) in which some singlet oxygen was found by trapping it with 2,5-dimethylfuran to produce hexene-2,5-dione. The general question of the possible role of molecular oxygen in the nifedipine photochemistry is important for an adequate understanding of the mechanism. Our experimental results indicated that oxygen was not required for the conversion of nifedipine to NTSP, and furthermore oxygen did not act as a major quencher of the photoreaction which is consistent with the proposed intramolecular mechanism. The resolution of the EPR spectra obtained under hypoxic

conditions was better than that under oxibiotic conditions. For hypoxic and oxibiotic conditions, the apparent peak-to-peak linewidths were found to be respectively ~0.7 G and ~0.8 G. The broader apparent peak-to-peak linewidth observed in the oxygenated aqueous dispersions could be explained by the usual Heisenberg spin exchange broadening of the EPR spectral lines through collisions of the free radicals with molecular oxygen.

4) Formation in the presence of added spin traps

By the use of added PBN, we compared the performance of endogenous NTSP with exogenous PBN as competitive spin traps in some EPR photochemical experiments involving nifedipine. Secondly, in the context of comparing exogenous and endogenous spin traps, we also examined whether or not NTSP itself could produce reactive radicals through its photochemistry. The rationale for choosing PBN as a competitive spin trap was its hydrophobicity which was like that of nifedipine and NTSP.

First, the EPR spectra for the irradiation of nifedipine in DMPC LUV systems without and with the addition of PBN were compared as displayed respectively in Figures 4.3.4a and 4.3.4b. The two spectra are very similar with respect to both the types of radicals observed and their amplitudes. Therefore, the addition of PBN had almost no measurable effect on the observed spectra. The EPR spectra of PBN spin adducts usually consist of three doublets with a relatively small variation (Evans, 1979). If PBN really formed adducts with the reactive radicals produced in the reaction, their EPR spectra should be totally different from that of NTSP adducts. The observation of very similar spectra in Figures 4.3.4a,b indicated that PBN was ineffective as a spin trap compared with the endogenous NTSP. This may be attributed to the existence of

molecular association between NTSP and various nifedipine derived radical products.

The corresponding results are shown for the irradiation of NTSP samples, both in the absence and presence of PBN, in Figures 4.3.5a and 4.3.5b. Both spectra are very similar, and furthermore both are much weaker but similar to that of Figure 4.3.4 which was the result observed for the nifedipine irradiations. On the basis of this spectral similarity with weaker amplitudes, we conclude that the NTSP radical adducts were derived from the presence of small amounts of nifedipine in the NTSP product which was only about 95% pure. In the context of this interpretation, the further addition of PBN to this system gave no new information relative to the stronger nifedipine photochemical result of Figure 4.3.4. It is clear that NTSP by itself does not produce any reactive radicals which can be detected, and it only functions as an endogenous spin trap with high yields in the photochemical reaction of nifedipine.

5) Formation in organic solutions

The EPR spectra of free radicals derived from nifedipine photochemistry were studied in several organic solvents as reaction media for a comparison with the lipid and protein results. In these homogeneous solutions, we were surprised to discover that although stable free radicals were produced, they did not have the well resolved EPR spectra which were typical of our lipid dispersion experiments. Typical experimental EPR results measured in benzene and ethanol solutions are shown in Figure 4.3.11.

In this respect, our results are different from the well resolved EPR spectra reported in various organic solvents (Stasko *et al*, 1994). On the basis of these well resolved spectra, they were able to propose the essential structural components of two radicals, designated A and B (Figure 1.3.2), which were consistent with the EPR spectral

results. We tried all of the solvents reported by the previous workers, and we tried various nifedipine concentrations; but we were unable to acquire EPR spectra of any better resolution than that reported in Figure 4.3.11. This observation was not due to high concentrations of free radicals which can cause line broadening through Heisenberg spin exchange broadening. For instance, the free radical concentration in ethanol solution was only about 1 μM which is much less than the concentrations obtained from the LUV lipid dispersions (usually 5 ~ 20 μM). Another line broadening mechanism such as the presence of paramagnetic impurities seems to be extremely unlikely because of the purity of the solvents which were used for solutions. On the other hand, dimerization of free radicals could give rise to some broadening through the spin exchange mechanism. However, on the basis of our observations, it is appears most likely that various reactions of the free radicals are responsible for the lower concentrations of the radicals observed in solution. Furthermore, in our hands, the spectra measured in solution were always different from those seen in LUV dispersions which clearly demonstrates that different stable free radicals were produced in the homogeneous solutions.

5.3.2 Radical Structures

As mentioned in the Introduction, Misik *et al* (1991) first suggested the potential spin trapping property of illuminated nifedipine when they studied its antioxidative activity on lipid peroxidation. The spin trapping property of illuminated nifedipine was attributed to the production of the nitroso compound, NTSP, which was confirmed by trapping free radicals formed in the thermal decomposition of 2,2'-azobiisobutyronitrile and radicals formed by photolysis of di-*tert*-butylperoxide. The very efficient spin trapping property of NTSP was also confirmed in our experiments by the comparison of the EPR spectra with or without the addition of PBN in DMPC liposome systems of nifedipine and NTSP.

The free radicals detected in our experiments may come from several possible pathways in the absence of exogenous spin traps. The involvement of NTSP as an endogenous spin trap facilitates the trapping of some very specific free radicals. which are derived from the specific chemical structure of nifedipine. For instance, a homogeneous break at the C_4- hydrogen bond causes the formation of a carbon-centred radical which can be stabilized by the electronic conjugation effect of the 7-electron $n^{\cdot}_{N}$-π_{C2-C3}-$n^{\cdot}_{C4}$-π_{C5-C6} dihydropyridine ring system as shown in Figure 5.3.2, structure I. Some other pathways may be related to the spin trapping property of NTSP as shown in Figure 1.3.1. Here, we underline the fact that NTSP is a major product in the photochemistry. NTSP may trap a carbon-centred radical formed in the ring of dihydropyridine in an intermolecular (Figure 5.3.2, structure II) or intramolecular way (Figure 5.3.2, structure III). NTSP may also trap or abstract some small radical pieces such as a hydrogen radical (Figure 5.3.2, structure IV), possibly formed in the process of the photodegradation. In order to determine the structures of the radicals detected in our experiments, we tried to analyze and simulate the spectra in a logical manner.

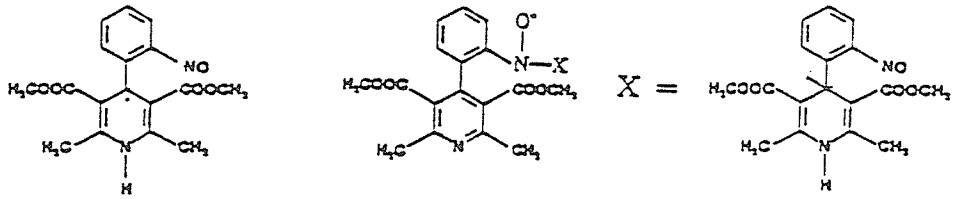

(I) (II)

(III)* (IV)*

Figure 5.3.2 Possible structures for the radicals detected in the photochemical experiments

* Reported by Stasko *et al* (1994) (see Figures 1.3.2).

1) One-radical approach:

As a first attempt at spectral simulation, we tried to interpret the experimental spectra in terms of one radical. On inspecting the EPR spectra obtained from DMPC LUVs shown in Figures 4.3.3 and 4.3.4 and from benzene solution shown in Figure 4.3.11a, we found a common nitrogen ($I = 1$) hyperfine splitting value of 12 ± 1 gauss. We assumed that this splitting constant came from a stable nitroxide type of radical and not from an unstable carbon-centred radical (e.g., Figure 5.3.2, structure I). Further analyzing the spectrum as shown in Figure 4.3.3, we initially proposed some approximate splitting constants which are reported in Part I of Figure 5.3.4. However, the simulated spectrum which resulted from these splitting constants did not give a satisfactory fit to the experimental spectrum of Figure 4.3.3a. Of particular concern was the fact that the spectral width of the simulation was about 10 gauss less than that of the experimental spectrum.

We considered several models including one where we attributed splitting constants to a second and even a third nitrogen atom which were both present in the presumed structure. However, we finally rejected this model because of the probable lack of extensive electron spin density delocalization in a nonaromatic system. This was confirmed when we compared the result of PBN trapping phenyl radical and o-nitrophenyl radical (Figure 5.3.3) (Janzen *et al*, 1982; Xu *et al*, 1985). With reference to these PBN spin adduct models, we found that the addition of a nitro group in a δ-position did not cause any new spectral splitting besides exerting its strong effect on the splitting constants of the α-N and β-H atoms. Therefore, we came to the conclusion that the unique radical structure which we were considering was insufficient to account for the experimental spectrum which we wanted to simulate.

a)

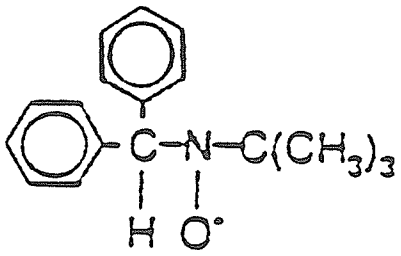

a_N 14.57 G, a_H 2.16 G;

b)

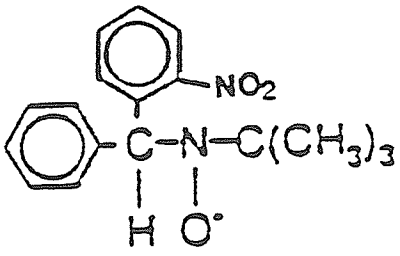

a_N 13.90 G, a_H 2.78 G.

Figure 5.3.3 The effect of the o-nitro group on the splitting constants observed in the EPR spectra for the spin adducts of PBN with phenyl and o-nitrophenyl radicals

2) Two-radical approach:

During the course of our work, the previously mentioned study (Stasko *et al*, 1994) appeared in the literature. This latter work proposed for the first time that two stable radicals were produced by the nifedipine photochemistry, and these workers used a light source with wavelengths greater than 365 nm which was similar to the light source of this work. The general molecular structures of the two radicals which they proposed are shown in Figure 1.3.2. The splitting constants obtained from the reported work (Stasko *et al*, 1994) are shown in Part II of Figure 5.3.4.

According to the splitting constants of the two radicals reported in Stasko's work, we then simulated the EPR spectra for these radicals. Then, by using a spectrum addition program, we added the two spectra together at various relative ratios. We discovered that the added simulated spectra did give a reasonable fit to the experimental spectrum of Figure 4.3.3a when we chose a value of 1:(0.65±0.05) for the radical A to radical B ratio. Stasko et al specified the structure shown in Figure 5.3.2 (III) as one possible radical. In fact, both the structures II and III shown in Figure 5.3.2 could give an EPR spectrum which was similar to that attributed to radical A (Stasko *et al*, 1994).

The presence of the two different radical types, A and B, can explain the EPR results in our experiments. The results of the simulations are shown in Figure 5.3.5. where reasonable agreement between the experimental and simulated spectra is evident.

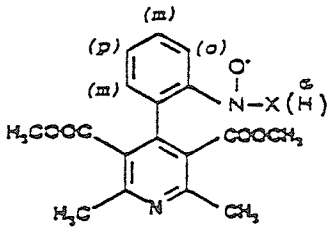

For Radical A, the substituent is X (see Figure 5.3.2, structure II);

For Radical B, the substituent is H.

I). Estimated splitting constants by using a one radical model in the present work:

a_N 12.04 ± 0.05 G;

2x $a_{H(m)}$ 1.06 ± 0.05 G; *aH(o)* 3.28 ± 0.05 G;

aH(p) 3.39 ± 0.05 G.

II). Reported splitting constants (Stasko *et al*, 1994):

For radical A:

a_N 10.26 G;

2x $a_{H(m)}$ 0.95 G; *aH(o)* 3.10 G; *aH(p)* 3.22 G.

For Radical B:

a_N 9.08 G; $a_{H(\alpha)}$ 12.16 G;

2x $a_{H(m)}$ 1.10 G; *aH(o)* 2.95 G; *aH(p)* 3.15 G.

Figure 5.3.4 The splitting constants and their designation for radical A and radical B

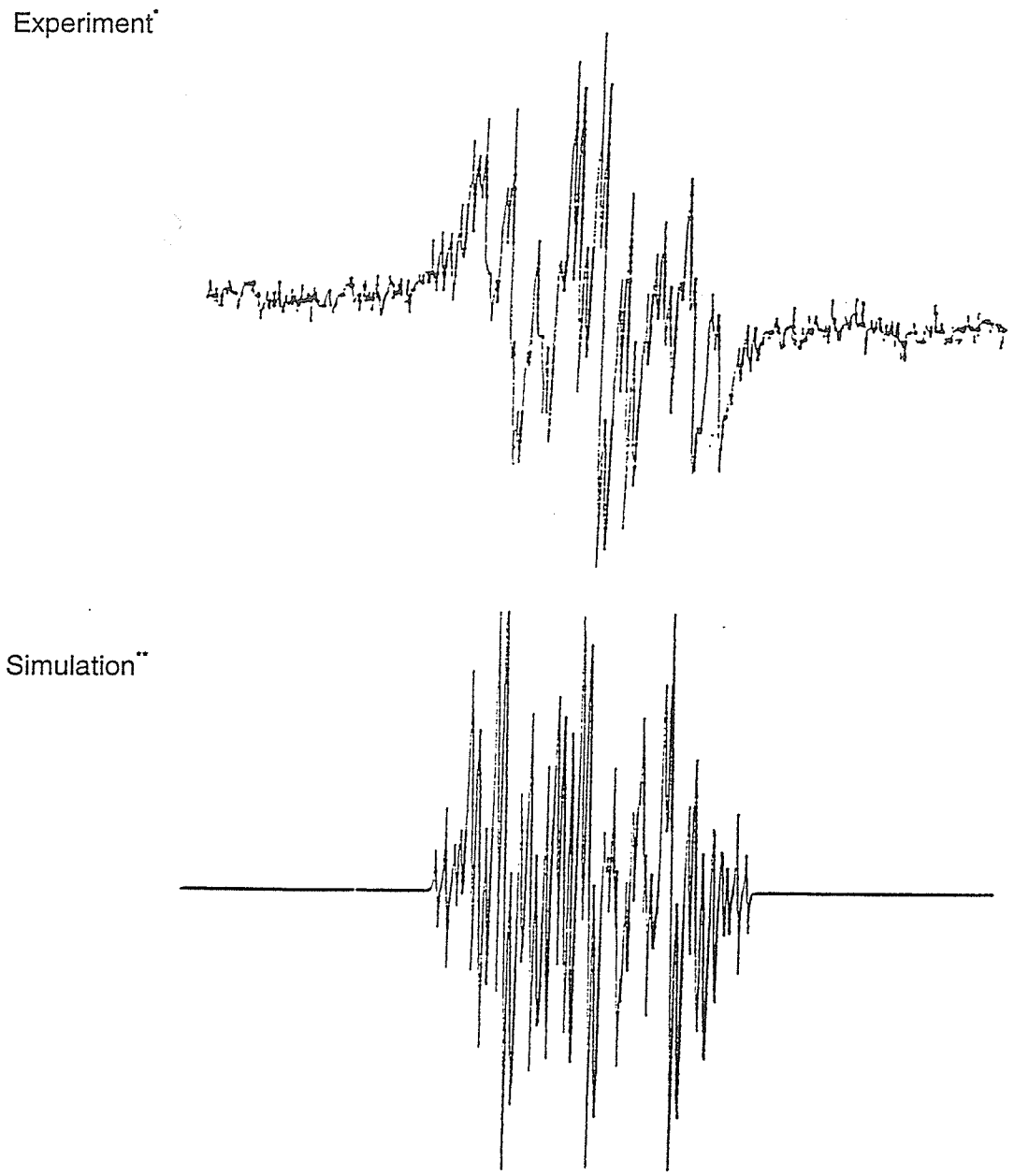

Figure 5.3.5 Experimental and simulated EPR spectra for the detected radical adducts

*: Experimental spectrum obtained from the present work; **: Simulated spectrum based on the reported splitting constants (Stasko *et al*, 1994) for a 1.0:0.65 mixture of radicals A and B .

5.3.3 Formation Pathways

It is clear that our work confirmed that NTSP acted as an endogenous spin trap and gave rise to the detected stable radical adducts. However, the proposed carbon-centred free radical shown in Figure 5.3.2 (structure I) was not observed. The spectrum simulation results indicated the presence of only two radicals A and B (Figure 5.3.2, structures II and IV). In this interpretation, there was no doubt about the structure of radical B (Figure 5.3.2, structure IV). However, the precise structure of the X group in radical A has not been clarified at present. Stasko *et al* (1994) proposed a general formula and several possible compounds for radical A (see Figure 1.3.2). Furthermore, one favorable structure was specified for radical A (Figure 5.3.2, structure III). We proposed a similar structure as shown in Figure 5.3.2 (structure II), including a specific X group. This latter structure could give the same EPR spectrum as radical A as reported (Stasko *et al*, 1994). Furthermore, the formation pathway of the radical A can be explained based on the proposed photochemical mechanism of the present work.

Stasko *et al* (1994) first proposed a formation pathway of the radical A by hydrogen abstraction through a hydrogen-bond dimer as an intermediate in the nifedipine photochemistry. However, they could not explain adequately the lag time between the generation of the two radicals. Although the nitrosobenzene moiety of NTSP can also abstract a hydrogen atom from nifedipine and form a free radical (Figure 5.2.1, reaction c), it seems unlikely that this will occur rapidly in nifedipine or in any of the derived photochemical products. The EPR results (Stasko *et al*, 1994) indicated that the X group in the radical adduct A was an EPR silent substituent and that the hydrogen in radical B originated from the nifedipine skeleton. Radical A with an EPR silent substituent was formed immediately upon irradiation, and then radical B with a hydrogen substituent came

up after prolonged irradiation. This means that radical B was formed after the formation of radical A according to the work (Stasko *et al*, 1994). As shown in Figure 5.3.6, if radical B was really formed as a result of NTSP first abstracting a hydrogen atom, it should be observed as a free radical, probably simultaneously with the observation of radical A. Obviously, this is not consistent with the experimental results (Stasko *et al*, 1994). Therefore, instead of the pathway of hydrogen abstraction, another route may be more pertinent as a mechanism for forming the stable trapped radicals.

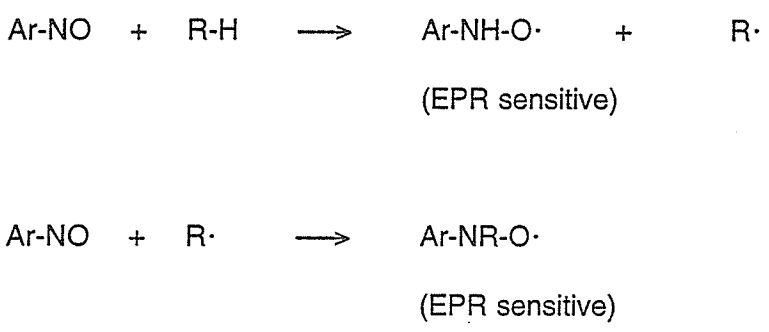

Figure 5.3.6 Formation of radicals predicted from the hydrogen abstraction by NTSP

From the mechanism we proposed (Figure 5.2.2), we may explain the lag time between the observation of radical A and radical B. In the following discussion, it is assumed that the dehydration of the 1,4-dihydro-4-pyridinol derivative (Figure 5.2.2, structure V) occurs by a two-step free radical formation mechanism.

First, we propose that the C_4-OH bond of structure V in Figure 5.2.2 must undergo a homolytic fission into a carbon-centred radical and a hydroxyl radical. This process could be concerted with NTSP abstracting the hydroxyl group as it forms, or the process could

be consecutive with NTSP trapping the hydroxyl radical through a dimer or even a termolecular complex. The radical Ar-NO˙-OH has not been observed by EPR so far, and we have assumed that it is very unstable in agreement with other workers (Levy and Cohen, 1979). By intermolecular or intramolecular trapping, the radical adduct of NTSP and the carbon-centred radical, 2'-nitrosophenyl-1,4-dihydropyridin-4-yl radical (Figure 5.3.2, structure I) could form as radical A in two different structures as previously shown in Figure 5.3.2 (structures II and III). The ring strain associated with a 4-membered ring in the radical (Figure 5.3.2, structure III) may prevent its formation by an intramolecular route. Therefore, the structure II formed by an intermolecular trapping pathway may be a more reasonable structure for the stable radical A.

Secondly, we propose that radical B (Figure 5.3.2, structure IV) could be formed by NTSP trapping a hydrogen radical or abstracting a hydrogen atom. The hydrogen could be the N^1 - H in the 1,4-dihydropyridine of structure V in Figure 5.2.2. The hydrogen coming from either of the two methyl groups in the pyridine ring could also not be completely excluded. Furthermore, the formation of the conjugated system from the 1,4-dihydropyridin-4-yl ring radical may promote the leaving of the hydroxyl group and retard the departure of the hydrogen atom, resulting in the lag time between the formation of the two radicals. In addition, the existence of a dimer complex would promote the intermolecular mode of radical trapping by NTSP. Finally, the observation of a faster photochemical reaction in liposome bilayer membranes possibly points to the existence of either a nifedipine-radical or NTSP-radical dimer complex which would promote faster spin adduct formation reactions in the bilayer membranes.

The possible pathways which we have discussed for the formation of the radicals are summarized in Figure 5.3.7.

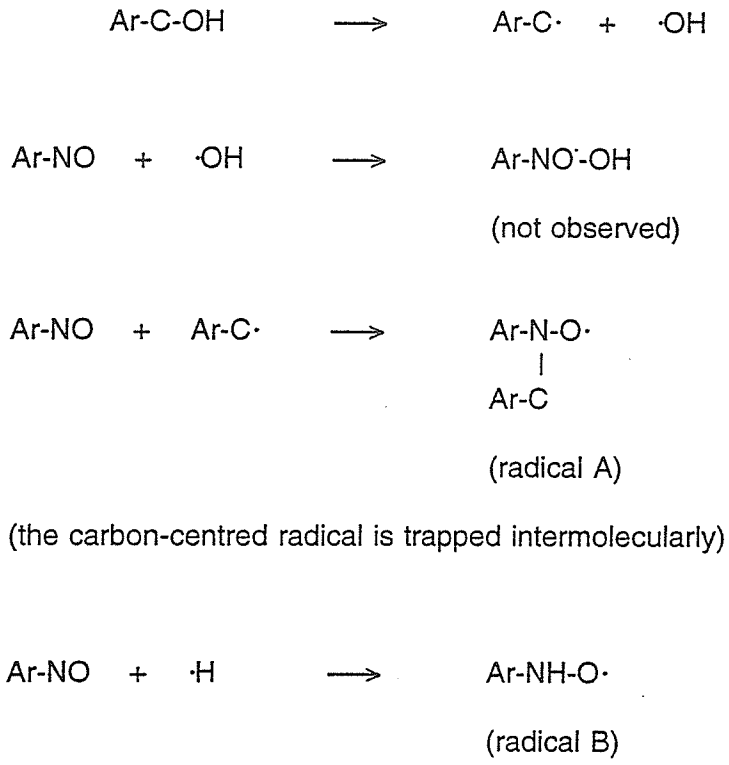

Figure 5.3.7 Possible formation pathways of the detected radical adducts

PART VI. CONCLUSIONS

6.1 CONCLUSIONS

1) Biological interactions

Nifedipine was incorporated in the bilayer membranes of DMPC and DHPC aqueous lipid dispersions, first in the form of multilamellar vesicles (MLVs) by vortexing and secondly in the form of large unilamellar vesicles (LUVs) by the extrusion technique (Nayar *et al*, 1989). Nifedipine was also absorbed on bovine and human albumin proteins in aqueous solutions by the vortexing method. The concentrations of nifedipine in the samples were measured by the method of first derivative UV-VIS spectrometry which was based on the fact that NTSP does not have any significant absorption at wavelengths > 380 nm while nifedipine has a characteristic first derivative absorption minimum around 400 nm.

Nifedipine was usually incorporated in DMPC LUVs and in DHPC LUVs at the concentrations of 2 ± 0.5 mM. The molar ratios of DMPC/NFDP and DHPC/NFDP were in the range of 12 ~ 25 in the present work. The high concentrations of nifedipine in lipid indicated that the incorporated nifedipine should be distributed in the bilayer membranes of the liposomes. In the aqueous albumin solutions, the nifedipine concentration which was absorbed by protein was in the range of 0.5 - 2.0 mM. The interesting result of nifedipine to bovine albumin association showed that maximum molar ratios of nifedipine bound to the protein were close to 1 ([NFDP]/[BSA] = 1 ± 0.1). The approximate 1:1 molar ratio of NFDP/BSA implied that nifedipine may be absorbed only at specific binding sites on the protein. It was possible that one nifedipine molecule really interacted with one albumin macromolecule. But other binding variations such as some proteins having zero, others one, and some more than one molecule of nifedipine attached cannot be excluded on the basis of the present data.

The EPR study further indicated that the biological interactions of nifedipine with the bilayer membranes of the C_{14} saturated carbon chains and with albumins were very

different. Nearly isotropic EPR spectra with very high spectral resolution for the free radicals were obtained from both DMPC and DHPC LUVs. This result clearly indicated that the nifedipine molecule was relatively mobile in the saturated chain bilayer membranes of the LUV vesicles. However, nifedipine was strongly immobilized upon binding to albumin proteins as demonstrated by the highly anisotropic nature of the EPR spectra of the free radicals formed in the protein systems. In the protein aqueous solutions, nifedipine and its derived free radicals clearly stay bound to high affinity binding sites. There are no such sites available in the bilayer membranes of the LUVs, and hence greater mobility was always observed in the vesicle systems. Finally, it is important to mention that the free radical spin adducts are relatively large molecules; and they would also have the poor aqueous solubility which is characteristic of nifedipine itself.

2) Dimer-complex formation

Nifedipine's self-association may play an important role in the photodegradation of nifedipine and also in the formation of the NTSP radical adducts. By UV-VIS spectroscopic methods, we measured the absorptivities of 1-20 mM solutions of nifedipine in ethanol and 1-butanol as well as for 1-10 mM solutions of nifedipine in 1-octanol. As a first attempt, we tried to evaluate the equilibrium dimer formation constants (K) and the extinction coefficients (E_D) in the various solvents by employing an iteration method based on the proposed Equation [5] (page 17). However, this method was not successful probably due to the close similarity between the absorption profiles of the monomer and the dimer complex. Assuming that the monomer and dimer spectra were very similar, we simplified the association equation to that of Equations [13] and [15] (page 58 - 59). The simplifying assumption was that the E_D and E_M values were identical, and this allowed us to estimate the dimer-complex formation equilibrium constants (K) as 7.98 ± 45%, 13.6 ± 26% and 49.3 ± 8% (M^{-1}), respectively in ethanol, in 1-butanol and in 1-octanol

solutions.

The formation of the nifedipine dimer complex was apparently stronger as the solvents became more hydrophobic according to the trend in the estimated K values for ethanol, 1-butanol, and 1-octanol solutions. On the basis of our absorption spectral observations for nifedipine in these solvents, the hydrogen bonded dimer complex appears to be probable. It is even possible that there is more than one complex type such as dimers, trimers and even the association of nifedipine with its various photochemical products. We estimated that about 10% of nifedipine was dimerized in the 2.5 mM nifedipine solution in 1-octanol. Compared with 1-octanol, DMPC and DHPC lipids should have higher hydrophobicities in their bilayer membranes. Therefore, if dimerization is enhanced by hydrophobicity in the membrane environments, nifedipine could have an even greater extent of dimerization in these bilayer lipid membranes.

3) Photodegradation mechanism

It was confirmed that 2,6-dimethyl-4-(o-nitrosophenyl-3,5-dimethylpyridine dicarboxylate (NTSP) was the major photochemical product which probably functions as a spin trap. The photochemical kinetic study revealed a faster conversion of nifedipine to NTSP in DMPC aqueous dispersions than that seen in ethanol solution for similar overall concentrations. The faster kinetics could be explained by the promotion of a higher dimerization of nifedipine in the bilayer membranes of the liposomes which we attribute to the higher hydrophobicity of these membranes.

A mechanism of a C_4-hydrogen atom transferring to the ortho nitro group for the conversion of nifedipine to NTSP was proposed in this work. The photo-excited nitro group of nifedipine abstracts the C_4-hydrogen to form a *aci*-nitro compound which undergoes a concerted series of intramolecular rearrangements to form the 2'-nitrosophenyl-1,4-dihydropyridinol derivative as an intermediate. This intermediate is then aromatized by

intramolecular dehydration to 2'-nitrosophenyl-pyridine (NTSP) (Figure 5.2.2, structure VI). In the mechanism, the 1,4-dihydro-4-pyridinol derivative was proposed as a key intermediate. Although we did not find any direct evidence to prove the presence of the 1,4-dihydro-4-pyridinol derivative as an intermediate in the proposed mechanism, it gives an explanation for the formation pathway of the detected radical adducts, particularly for the observation that radical A is formed before radical B.

4) Radical formation

The stable radicals which were involved in the nifedipine photochemistry were carefully studied by EPR spectroscopy. The comparison of EPR studies under oxibiotic and hypoxic conditions (Table 4.3.3 & Figure 4.3.3) did not show any indication of an involvement of oxygen in the formation of radicals, even as a quencher. The concentrations of the radicals in the liposome dispersions and in the protein aqueous solutions were usually about 10 to 20 μM with respect to the initial nifedipine concentrations of about 2 ± 0.5 mM. The spectral simulation of a higher resolution spectrum (Figure 4.3.3a) obtained from nifedipine/DMPC LUVs revealed the presence of both radical A and radical B with a stoichiometric ratio for A:B of 1:(0.65 ± 0.05). Radical B was assumed to be the same as that suggested by Stasko *et al* (1994) (see Figure 1.3.2b). However, in the case of radical A, we proposed another structure (Figure 5.3.2, structure II) which was different from the structure suggested by Stasko *et al* (1994). Our proposed structure is also consistent with the observed hyperfine splitting constants for radical A. The proposed structures for the two radicals can be simply shown as the following:

(radical A) (radical B)

For the two above stable radical adducts observed by EPR, their common mechanism of formation was explained as shown in Figure 5.3.7. The carbon-centred radical at the C_4 position was formed first by the breaking of the C_4-OH bond, and radical A was formed by NTSP intermolecularly trapping the carbon-centred radical, presumably through a dimer complex. Secondly, Radical B was formed by NTSP trapping a hydrogen radical possibly derived from the breaking of the N_1-H bond in the dihydropyridinyl ring. Any dimer complex between nifedipine and NTSP could also have promoted the faster formation of the radical A through the intermolecular reaction of a radical intermediate with the nearby NTSP.

In this work, we have carried out the incorporation of nifedipine in aqueous liposome dispersions and in albumin protein solutions. By working with organic solvents, we estimated the equilibrium dimer-complex formation constants for nifedipine. These results were then applied to our discussion of the photochemical mechanism which produces free radicals following the conversion of nifedipine to NTSP. Our proposed mechanism involved the 1,4-dihydro-4-pyridinol derivative as a key intermediate. The formation pathway of the two observed stable radical adducts, A and B, was also explained based on the proposed photochemical mechanism.

For further work, it is necessary to do more work on the interaction of nifedipine with albumins, particularly on how nifedipine possibly complexes with the proteins at very specific sites. Secondly, we would suggest that it is a worthwhile goal to try to confirm the presence of the 1,4-dihydro-4-pyridinol derivative in the photochemical mechanism. Finally, it would be pertinent to study the properties of NTSP itself, particularly its tendency for self-association and for its association with nifedipine. This information would help to elucidate how NTSP traps the radicals derived from the nifedipine photochemistry.

PART VI. REFERENCES

Antonin, K., Petr, T. and Igor, G. (1984): "Interaction of ^{13}C NMR chemical shifts of Hantzsch's pyridines and 1,4-dihydropyridines", **Collect. Czech. Chem. Commun.**, 49(10):2393-2399.

Bechard, S.R., Quaraishi, O. and Kwong, E. (1992): "Film coating: effect of titanium dioxide concentration and film thickness on the photostability of nifedipine", **Int. J. Pharm.**, 87:133-139.

Benesi, H.A. and Hildebrand, J.H. (1949): "A spectrophotometric investigation of the interaction of iodine with aromatic hydrocarbons", **J. Amer. Chem. Soc.**, 71:2703-2707.

Berson, J.A. and Brown, E. (1955a): "Studies on dihydopyridines. I. The preparation of unsymmetrical 4-aryl-1,4-dihydropyridines by the Hantzsch-Beyer synthesis", **J. Amer. Chem. Soc.**, 77:447-450.

Berson, J.A. and Brown, E. (1955b): "Studies on Dihydropyridine. II. The photochemical disproportion of 4-(2'-nitrophenyl)-1,4-dihydropyridines", **J. Amer. Chem. Soc.**, 77:447-450.

Brock, T.G., Nagaprakash, K., Margolis, D.I. and Smolen, J.E. (1994): "Modelling degranulation with liposomes: effect of lipid composition on membrane fusion", **J. Membr. Biol.**, 141(2):139-148.

Bruner, J., Skrabal, P., and Hauser, H. (1976): "Single bilayer vesicles prepared without sonication physico-chemical properties", **Biochim. Biophys. Acta**, 455:322-332.

Carlucci, G., Colanzi, A. and Mazzeo, P. (1990): "Determination of 2,6-dimethyl-4-(2'-nitrosophenyl)-3,5-pyridinedicarboxylic acid dimethylester in nifedipine by derivative UV-Spectrophotometry in bulk material and pharmaceutical forms", **Farmaco**, 45:751-755.

Carvalho, C.M., Oliveira, C.R., Lima, L.P., Leysen, J.E., and Carvalho, A.P. (1989): "Partition of Ca antagonists in brain plasma membranes", **Biochem. Pharmacol.**, 38:2121-2127.

Deamer, D. and Bangham, A.D. (1976): "Large volumes liposomes by an ether vaporization method", **Biochim. Biophys. Acta**, 443:629-635.

De Mayo, P. (1960): "Ultraviolet photochemistry of single unsaturated system", *in* **Advances in Organic Chemistry** (Ed., Rapael, R., Taylor, E. and Wynberg, H.), 2:367-425.

Ebel, S., Schutz, H. and Hornitschek, A. (1978): "Untersuchungen zur analyitk von nifedpin unter besonderer berucksichtigung der bei lightexpotion entsteenden umwandlungsprodukte", **Arzneim. Forsch.**, 22:2188-2193.

Edwards, D.I. (1986): "Reduction of nitroimidazole *in vitro* and DNA damage", **Biochem. Pharmacol.**, 35:53-58.

Elorza, B., Elorza, M.A., Sainz, M.C. and Chatres, J.R. (1993): "Comparison of particle size and encapsulation parameters of three liposomal preparations", **J. Microencapsul.**, 10(2):237-248.

Evans, C.A. (1979): "Spin Trapping", **Aldrichchimica Acta**, 12:23-29.

Floyd, R.A., Lewis, C.A. and Wong, P.K. (1984): "High-pressure liquid chromatography-electrochemical detection of oxygen free radicals", *in* **Methods in Enzymology**, 105:231-237.

Hagiwara, S. and Byerly, L. (1981): "Calcium channel", **Annu. Rev. Neurosci.**, 4:69-125.

Herbette, L.G., Van Erve, Y.M.H. and Rhodes, D.G. (1989): "Interaction of 1,4-dihydropyridine calcium channel antagonists with biological membranes: Lipid bilayer partitioning could occur before drug binding to receptors", **J. Mol. Cell Cardiol.**, 21:187-201.

Hoster, F.A. (1975): "Pharmacokinetics of nifedipine-^{14}C in man", **2nd International Adalat Symposium.** (1974, Amsterdam), Springer-Verlag, Berlin, 124-127.

Hosey, M.M. and Lazdunski, M. (1988): "Calcium channels: molecular pharmacology, structure and regulation", **J. Membr. Biol.**, 104:81-105.

Jacobsen, P., Pederson, O.L. and Mikkelsen, E. (1979): "GC determination of nifedipine and one of its metabolites using electron capture detector", **J. Chromatography.**, 162:81-87.

Jaffe, H.H. and Orchin, M. (1962): "Theory and Applications of ultraviolet spectroscopy", John Wiley and Sons, Inc..

Janzen, E.G., Coulter G.A., Oehler U.M. and Bergsma J.P. (1982): "Solvent effects on the nitrogen and β-hydrogen hyperfine splitting constants of aminoxyl radicals obtained in spin trapping experiments", **Can. J. Chem.**, 60:2725-2733.

Janzen, E.G. and Haire, D.L. (1990): "Two decades of spin trapping", **Advances in Free Radical Chemistry.**, 1:253-295.

Kleinbloesem, C.H., Van Brummelen, P., Van De Linde, J.A., Voogd, P.J. and Breimer, D.D. (1984): "Nifedipine: Kinetics and dynamics in healthy subjects", **Clin. Pharm. Thera.**, 35:742-749.

Knowles, P.F., Marsh, D. and Rattle, H.W.E. (1976): "Magnetic resonance of biomolecules: An introduction to the theory and practice of NMR and ESR in biological systems", John Wiley & Sons, Ltd:.

Kracma, J., Kracmarova, J., Kovarova, A. and Stejskal, A. (1988): "UV spectrometry in drug control. 37: New active substances containing benzene, pyridine and quinoline chromophores. Part 8: Impact of substitution and solvent", **Pharmazie,** 43(3):173-176.

Kroneberg, G. and Krebs, R. (1980): "Pharmacology of nifedipine", **4th International Adalat Symposium** (1979), 14-24.

Leighton, P.A. and Lucy, F.A. (1934): "Photoisomerization of the o-nitrobenzaldehydes. I. Photochemical results", **J. Chem. Phys.**, 2:756-759.

Levy, N. and Cohen, M.D. (1979): "Photoreduction of 4-cyano-1-nitrobenzene in propan-2-ol", **J. Chem. Soc. Perkin Trans.**, II:553-558.

Majeed, I.A., Murray, W.J., Newton, D.W., Othman, S. and Al-turk, W. (1987):

"Spectrophotometric study of the photodecomposition kinetics of nifedipine", **J. Pharm. Pharmacol.**, 39:1044-1046.

Mak, I.T., Boehme, P. and Weglicki, W.B. (1992): "Antioxidant effects of calcium channel blockers against free radical injury in endothelial cells: Correlation of protection with preservation of glutathione levels", **Circu. Res.**, 70:1099-1103.

Mak, I.T. and Weglicki, W.B. (1990): "Comparative antioxidant activities of propranolol, nifedipine, verapamil and diltiazem against sarcolemmal membrane lipid peroxidation", **Circ. Res.**, 66:1449-1452.

Marsh, D. (1990): "Handbook of lipid bilayers", Chemical Rubber Co., Boca Raton, 135-162.

Matsuda, Y., Teraoka, R. and Sugimoto, I. (1989): "Comparative evaluation of photostability of solid-state nifedipine under ordinary and intensive light irradiation conditions", **Int. J. Pharm.**, 54(3):211:221.

Mauser, H. and Hertzer, H. (1965): "Photoreduction of nitrobenzene in MeOH", **Z. Naturforsch**, 20b(3):200-203.

McConnell, H.M. and McFarland, B.G. (1970): "Physics and chemistry of spin labels", **Quart. Rev. Biophys.**, 3:91-136.

Miller, R.J. (1987): "Multiple calcium channels and neuronal function", **Science**, 235:46-52.

Misik, V., Ondrias, K. and Gergel, D. (1993): "Antioxidative properties of cardioactive drugs", **Bratisl. Lek. listy**, 94:66-70.

Misik, V., Stasko, A., Gergel, D. and Ondrias, K. (1991): "Spin-trapping and antioxidant properties of illuminated and nonilluminated nifedipine and nimodipine in heart homogenate and model system", **Mol. Pharmacol.**, 40:43-439.

Nayar, R., Hope, M.J. and Cullis, P.R. (1989): "Generation of large unilamellar vesicles from long-chain saturated phosphatidylcholines by extrusion technique", **Biochim. Biophys. Acta**, 986:200-206.

Nayler, W.G. (1988): "Calcium Antagonists", London, Academic Press.

Nayler, W.G. (1990): "Classification and tissue selectivity of calcium antagonists", **Zeitschr. Kardiol.** 79(suppl 3):107-111.

O'Haven, T.C. and Green, G.L. (1976): "Numerical error analysis of derivative spectrometry for the quantitative analysis of mixture", **Anal. Chem.**, 48:312-318.

Ondrias, K., Misik, V., Gergel, D. and Stasko, A. (1989): "Lipid peroxidation of phosphatidylcholine liposomes depressed by the calcium channel blockers nifedipine and verapamil and by the antiarrhythmic-antihypotensive drug stobadine", **Biochim. Biophys. Acta**, 1003:238-245.

Ondrias, K., Misik, V., Stasko, A., Gergel, D. and Hromadova, M. (1994): "Comparison of antioxidant properties of nifedipine and illuminated nifedipine with nitroso spin traps in low density lipoproteins and phosphatidylcholine liposomes", **Biochim. Biophys. Acta**, 1211:114-119.

Opie, L.H. (1990): "Clinical use of calcium channel antagonistic drugs", Kluwer Academic, Boston.

Orger, B.H. (1972): "Reduction of nitrogen-containing compounds", *in* **Photochemistry**, (Bryce-Smith, D., ed.), Burlington House, London, 3:644-656.

Perkampus, H.H. (1992): "UV-VIS spectroscopy and its applications", Springer-Verlag Berlin, Heidelberg.

Philips, A.P. (1951): "Substituted dihydropyridines to Hantzsch's pyridine synthesis", **J. Amer. Chem. Soc.**, 73:2248.

Ramemsch, K.D. and Sommer, J. (1983): "Pharmacokinetics and metabolism of nifedipine", **Hypertension**, 5:II-18 - II-24.

Sachs, F. and Hilpert, S. (1904): **Chem. Ber.**, 34:2040.

Sadana, G.S. and Ghogare, A.B. (1991): "Mechanistic studies on photolytic degradation of nifedipine by use of ^{1}H-NMR and ^{13}C-NMR spectroscopy", **Int. J. Pharm.**, 70:195-

199.

Saunders, L., Perrin, J. and Gammack, D.B. (1962): "Ultrasonic irradiation of some phospholipid sols", **J. Pharm. Pharmacol.**, 14:567-572.

Schlossman, K., Medenwald, H. and Rosenkranz, H. (1975): "Investigation on the metabolism and protein binding of nifedipine", **2nd International Adalat Symposium** (1974, Amsterdam), Springer-Verlag, Berlin, 33-39.

Shim, S.C., Pae, A.N. and Lee, Y.J. (1988): "Mechanistic studies on the photochemical degradation of nifedipine", **Bull. Korea Chem. Soc.**, 9(5):271-274.

Stasko, A., Brezova, V., Biskupic, S., Ondrias, K. and Misik, V. (1994): "Reactive radical intermediates formed from illuminated nifedipine", **Free Radical Biol. Med.**, 17:545-556.

Sullivan, A.B. (1966): "Electron spin resonance studies of a stable arylnitroso-olefin adduct free radical", **J. Org. Chem.**, 31:2811-2817.

Swartz, H.M., Bolton, J.R. and Borg, D.C. (1972): "Biological Applications of Electron Spin Resonance", Wiley-Interscience, New York.

Syed, L.A. (1989): "Nifedipine", *in* **Analytical profiles of drug substances**, (Florey K., ed), Academic Press, 18:221-288.

Talsky, G. (1979): "Higher order UV derivative spectrophotometry of polycarbonates containing azo groups", **Makromol. Chem.**, 180:513-516.

Tanasescu, I. (1926): "The mechanism of the photochemical reactions of o-nitrobenzaldehyde and some of its condensation products", **Bull. Soc. Chim.**, 39:1443-1455.

Testa, R., Dolfini, E., Reschiotti, C., Secchi, C. and Biondi, P.A. (1979): "Gas-liquid chromatographic determination of nifedipine, a light sensitive drug, in plasma", **Farmaco.**, 34:463-473.

Thoma, K. and Kerker, R. (1992a): "Photoinstability of drugs. Part 2. the behaviour of

visible light-absorbing drugs in simulated daylight", **Pharm. Ind.**, 54(3):287-283.

Thoma, K. and Kerker, R. (1992b): "Photoinstability of drugs. Part 3. photodegradation and stabilization of nifedipine in dosage forms", **Pharm. Ind.**, 54(4):359-365.

Thoma, K. and Kerker, R. (1992c): "Photoinstability of drugs. Part 4. the decomposition products of nifedipine", **Pharm. Ind.**, 54(4): 465-468.

Thoma, K. and Klimek, R. (1985): "Studies on photoinstability of nifedipine. Part 1: kinetics of degradation and reaction mechanism", **Pharm. Ind.**, 47(2):207-215.

Thomas, S.E. and Wood, M.L. (1986): "Photosensitivity reactions associated with nifedipine", **Br. Med. J.**, 292:992.

Tirzit, G.D., Kirule, I.E., Baumane, I.K., Gavar, R.A., Stradyn, I.P. and Dubur, G.Y. (1984): "Mechanism of the antioxidant action of 2,6-dimethyl-3,5-dimethoxycarbonyl-4-(2-nitrophenyl)-1,4-dihydro-pyridine", **Khim. Geterotsikl. Soedin.**, 8:1120-1122.

Van Zwieten, P.A. (1989): "Clinical Aspects of calcium entry blockers", Basel, Karger.

Vargas, F., Rivas, C. and Machado, R. (1992): "Photodegradation of nifedipine under aerobic conditions: evidence of formation of singlet oxygen and radical intermediate", **J. Pharm. Sci.**, 81(4):399-400.

Wang, S. and Cheng, X. (1991): "Photodegradation kinetics of nifedipine", **Zhongguo Yaoke Daxue Xuebao**, 22(1):1-4.

Weglicki, W.B., Mak, I.T. and Simic, M.G. (1990): "Mechanisms of cardiovascular drugs as antioxidants", **J. Mol. Cell Cardiol.**, 22:1199-1208.

Wertz, J.E. and Bolton, J.R. (1972): "Electron spin resonance elementary theory and practical applications", McGraw-Hill, New York.

Xu, G., Zhao, Y., Suen, X., Liu, Y. and Song, X. (1985): "ESR study of the active radicals produced by the photolysis of arenediazonium salts and their crown ether complexes", **Wuli Huaxuebao Xuebao**, 1(4):329-334.

PART VIII. APPENDICES

Appendix A.

Modified Benesi-Hildebrand Theory

For a dimerization of any compound, an equilibrium of its monomer (M) and the dimer (D) in the reaction is assumed:

$$2\,M \quad \rightleftharpoons \quad M_2 \text{ (or D)} \qquad (D = M_2)$$

At equilibrium, we can define the equilibrium constant:

$$K = C_D / C_M^2 \qquad \text{(Eq.1)}$$

Here,

K : equilibrium dimerization constant with units of M^{-1};

C_D : concentration of the dimer at equilibrium;

C_M : concentration of the monomer at equilibrium.

1) For stoichiometry considerations, assume C to be the initial concentration of the monomer and x to be the concentration of the dimer at equilibrium,

Then, $C_D = x$,

$C = C_M + 2\,C_D = C_M + 2x$

or $C_M = C - 2x$

From Eq.1 $K = C_D / C_M^2 = x / (C - 2x)^2$

$(C^2 - 4Cx + 4x^2)K - x = 0$

$4Kx^2 - (4KC + 1)x + KC^2 = 0$

$$x = \frac{4KC+1 \pm \sqrt{(8KC+1)}}{8K} \qquad \text{(Eq.2)}$$

here, the K value is unknown.

2) For UV-VIS spectral methodology considerations, assume that both monomer and dimer obey Beer's Law at the measured wavelength and an overlapped absorbance should be:

$$A = E_D C_D d + E_M C_M d \qquad \text{(Eq.3)}$$

here,

A : experimental absorbance;

E_D : molar extinction coefficient of the dimer;

E_M : molar extinction coefficient of the monomer.

d : optical pathlength of a cuvette (cm)

At low concentration, it is assumed that no dimer forms. The absorbance of the system at low concentration will be

$$A_0 = E_M C_0 d \qquad \text{(Eq.4)}$$

here,

A_0 : absorbance of the monomer at low concentration without the formation of dimer;

C_0 : concentration of the monomer at low concentration without the formation of dimer;

Divide Eq.3 by Eq.4:

$$\frac{A}{A_0} = \frac{E_M C_M + E_D C_D}{E_M C_0}$$

$$\because \quad C_D = x \quad \text{and} \quad C_M = C - 2x$$

$$\therefore \quad \frac{A}{A_0} = \frac{E_M (C - 2x) + E_D x}{E_M C_0} \qquad \text{(Eq.5)}$$

Rearrange Eq.5 and solve for x:

$$\frac{A}{A_0} = \frac{E_M C + (E_D - 2E_M)x}{E_M C_0}$$

$$\frac{A}{A_0} = \frac{C}{C_0} + \frac{(E_D / E_M - 2)x}{C_0}$$

$$x = \frac{C_0\left(\frac{A}{A_0} - \frac{C}{C_0}\right)}{\frac{E_M}{(E_D - 2E_M)}} \qquad \text{(Eq.6)}$$

3) Combine Eq.2 and Eq.6, and eliminate x, then rearrange, the final equation is obtained as the following:

$$E = \frac{E_M}{(E_D - 2E_M)} = \frac{4CK + 1 \pm \sqrt{(8CK + 1)}}{8C_0K\left(\frac{A}{A_0} - \frac{C}{C_0}\right)} \qquad \text{(Eq.7)}$$

here, A, A_0 and E_M are determined from experimental values; C_0 and C are well determined by the preparations of the solutions; E_D and K are unknown. E_D is wavelength dependent and K is independent on wavelength and concentration.

4) Proposed iterative method for the solution of the equation 7:

i. Propose K values at specific λ;

ii. Calculate E_M / (E_D - $2E_M$) and then E_D from the corresponding K value at this specific λ;

iii. The K value should be the same at all wavelengths, however the value of E_D is obviously a function of wavelength.

Appendix B.

The UV-VIS Absorbance Data and the K Value Estimation for Nifedipine in Alcoholic Solutions

In the following Tables, these definitions apply:

K	:	equilibrium dimer-complex formation constant (M^{-1});
E_M	:	molar extinction coefficient of nifedipine monomer $(M \cdot cm)^{-1}$;
A_0	:	absorptivity for 1 mM nifedipine solution for a 1 mm cuvette;
A	:	calculated absorptivity by multiplying a factor of 20.37 to the absorptivity obtained from the 10 mM or 20 mM nifedipine solutions from a 0.0491 mm cuvette;
A/A_0	:	the ratio of A/A_0;
ΔA	:	for 10 mM nifedipine solution, $\Delta A = 10 \cdot A_0 - A$, and for 20 mM nifedipine solution, $\Delta A = 20 \cdot A_0 - A$;
x	:	the estimated concentration of nifedipine dimer complex;
Av.	:	average data;
S_R	:	relative standard deviation (%).

1) The absorbance data and the K value estimation for nifedipine in ethanol solution

λ (nm)	E_M $(M\cdot cm)^{-1}$	A	A/A_0	ΔA	x (mM)	K (M^{-1})
400	1610	2.852	17.714	0.368	2.29	9.60
390	2660	4.848	18.226	0.472	1.77	6.56
380	3790	6.967	18.362	0.613	1.62	5.75
370	4570	8.433	18.383	0.707	1.55	5.41
360	4940	9.105	18.431	0.775	1.57	5.52
350	5000	9.085	18.170	0.915	1.83	6.85
340	4990	8.983	18.002	0.997	2.00	7.80
330	4990	9.004	18.044	0.976	1.96	7.56
320	4910	8.555	17.424	1.265	2.58	11.78
310	4400	7.720	17.545	1.080	2.45	10.78
300	4000	6.905	17.262	1.095	2.74	12.98
290	3730	6.315	16.930	1.145	3.07	15.98
280	3510	4.644	13.231	2.376	6.77	162.13
270	4070	6.926	17.017	1.214	2.98	15.14
260	6100	10.645	17.466	1.575	2.58	11.70
250	10440	19.107	18.302	1.773	1.70	6.16
240	19850	36.544	18.410	3.156	1.59	5.62
230	20310	37.440	18.434	3.180	1.57	5.50
220	16530	30.575	18.497	2.485	1.50	5.21
210	19090	35.872	18.791	2.308	1.21	3.91
Av.					2.03	7.98
S_r(%)					27.3	45.6

2) The absorbance data and the K value estimation for nifedipine in 1-butanol solution

λ (nm)	E_M $(M \cdot cm)^{-1}$	A	A/A_0	ΔA	x (mM)	K (M^{-1})
400	1700	2.913	17.135	0.487	2.86	14.07
390	2800	4.868	17.387	0.732	2.61	11.98
380	3910	6.802	17.400	1.018	2.60	11.90
370	4630	8.026	17.334	1.234	2.67	12.39
360	4880	8.515	17.448	1.245	2.55	11.50
350	4860	8.474	17.436	1.246	2.56	11.59
340	4820	8.372	17.369	1.268	2.63	12.11
330	4850	8.392	17.304	1.308	2.70	12.64
320	4610	7.863	17.056	1.357	2.94	14.78
310	4180	7.106	17.007	1.254	3.00	15.31
300	3790	6.417	16.930	1.163	3,07	15.97
290	3550	5.867	16.526	1.233	3.47	20.38
280	3370	5.500	16.320	1.240	3.68	23.03
270	3960	6.559	16.563	1.361	3.44	19.95
260	6030	10.266	17.026	1.794	2.98	15.07
250	10560	18.455	17.447	2.665	2.52	11.29
240	20240	35.586	17.582	4.894	2.42	10.52
230	20010	34.792	17.387	5.228	2.61	11.97
220	16230	28.212	17.383	4.248	2.62	12.01
210	19030	33.733	17.747	4.287	2.25	9.38
Av.					2.81	13.58
S_r(%)					13.3	26.0

3) The absorbance data and the K value estimation for nifedipine in 1-octanol solution

λ (nm)	E_M $(M\cdot cm)^{-1}$	A	A/A_0	ΔA	x (mM)	K (M^{-1})
400	1710	1.365	7.981	0.345	2.02	56.70
390	2790	2.261	8.104	0.529	1.90	49.20
380	3850	3.117	8.095	0.733	1.90	49.65
370	4990	3.667	8.166	0.823	1.83	45.69
360	4700	3.830	8.148	0.870	1.85	46.67
350	4690	3.830	8.165	0.860	1.83	45.73
340	4680	3.830	8.183	0.850	1.82	44.80
330	4730	3.830	8.096	0.900	1.90	49.59
320	4490	3.646	8.121	0.844	1.88	48.27
310	4050	3.280	8.098	0.770	1.90	49.50
300	3680	2.974	8.082	0.706	1.92	50.51
290	3450	2.791	8.089	0.659	1.91	50.02
280	3290	2.648	8.049	0.642	1.95	52.49
270	3950	3.178	8.045	0.772	1.95	52.68
260	6100	4.868	7.981	1.232	2.02	56.85
250	10620	8.555	8.056	2.065	1.94	52.07
240	20470	16.887	8.250	3.583	1.75	41.44
230	19960	16.377	8.205	3.583	1.80	43.69
220	16460	13.342	8.106	3.118	1.89	49.10
210	20090	16.926	8.111	3.794	1.89	48.77
Av.					1.89	49.03
S_r(%)					3.59	8.0

Appendix C.

The Data of Double Integral (DI) for Standard Nitroxide Sample

Sample: 4-Hydroxyl-2,2,6,6-tetramethylpiperidin-1-yloxy (Tempol)

Concentration: 100 μM in pH 7.4 HEPES/NaCl buffer

The concentrations of radicals in liposomes and in proteins could be determined by the following equation based on the calculation of double integral values of EPR spectra measured for the above Tempol/buffer standard solution. If all other experimental conditions such as modulation amplitude and microwave power are the same, the radical concentrations in the measured samples can be determined. The following Tables give the calculated results of double integrals of EPR spectra for the Tempol standard solution measured under different experimental conditions.

$$C_m = \frac{A_m G_s N_s}{A_s G_m N_m} C_s$$

Here,

A_s, A_m : double integral value for the standard sample and for the measured sample;

G_s, G_m : receiver gain for the standard sample and the measured sample;

N_s, N_m : number of scans for the standard sample and for the measured sample;

C_s, C_m : radical concentration in the standard sample and in the measured sample.

1). Double integral data for the Tempol standard sample in glass capillary

NO.	M.A.(G)[a]	M.P.(mW)[b]	T°C	A_s
GA1	0.8	10	27	888
GA2	0.5	10	27	539
GA3	0.5	1	27	189
GA4	0.25	10	27	261
GA5	0.8	10	37	968
GA6	0.5	10	37	619
GA7	0.5	1	37	200
GA8	0.25	10	37	312
GA9	0.8	10	47	1061
GA10	0.5	10	47	661

Notes:

a) M.A.: modulation amplitude, unit of gauss; b) M.P.: microwave power, unit of mW; Experimental conditions: receiver gain (G_s): 10 x 10^2; number of scan: 4; 60 μl sample volume in glass capillary under oxibiotic conditions.

2) Double integral data for the Tempol standard sample in double teflon tubes

NO.	M.A.(G)[a]	M.P.(mW)[b]	G_s (x10^2)	T°C	A_s
GB1	0.8	10	8	27	929
GB2	0.5	10	10	27	587
GB3	0.5	1	10	27	196
GB4	0.25	10	10	27	297
GB5	0.8	10	8	37	944
GB6	0.5	10	10	37	612
GB7	0.5	10	10	37	196
GB8	0.25	1	10	37	301
GB9	0.8	10	8	47	1022
GB10	0.5	10	10	47	670

Notes:

a) M.A.: modulation amplitude, unit of gauss; b) M.P.: microwave power, unit of mW; Experimental conditions: number of scan: 4; 70 x 2 µl sample volume in teflon tubes under hypoxic conditions.